Recent experimental studies of electron dephasing in metal and semiconductor mesoscopic structures

2002 J. Phys.: Condens. Matter 14 R501

(http://iopscience.iop.org/0953-8984/14/18/201)

INSTITUTE OF PHYSICS PUBLISHING JOURNAL OF PHYSICS: CONDENSED MATTER

J. Phys.: Condens. Matter **14** (2002) R501–R596 PII: S0953-8984(02)16903-7

TOPICAL REVIEW

Recent experimental studies of electron dephasing in metal and semiconductor mesoscopic structures

J J Lin[1,3] **and J P Bird**[2,3]

[1] Institute of Physics, National Chiao Tung University, Hsinchu 300, Taiwan
[2] Department of Electrical Engineering, Arizona State University, Tempe, AZ 85287, USA

E-mail: jjlin@cc.nctu.edu.tw and bird@asu.edu

Received 13 February 2002
Published 26 April 2002
Online at stacks.iop.org/JPhysCM/14/R501

Abstract

In this review, we discuss the results of recent experimental studies of the low-temperature electron dephasing time (τ_ϕ) in metal and semiconductor mesoscopic structures. A major focus of this review is on the use of weak localization, and other quantum-interference-related phenomena, to determine the value of τ_ϕ in systems of different dimensionality and with different levels of disorder. Significant attention is devoted to a discussion of three-dimensional metal films, in which dephasing is found to predominantly arise from the influence of electron–phonon (e–ph) scattering. Both the temperature and electron mean free path dependences of τ_ϕ that result from this scattering mechanism are found to be sensitive to the microscopic quality and degree of disorder in the sample. The results of these studies are compared with the predictions of recent theories for the e–ph interaction. We conclude that, in spite of progress in the theory for this scattering mechanism, our understanding of the e–ph interaction remains incomplete. We also discuss the origins of decoherence in low-diffusivity metal films, close to the metal–insulator transition, in which evidence for a crossover of the inelastic scattering, from e–ph to 'critical' electron–electron (e–e) scattering, is observed. Electron–electron scattering is also found to be the dominant source of dephasing in experimental studies of semiconductor quantum wires, in which the effects of both large- and small-energy-transfer scattering must be taken into account. The latter, *Nyquist*, mechanism is the stronger effect at a few kelvins, and may be viewed as arising from fluctuations in the electromagnetic background, generated by the thermal motion of electrons. At higher temperatures, however, a crossover to inelastic e–e scattering typically occurs; and evidence for this large-energy-transfer process has been found at temperatures as high as 30 K. Electron–electron interactions are also thought to play an important role in dephasing in ballistic quantum dots, and the results of recent experiments in this area are reviewed. A common feature of experiments, in both dirty metals

[3] Authors to whom any correspondence should be addressed.

0953-8984/02/180501+96$30.00

and ballistic and quasi-ballistic semiconductors, is found to be the observation of an unexpected 'saturation' of the dephasing time at temperatures below a kelvin or so. The possible origins of this saturation are discussed, with an emphasis on recent experimental investigations of this effect.

Contents

1. Introduction

The electron dephasing time, τ_ϕ, is a quantity of fundamental interest and importance in metal and semiconductor mesoscopic structures. Both theoretical and experimental investigations of τ_ϕ in various (one, two, three, and zero) dimensions have advanced significantly over the last 20 years. These advances have largely been due to the observation, in mesoscopic metals and semiconductors, of a variety of prominent quantum-interference phenomena. Among these phenomena are included weak localization in films and wires [1–7], universal conductance fluctuations in disordered quantum wires [8], and Aharonov–Bohm oscillations [9], and persistent currents [10], in mesoscopic rings. In many cases, these quantum-interference phenomena are observed in weakly disordered systems, in which electrons are able to undergo *multiple* elastic scattering at low temperatures, before the coherence of their wavefunction is randomized. The electron dephasing time τ_ϕ (together with the spin–orbit scattering time τ_{so}) totally controls the magnitude and temperature (T) dependence of the quantum-interference effects[4], and is given by [3, 7]

$$\frac{1}{\tau_\phi(T,l)} = \frac{1}{\tau_\phi^0(l)} + \frac{1}{\tau_i(T,l)}, \tag{1}$$

[4] Strictly speaking, with universal conductance fluctuations and the Aharonov–Bohm effect, there is also the influence of thermal averaging that needs to be taken into account.

where l is the electron elastic mean free path, τ_ϕ^0 is presumed to be independent of temperature, and τ_i is the relevant inelastic electron scattering time(s) in question[5]. As is evident from equation (1), the temperature dependence of τ_ϕ is controlled entirely by the temperature dependence of τ_i, while τ_ϕ^0 determines the value of the dephasing time in the limit of very low temperatures. In addition to being temperature dependent, τ_i is also dependent on the disorder (i.e. electron elastic mean free path l). The zero-temperature dephasing time, $\tau_\phi^0 \equiv \tau_\phi(T \to 0)$, has remained the subject of a long-standing puzzle, which has very recently attracted vigorous renewed interest and is currently under much theoretical and experimental debate. The central question is whether τ_ϕ^0 should reach a finite or infinite value as the temperature tends to zero. Among the current opinions that exist on this matter, it has been suggested that the saturated value of τ_ϕ^0 should depend on the specific sample geometry [11], the level of disorder in the structure [12, 13], the microscopic qualities of the defects [14, 15], or e–e scattering mediated by the magnetic exchange interaction [16]. In addition, it is also widely accepted that the temperature and disorder behaviour of both τ_i and τ_ϕ^0 are very sensitive to the effective dimensionality of the sample [7, 11].

Since the realization of weak-localization effects, the dependence of the dephasing time on temperature and the mean free path has been widely studied in various mesoscopic systems, including metals [1, 7], semiconductors [17], and superconductors [7]. The establishment of the electron dephasing (or phase-breaking) length:

$$L_\phi = \sqrt{D\tau_\phi} \tag{2}$$

as the key length scale in the quantum-interference phenomena has prompted extensive investigations in systems of differing effective dimensionality. The electron diffusion constant $D = v_F^2\tau/d$ in diffusive systems, where v_F is the Fermi velocity, τ is the electron elastic mean free time, and d is the effective dimensionality of the system under study. The diffusion constant appears in the problem as a consequence of the *diffusive* motion of conduction electrons in the weakly disordered regime. This is the regime where perturbative calculations are valid and theoretical predictions can be quantitatively compared with experimental measurements. (Later on, we will discuss the results of experiments performed on quasi-ballistic quantum wires, and ballistic quantum dots, in which systems the assumption of diffusive motion may no longer hold.) Usually, the dephasing length L_ϕ can be a (few) thousand ångström(s) or longer at liquid-helium temperatures in disordered metals [18, 19], and it can be even longer in high-mobility mesoscopic semiconductors [20]. Therefore, films less than a few hundred ångströms thick will reveal two-dimensional behaviour with regard to the quantum-interference effects, while narrow channels with widths less than this will exhibit one-dimensional behaviour. Recently, progress has even been made in the study of *zero-dimensional* systems, such as semiconductor quantum dots [20] and granular metal particles [21], whose spatial dimensions can *all* be smaller than the dephasing length.

Owing to extensive theoretical and experimental studies of weak-localization, and other quantum-interference, effects over the course of the past two decades, it is now known that the microscopic processes that determine τ_ϕ can essentially be ascribed to four different origins. It is furthermore understood that a number of these dephasing processes may coexist in real systems, with one or two mechanisms typically dominating, dependent on the system dimensionality, the level of disorder, and the measurement temperature. The four important dephasing mechanisms, and the particular experimental circumstances under which these might dominate, are categorized as follows.

[5] In the case of superconductors, and at temperatures very close to the transition temperature T_c, τ_i is essentially the dephasing time due to superconducting fluctuations $1/\tau_i \approx 1/\tau_{e-sf}$, while at temperatures well above T_c, τ_i is limited by e–ph scattering in three dimensions, $1/\tau_i \approx 1/\tau_{ep}$, and by e–e scattering in one and two dimensions, $1/\tau_i \approx 1/\tau_{ee}$.

(a) In three-dimensional, weakly disordered, conductors ($L_\phi < L_x, L_y, L_z$), electron–phonon (e–ph) scattering is the sole dominant inelastic dephasing process [22–24], i.e. $1/\tau_{\rm i}(T, l) \approx 1/\tau_{ep}(T, l)$. Thus far, three-dimensional weak-localization effects have been studied using thick granular films [25–27], thick quench-condensed metal films [28], doped semiconductors [17], metallic glasses [29, 30], and polycrystalline metallic alloys [31, 32]. However, the behaviour of $1/\tau_{ep}$ in the presence of disorder in mesoscopic three-dimensional systems is still not fully understood. In particular, experimental results vary widely and are frequently in disagreement with theoretical predictions [22, 33].

(b) In three-dimensional, strongly disordered, conductors, e–e scattering is very sensitive to the critical (as opposed to diffusive) current dynamics, resulting in the e–e scattering rate $1/\tau_{EE}$ dominating over the e–ph scattering rate [34], i.e., $1/\tau_{\rm i}(T, l) \approx 1/\tau_{EE}(T, l)$. Thus far, theoretical and experimental studies of the 'critical' e–e scattering time $\tau_{EE}(T, l)$ in conductors near the mobility edge have not attracted much attention. (We use the notation τ_{EE} to distinguish the 'critical' e–e scattering time near the Anderson transition from the more familiar Nyquist and inelastic e–e scattering time, usually denoted by τ_{ee}.)

(c) In metals and semiconductors at low temperatures, *small*-energy-transfer ('quasielastic') e–e scattering is the dominant dephasing process, giving rise to $1/\tau_{ee} \propto T$ in two dimensions, and $1/\tau_{ee} \propto T^{2/3}$ in one dimension [35]. Among the four dephasing processes discussed here, this 'Nyquist' dephasing mechanism is the most widely studied and best understood [10]. Physically, such quasielastic e–e collisions are equivalent to the interaction of an electron with the fluctuating electromagnetic field produced by all the other electrons, i.e. dephasing by the equilibrium Nyquist noise.

(d) In mesoscopic systems at very low temperatures, a 'saturation' of the electron dephasing rate, $1/\tau_\phi(T, l) \approx 1/\tau_\phi^0(l)$, is often observed [11, 12, 36, 37]. The underlying physics of this *extremely weakly* temperature-dependent dephasing time is currently the source of intensive debate [14]. While some authors argue that the saturation is caused by extrinsic mechanisms, such as magnetic spin–spin scattering [16, 38–40], hot-electron effects [24, 41], electromagnetic noise sources [35, 42] or non-equilibrium effects [43], other authors yet argue for an intrinsic quantum origin, such as the effect of e–e interaction in a disordered metal [44, 45]. In addition, the role of the interaction between conduction electrons and dynamical defects, such as two-level systems (TLS), has also been widely investigated [14, 15].

In this review paper, we will concentrate our discussions on available theoretical predictions, and experimental results for the different low-temperature dephasing mechanisms. While we will present experimental results for all four mechanisms identified above[6], our main interest will focus on reviewing recent studies of the e–ph scattering time τ_{ep}, the 'critical' e–e scattering time τ_{EE}, and the saturation of the dephasing time τ_ϕ^0. We shall focus on a discussion of the inelastic electron dephasing times in mesoscopic metals and semiconductors, with significantly different material characteristics. Both the temperature and disorder dependences of τ_{ep}, τ_{EE}, and τ_ϕ^0 will be discussed. We shall see that:

(a) In the case of the e–ph scattering time, a significant body of experimental results, obtained for various materials, do not support the existence of a universal dependence of $1/\tau_{ep}$ on disorder. As for the temperature dependence of $1/\tau_{ep}$, experiments *frequently* (but not

[6] The spin–orbit scattering time $\tau_{\rm so}$, which is another important timescale in quantum-interference phenomena [1, 46], will only be mentioned where necessary. The microscopic origin and physical properties of $\tau_{\rm so}$ in metals have recently been extensively explored by Bergmann and co-workers [47].

always) reveal an unexpected T^2 dependence, in disagreement with standard theoretical concepts [48] regarding the e–ph interaction in disordered metals.

(b) In the case of $1/\tau_{EE}$, a linear temperature dependence, as well as the absence of any disorder dependence have been found in very low-diffusivity bulk systems, i.e. $1/\tau_{EE} \propto Tl^0$. Such behaviour can be qualitatively understood in terms of the current theory for inelastic e–e scattering in three-dimensional conductors near the mobility edge. Consequently, there is a crossover of inelastic electron dephasing in disordered systems, from e–ph scattering to critical e–e scattering, as the level of disorder is increased and the systems move significantly toward the Anderson transition.

(c) We will address the issue of the 'saturation' behaviour of the electron dephasing time at very low temperatures. The issue of whether there might be an *intrinsic* microscopic dephasing process causing a finite τ_ϕ^0 at very low temperatures is extremely controversial and is still open to debate. We will discuss several systematic experimental observations, involving different materials (metals and semiconductors), and transport regimes (diffusive, quasi-ballistic and ballistic). We shall see that these studies place important physical constraints on the development of a successful theory that will ultimately be able to account for the saturation.

1.1. Dephasing, dephasing time τ_ϕ, and inelastic scattering time $\tau_{\rm i}$

The dephasing (also called phase-breaking or decoherence) time τ_ϕ in mesoscopic physics is the timescale for a conduction electron to stay in a given exact one-electron energy eigenstate in the presence of *static* impurities. The transitions between these eigenstates are due to e–ph, e–e, electron–dynamical defect (e.g. TLS, or defects possessing some internal degree of freedom), or electron–magnetic-impurity interactions [14]. In the context of quantum-transport phenomena such as weak localization, universal conductance fluctuations, and various quantum-interference oscillations (i.e. h/e and $h/2e$ oscillations in connected structures), τ_ϕ determines the energy and length scales at which quantum behaviour is seen. A considerable amount of theoretical and experimental study has been directed toward understanding the mechanisms responsible for the loss of phase coherence and the dependences of these mechanisms on temperature, disorder, and dimensionality. It is well established that, in the *diffusive* regime, τ_ϕ (and also $\tau_{\rm i}$) is very sensitive to the system dimensionality.

While τ_ϕ relates directly to the dephasing processes, $\tau_{\rm i}$ is an inelastic quasiparticle lifetime related to the inverse of the one-electron self-energy. These two timescales are therefore closely connected, but *not necessarily* the same. The difference between $\tau_{\rm i}$ and τ_ϕ arises from processes with *small energy transfer*. This difference is particularly pronounced for the Nyquist e–e contribution in *reduced* dimensions. Physically, the small-energy-transfer e–e scattering is equivalent to the interaction of a conduction electron with the fluctuating electromagnetic field, produced by all other surrounding electrons in the system. This thermal, fluctuating (i.e. randomly time- and space-dependent), electric field is called the equilibrium Nyquist or Johnson noise. Due to the statistical nature of these fluctuations, such a scattering is different for each electron, thus the electronic ensemble loses it coherence [49]. In the case of a *lower-dimensional* system, and in the *diffusive* regime, we can have $\tau_\phi \ll \tau_{\rm i}$, with $1/\tau_\phi$ being dominated by very small-energy scattering processes. (That is, small-energy-transfer processes do not much affect $1/\tau_{\rm i}$.) For example, in two dimensions, the inelastic e–e dephasing time $1/\tau_{\phi,ee} \propto T$, while the e–e scattering time $1/\tau_{{\rm i},ee} \propto T \ln T$, at low temperatures. In one dimension, on the other hand, $1/\tau_{\phi,ee} \propto T^{2/3}$ and $1/\tau_{{\rm i},ee} \propto T^{1/2}$. Usually, the more weakly temperature-dependent Nyquist e–e scattering therefore dominates τ_ϕ at temperature below a few kelvins, and e–ph scattering dominates at even higher temperatures (in metals).

The situation is completely different in a *three-dimensional* system and in the *diffusive* regime, where we can have $\tau_\phi \approx \tau_i$ for e–ph scattering. This approximate equality of τ_ϕ and τ_i for three-dimensional systems follows primarily from the fact that *large-energy-transfer* ($\sim k_B T$) scattering dominates both τ_ϕ and τ_i in bulks. For the e–ph contribution to inelastic scattering, processes with small energy transfer are suppressed by the e–ph vertex [50]. As a consequence, one expects that the e–ph dephasing time and inelastic e–ph scattering time should be almost identical: $1/\tau_{\phi,ep} \approx 1/\tau_{i,ep}$. Typically, one finds $1/\tau_{ep} \approx 1/\tau_\phi \propto T^p$ with the exponent of temperature $p \approx 2$–4, depending on the system specifics and dimensionality. Notably, in this case, it is also true that $\tau_\phi \approx \tau_i$ for e–e scattering. However, the three-dimensional e–e process is usually not seen in experiment. This is mainly because the crossover from the e–ph process to the e–e process in three dimensions should usually occur only at the experimentally unexplored sub-mK regime. (Besides, as $T \to 0$, τ_ϕ can often be dominated by the saturated time τ_ϕ^0, and thus an evaluation of the temperature-dependent contribution to τ_ϕ can be less certain.)

1.2. Objective of this review

Before discussing the organization of this review paper, it is worthwhile mentioning our motivations for writing an *experimental* review on recent developments on the dephasing time in mesoscopic systems. Twenty years have now passed since the first discovery of weak-localization effects in disordered conductors and, while a number of careful studies have been performed in this area, a new generation of young investigators have also been attracted to this exciting field. For this reason, we feel that an updated experimental review might be helpful for introducing these researchers to the current status of this field. In addition, since the pioneering studies of quantum-interference effects, new experimental results have continued to be reported in the literature, providing very useful quantitative information on the temperature and disorder dependence of τ_ϕ. Systematic experimental studies, as a function of a wide range of sample parameters, can now be undertaken, due to the ability to perform highly controlled measurements on well-characterized samples. Consequently, over the course of the past decade, a central theme of research in this area has become the quantitative study of dephasing mechanisms, rather than the study of the quantum-interference effects themselves, which provided the main theme of interest in the early years of this field. Finally, we note that, while many excellent reviews already exist concerned with a discussion of quantum-interference effects [1–7], there has essentially thus far been no review that has focused on the properties of the electron dephasing times. We also believe it is worthwhile to discuss together both mesoscopic metals and semiconductors, because the forms of inherent, microscopic physics of the electron dephasing in these two kinds of material are very similar and closely related. With these various issues in mind, we have been stimulated to undertake this current review.

The organization of the rest of this review is as follows. In section 2, we discuss the use of magneto-transport studies to extract the various dephasing times. It is hoped that this section will be of use to those researchers who are interested in the problem of electron dephasing, but who are not very familiar with quantum-interference effects. In particular, we elaborate on several novel examples to illustrate that the extracted electron dephasing times can be *extremely* reliable. In section 3, we concentrate on the electron dephasing times in mesoscopic disordered metals, focusing especially on three-dimensional polycrystalline metals. In section 4, we focus on measurements of the electron dephasing time in semiconductor quantum wires and dots, in which electron transport is typically much *cleaner* than in metals. In section 5, we present our conclusions, and attempt to provide a consistent overview of the various studies performed in different metal and semiconductor mesoscopic structures.

2. Determining the dephasing time in mesoscopic systems

In this section we briefly review the different techniques that are used to determine the value of the dephasing time τ_ϕ in metal and semiconductor mesoscopic structures, such as quantum wires and dots. The main experimental technique here involves extracting estimates for the dephasing time from either the weak-localization lineshape, or the conductance fluctuations, observed in the magnetoresistance of these structures at liquid-helium temperatures and below.

Weak localization of conduction electrons in disordered metals was first theoretically predicted, and experimentally observed, in 1979, and has remained the subject of continued interest since this time. In addition to more conventional mesoscopic metals and semiconductors, weak localization has also been studied in novel materials such as quasicrystals [51], carbon nanotubes [52], and high-temperature superconductors [53]. The weak localization is due to coherent backscattering of two, time-reversed, partial-electron-wave amplitudes, which traverse a closed loop and return to the origin within a timescale of τ_ϕ. Physically, τ_ϕ is the average timescale over which the phase coherence of the conduction electron is maintained. It was soon realized that any time-reversal-invariance 'breakers', including e–ph, e–e, and magnetic spin-flip scattering, would suppress weak localization. In 1980, Hikami *et al* [46] considered how the weak-localization effects might be suppressed by an external magnetic field. In particular, they calculated the magnetoresistance for two dimensions. Their result was explicitly expressed in terms of the various electron dephasing times. Their work immediately prompted extensive experimental investigations of the low-field magnetoresistance of thin metal films and semiconductor inversion layers. Soon afterward, the magnetoresistance in one dimension [54, 55], and that in three dimensions [56, 57], were also calculated. Thus, in principle, the low-temperature value of τ_ϕ can be extracted from weak-localization measurements, which therefore represent a powerful diagnostic tool. This tool has now been applied to various materials systems, including normal metals, superconductors, and semiconductors. While studies in all dimensions are possible, most experimental measurements reported in the literature have been focused on two dimensions. This is mainly because one-dimensional samples are less readily experimentally available, while the weak-localization effects in three dimensions are much less pronounced than in lower dimensions, rendering it previously less appealing to study these effects using either one or three dimensions.

In this section, we first explain how τ_ϕ can be determined from magnetoresistance measurements. We then use a few examples to indicate the feasibility of this experimental method, demonstrating that such studies can lead to *very reliable* and *quantitative* estimates of τ_ϕ, over a *wide* range of temperature and disorder[7]. This degree of reliability is not always achievable using other experimental methods. For instance, we will demonstrate that the inelastic electron scattering time $\tau_{\rm i}$ measured in a given material system accurately mimics the relevant microscopic inelastic process as the sample is made larger and as it changes progressively from one, to two, and, finally, to three dimensions. More precisely, it is known that the temperature and disorder dependences of $\tau_{\rm i}$ in a given material system depend strongly on the sample dimensionality. In lower dimensions, the Nyquist e–e scattering dominates the dephasing process at low temperatures, while in three dimensions, e–ph scattering is the strongest source of dephasing. In addition, we will show that, in the case

[7] Strictly speaking, it should be noted that the magnetoresistance measurements actually yield very reliable and quantitative estimates of the dephasing length. The value of the dephasing time is then computed through equation (2), using the independently determined diffusion constant D. (The experimental method for evaluating D is discussed in section 3.) Although the estimate for D in metals and alloys with complex Fermi surfaces can be subject to an uncertainty of a factor of $\sim$2, the temperature and disorder dependence of τ_ϕ extracted in this manner is highly reliable.

of a superconducting sample, the weak-localization studies correctly determine the transient lifetime of the superconducting fluctuations at temperatures closely above the superconducting transition temperature, T_c. A few other examples will also be discussed, to demonstrate that weak-localization effects are now sufficiently understood and can be used as a powerful probe of the electron scattering times. Indeed, estimates for L_ϕ determined from weak-localization measurements have been compared with the results of studies of conductance fluctuations, and Aharonov–Bohm oscillations in single rings, and have been found to be in reasonable agreement with one another [58].

2.1. Low-field magnetoresistance

2.1.1. Weak localization in disordered metals and semiconductors. Over the past two decades, it has come to be understood that weak-localization effects result in noticeable 'anomalous' magnetoresistance in disordered conductors at low temperatures and at low magnetic fields [1,3–5,7,59,60]. An analysis of these magnetoresistance curves has been found in turn to provide quantitative information of the various electron dephasing mechanisms. In practice, even a *weak* magnetic field B can cause a noticeable phase difference between the two complementary partial-wave amplitudes involved in coherent backscattering, since these time-reversed paths can be thousands of ångströms long ($L_\phi \gg l$) at liquid-helium temperatures. Here, a weak magnetic field means one for which the classical magnetoresistance due to the Lorentz force is negligibly small[8]. On the other hand, it is understood that one is dealing with external magnetic fields $B > B_\phi = \hbar/4\pi D\tau_\phi$ such that the weak-localization effects are suppressed. Since the quantum-interference effects in reduced dimensions have been extensively reviewed in the literature, we will focus mainly on mesoscopic three-dimensional systems to illustrate the physics and experimental method of the weak-localization studies.

In a mesoscopic three-dimensional conductor, the weak-localization magnetoresistance at a given temperature T, $\Delta R(B) = R(B) - R(0)$, was calculated by Fukuyama and Hoshino [57]. In their calculations, in addition to the inelastic electron scattering, spin–orbit scattering and Zeeman splitting of spin subbands have also been taken into consideration. For superconducting materials at temperatures above the superconducting transition temperature, T_c, $\Delta R(B)$ has also been calculated [62, 63]. In this latter case, effects resulting from fluctuational superconductivity also need to be considered. When concerned with a temperature region close to, but still sufficiently far from the immediate vicinity of T_c (i.e. $2\pi k_B(T - T_c) \gg \hbar/\tau_\phi$), one must consider Maki–Thompson superconducting fluctuation effects. (On the other hand, in the immediate vicinity of T_c, one must also include a contribution from the Aslamazov–Larkin term [64].) In particular, it should be noted that Larkin has shown that the superconducting fluctuation contribution to $\Delta R(B)$ corresponding to the Maki–Thompson diagram has the same magnetic field dependence as the weak-localization contribution in the absence of spin–orbit scattering, but with opposite sign and with a coefficient called $\beta_{\text{Larkin}}(T)$ which diverges at T_c [62, 65]. The parameter $\beta_{\text{Larkin}}(T)$ is called the Larkin e–e attraction strength. The work of Larkin therefore nicely connects seemingly unrelated areas of research, i.e. weak-localization and fluctuational superconductivity.

[8] The magnitude of the classical magnetoresistance caused by the Lorentz force [61], $\Delta R(B)/R(0) \approx (\omega_c\tau)^2$, where $\omega_c = eB/m$ is the cyclotron frequency, is negligibly small in typical disordered conductors. For $l \approx 10$–100 Å, this classical magnetoresistance is of the order of 10^{-8}–10^{-6} in a magnetic field of 1 T. This is typically 3 to 4 orders of magnitude smaller than the weak-localization magnetoresistance. Moreover, this classical magnetoresistance is always positive while the weak-localization magnetoresistance can be either positive or negative, depending on the relative strength of the inelastic and spin–orbit scattering processes. These features distinguish the 'anomalous' weak-localization magnetoresistance from the normal classical magnetoresistance.

The total three-dimensional magnetoresistivity at a given temperature, $\Delta\rho(B) = \rho(B) - \rho(0)$, including both the weak-localization effects and Maki–Thompson term is given by [57, 62, 65]

$$\frac{\Delta\rho(B)}{\rho^2(0)} = \frac{e^2}{2\pi^2\hbar}\sqrt{\frac{eB}{\hbar}}\left(\frac{1}{2\sqrt{1-\gamma}}\left[f_3\left(\frac{B}{B_-}\right) - f_3\left(\frac{B}{B_+}\right)\right] - f_3\left(\frac{B}{B_2}\right) + \beta_{\text{Larkin}}(T)\, f_3\left(\frac{B}{B_\phi}\right) - \sqrt{\frac{4B_{\text{so}}}{3B}}\left[\frac{1}{\sqrt{1-\gamma}}(\sqrt{t_+} - \sqrt{t_-}) + \sqrt{t} - \sqrt{t+1}\right]\right), \tag{3}$$

where

$$t = \frac{3B_\phi}{2(2B_{\text{so}} - B_0)}, \qquad \gamma = \left[\frac{3g^*\mu_B B}{4eD(2B_{\text{so}} - B_0)}\right]^2, \qquad t_\pm = t + \tfrac{1}{2}(1 \pm \sqrt{1-\gamma}),$$

$$B_\phi = B_{\text{i}} + B_0, \qquad B_2 = B_{\text{i}} + \tfrac{1}{3}B_0 + \tfrac{4}{3}B_{\text{so}}, \qquad B_\pm = B_\phi + \tfrac{1}{3}(2B_{\text{so}} - B_0)(1 \pm \sqrt{1-\gamma}).$$

Here g^* is the electron Landé g-factor, and μ_B is the Bohr magneton. The characteristic fields B_j are defined by $B_j = \hbar/4eD\tau_j$, where j = i, so, and 0 refer to the inelastic, spin–orbit, and temperature-independent residual scattering times (fields). The exact expression for the function f_3 in equation (3) is an infinite series which was originally calculated by Kawabata [56]. In analysing the experimental results one can instead reliably use an approximate expression for f_3 given by Baxter *et al* [66], which was shown to be accurate to be better than 0.1% for all arguments y. The approximate expression derived by Baxter *et al* is [66]

$$f_3(y) \approx 2\left[\sqrt{2+\frac{1}{y}} - \sqrt{\frac{1}{y}}\right] - \left[\left(\frac{1}{2}+\frac{1}{y}\right)^{-1/2} + \left(\frac{3}{2}+\frac{1}{y}\right)^{-1/2}\right] + \frac{1}{48}\left(2.03 + \frac{1}{y}\right)^{-3/2}.$$

The term $\beta_{\text{Larkin}}(T) f_3(B/B_\phi)$ in equation (3) is the Maki–Thompson superconducting fluctuation contribution. This term is calculated in the weak-field limit $4eDB < 2\pi k_B(T - T_c)$. For larger magnetic fields, this term becomes a constant [63]. The value of the coefficient β_{Larkin} depends on temperature, but is not affected by spin–orbit scattering since this term is concerned with the singlet part of the e–e interaction in the Cooper channel [62, 65]. This contribution is suppressed in exactly the same manner as the weak-localization effects are in the presence of spin–spin scattering. Because β_{Larkin} has a logarithmic temperature dependence, this contribution can be significant even at temperatures well above T_c. Since fluctuational superconductivity is progressively suppressed by an increasing magnetic field, the Maki–Thompson contribution to $\Delta\rho(B)$ is always positive, in contrast to the contribution from the weak-localization effects (equation (3) except the $\beta_{\text{Larkin}} f_3(B/B_\phi)$ term), which can be either positive or negative, depending on the ratio $\tau_{\text{so}}/\tau_{\text{i}}$ and the strength of B. In the limit $\tau_{\text{so}}/\tau_{\text{i}} \gg 1$, the magnetoresistivity is negative. In the opposite limit, $\tau_{\text{so}}/\tau_{\text{i}} \ll 1$, the magnetoresistivity is positive for all magnetic fields. The latter effect is called weak *anti-localization*.

Measurements of $\beta_{\text{Larkin}}(T/T_c)$ have been reported for both polycrystalline and amorphous metals, including two-dimensional [67, 68] and three-dimensional [31, 69] samples. It is now well established that the Larkin theory can predict a very accurate value of $\beta_{\text{Larkin}}(T/T_c)$, once the magnitude of the superconducting transition temperature T_c for a given sample is determined (from an independent measurement).

As mentioned, equation (3) reveals that the sign and magnitude of the magnetoresistivity is totally determined by two parameters: τ_ϕ (i.e. B_ϕ) and τ_{so} (i.e. B_{so}), of which only τ_ϕ is temperature dependent. We notice that the definition $B_\phi = B_{\text{i}} + B_0$ leads directly to the expression $1/\tau_\phi(T) = 1/\tau_{\text{i}}(T) + 1/\tau_\phi^0$ defined in equation (1). Generally speaking, the size of the magnetoresistivity increases with decreasing temperature as τ_ϕ becomes correspondingly

longer. In the limit of very low temperatures, $1/\tau_{\rm i}$ can become extremely small and may then allow $1/\tau_\phi^0$ (if finite) to dominate. Under such circumstances, the magnetoresistivity curves might overlap closely and the weak-localization contribution saturates (see discussion in section 3 below).

2.1.2. One-dimensional weak localization in metal and semiconductor quantum wires. As was discussed in the preceding sections, weak localization is a quantum-mechanical enhancement of the resistance that arises due to the effect of coherent backscattering. While we have thus far focused our discussion of this effect on its observation in bulk metals, and thin metallic films, weak localization is also widely observed in metallic and semiconductor quantum wires. An important feature in these systems is that the conductance corrections provided by this effect exhibit a *one*-dimensional character when the dephasing length of the electrons exceeds the width of the wire ($L_\phi > W$). Similarly to in the discussion of weak localization in higher dimensions, however, application of a weak magnetic field breaks time-reversal symmetry and suppresses the weak localization, giving rise to a negative magnetoresistance. For a *diffusive* channel of length L and width W, and in the case where the effects of spin–orbit scattering can safely be neglected, the magnetoconductance lineshape associated with this suppression is predicted to take the form [54, 70]

$$\Delta G(B) = -\frac{2}{L}\frac{e^2}{h}\left[\frac{1}{D\tau_\phi} + \frac{1}{D\tau_B}\right]^{-1/2}. \tag{4}$$

In this equation, $\Delta G(B)$ is the change in conductance induced by applying a magnetic field B, D is the diffusion constant, and the timescale τ_B is defined such that

$$\tau_B = \frac{3}{4}\frac{l_m^4}{W^2 D}, \qquad l_m = \sqrt{\frac{\hbar}{eB}}. \tag{5}$$

By fitting the form of the low-field magnetoresistance to equation (4), values for the dephasing time can therefore be extracted. In figure 1, we show the results of magnetoresistance measurements of a GaAs/AlGaAs quantum wire [71]. The growth of the magnitude of the negative magnetoresistance with decreasing temperature reflects the associated increase in the dephasing time, and the solid curves through the experimental data represent the results of fits to the form of equation (4). It is clear that these fits account well for the magnetoresistance variations observed in experiment, thereby allowing one to extract reliable estimates for the dephasing time.

While weak-localization studies can be used to extract estimates for the dephasing time in quantum wires, considerable care needs to be taken when applying the predictions of theory to the results of experiment. An important feature in the weak-localization theory is the assumption of *diffusive* electron motion, which is easily violated in semiconductor quantum wires [72]. The high electron mobilities characteristic of these systems can result in values for the electron mean free path l that easily exceed several microns [73]. Charge diffusion in quantum wires realized from such materials may therefore be *quasi-ballistic* in nature, with diffusive motion along the length of the wire but ballistic carrier transport in the transverse direction. An important effect that may arise in such structures is *flux cancellation* of ballistic trajectories that backscatter via a series of *diffuse* boundary scattering events. The basic idea is that such trajectories enclose zero effective flux, so an *enhanced* magnetic field is required to suppress weak localization. Beenakker and van Houten have discussed this effect in considerable detail [70, 72, 74] and show that, in the presence of this flux cancellation,

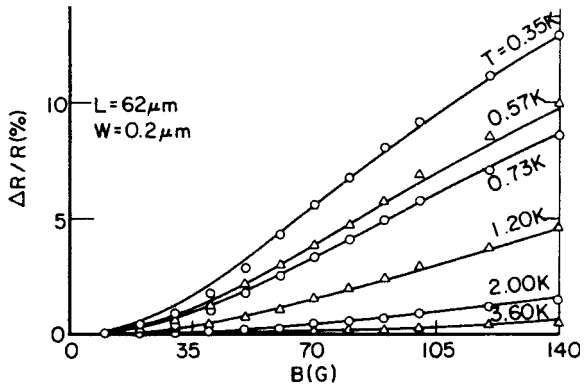

Figure 1. The temperature dependence of the magnitude of the negative magnetoresistance $\Delta R/R(0) = [R(B) - R(0)]/R(0)$ due to one-dimensional weak localization in a GaAs/AlGaAs quantum wire of length 62 μm and width 0.2 μm. This figure was reproduced with permission from [71]. Copyright 1987 by the American Physical Society.

equation (5) becomes modified according to

$$\tau_B = \begin{cases} C_1 \dfrac{l_m^4}{W^3 v_F}, & l_m^2 \gg WL \\ C_2 \dfrac{l_m^2 l}{W^2 v_F}, & Wl \gg l_m^2 \gg W^2. \end{cases} \tag{6}$$

In these equations, v_F is the Fermi velocity, and C_1 and C_2 are constants whose values depend on the nature of the boundary scattering in the wire ($C_1 = 9.5$ and $C_2 = 24/5$, while $C_1 = 4\pi$ and $C_2 = 3$, for specular, and diffusive, scattering, respectively). With these definitions, the weak-localization magnetoconductance takes the form

$$\Delta G(B) = -\frac{2}{L}\frac{e^2}{h}\left[\left(\frac{1}{D\tau_\phi} + \frac{1}{D\tau_B}\right)^{-1/2} - \left(\frac{1}{D\tau_\phi} + \frac{1}{D\tau_B} + \frac{1}{D\tau}\right)^{-1/2}\right]. \tag{7}$$

The main result of the flux-cancellation effect is to *enhance* the critical magnetic field required to suppress weak localization. For a *diffusive* channel with no flux cancellation, this field scale may be defined as [70]

$$B_{crit} = \frac{\hbar\sqrt{3}}{eWL_\phi}. \tag{8}$$

For a quasi-ballistic channel, however, this magnetic field scale is modified according to

$$B_{crit} = \begin{cases} \dfrac{\hbar}{eW}\left[\dfrac{C_1}{Wv_F\tau_\phi}\right]^{1/2}, & l_m^2 \gg Wl \\ \dfrac{\hbar}{eW}\dfrac{C_2 l}{W^2 v_F \tau_\phi}, & Wl \gg l_m^2 \gg W^2. \end{cases} \tag{9}$$

From a comparison of equations (8) and (9), we see that the enhancement of the critical field B_{crit} is of order $(l/W)^2 \gg 1$ in quasi-ballistic channels. Good agreement of experiment with these modified predictions has been found in a number of studies of quasi-ballistic, high-mobility, wires [75–77].

In addition to the effect of flux cancellation, it is also necessary to consider further modifications to the weak-localization magnetoresistance in *mesoscopic* quantum wires, whose

length may be comparable to the phase-breaking length. The weak-localization lineshape in such structures has been found to be strongly influenced by the geometric properties of their connecting probes, which result can be understood by considering that phase coherence of electrons decays over a length scale comparable to L_ϕ inside these regions [78]. By extending the usual theory for weak localization, quantitative predictions for the influence of specific probe geometries on the magnitude of the weak-localization magnetoresistance can be obtained [78].

2.2. The study of magneto-transport as a powerful probe of the dephasing time

In the above sections, we have discussed the underlying physics and theoretical predictions of weak-localization theory. Particularly, the weak-localization predictions for one dimension and three dimensions have been explicitly presented. The theoretical predictions for the magnetoresistance in two dimensions are well documented in the literature [3,4,7] and will not be presented here. We only notice that, in reduced dimensions, the relative orientation of the magnetic field to the film plane or wire axis is very important, because the magnetoresistances are highly anisotropic, due to the quantum-interference nature of the weak-localization effects. Owing to the accessibility of *quantitative* theoretical predictions such as equations (3) and (7), extensive measurements have been performed on various materials involving different dimensionalities. In short, the weak-localization predictions are found to describe very well the rich experimental observations. Moreover, over the years, weak-localization research has become a mature field and has proven to be the most powerful probe of τ_ϕ in mesoscopic metals and semiconductors[9]. As a matter of fact, the weak-localization effects are so well understood that these effects can now be 'tuned' in laboratories. For instance, the relative importance of different electron dephasing times can be adjusted by using tailor-made samples. Therefore, the *sign* and *magnitude* of the magnetoresistance in a given sample system can be manipulated in a controlled manner. To illustrate this point, we examine the systematic change in the magnetoresistance behaviour of a series of three-dimensional, tin-doped, $Ti_{73}Al_{27}$ alloys in figures 2 and 3. Figure 2 shows a plot of the normalized magnetoresistivities $\Delta\rho(B)/\rho^2(0)$ as a function of magnetic field B for a polycrystalline $Ti_{70}Al_{27}Sn_3$ alloy at several measurement temperatures. At low magnetic fields, the magnetoresistivities are positive at all measurement temperatures. At higher magnetic fields, the magnetoresistivities decrease with increasing B and become negative (not shown) if the applied magnetic field and/or measurement temperature is sufficiently high. The magnitude of $\Delta\rho(B)/\rho(0)$ is of the order of several parts in 10^{-4}. This figure clearly indicates that equation (3) can account well for the experimental results. Inspection of figure 2 reveals that the magnetoresistivities are larger at lower measurement temperatures, because τ_ϕ increases with decreasing T. (We notice that, in many cases, the magnetoresistivity might cease to grow with decreasing temperature as $T \to 0$; see section 3.)

Next, to further demonstrate the reliability of the weak-localization predictions, we plot in figure 3(a) the normalized magnetoresistivities at a given temperature of 3.0 K for a series of three-dimensional, tin-doped $Ti_{73-x}Al_{27}Sn_x$ alloys whose concentration of tin x varies progressively from 0 to 5. For this range of x, the alloys remain single phased and the residual resistivities of the samples are essentially the same, i.e., these alloys contain a similar level of disorder [82]. The parent $Ti_{73}Al_{27}$ phase is chosen because Ti possesses a moderately

[9] Extensions of the weak-localization theoretical predictions have also been carried out to deal with, for example, the negative magnetoresistance in the variable-range-hopping regime [79], the magnetoresistance in granular metals [80], and in ballistic quantum dots [20]. Such extensions make possible experimental extraction of τ_ϕ in cases beyond the weakly disordered regime. (Later on, however, we will notice and discuss why weak localization in ballistic dots may *not* be reliable.)

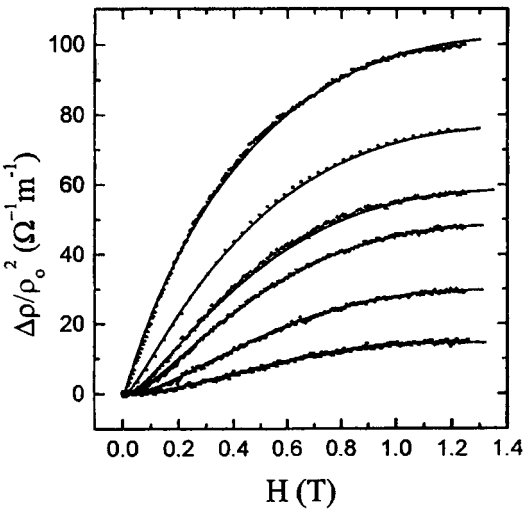

Figure 2. Normalized magnetoresistivities $\Delta\rho/\rho^2(0) = [\rho(B) - \rho(0)]/\rho^2(0)$ as a function of magnetic field for the three-dimensional $Ti_{70}Al_{27}Sn_3$ alloy at (from the top down) 2.00, 5.00, 8.00, 10.0, 15.0, and 20.0 K. The solid curves are the predictions of equation (3). This figure was reproduced with permission from [82]. Copyright 1999 by the American Physical Society.

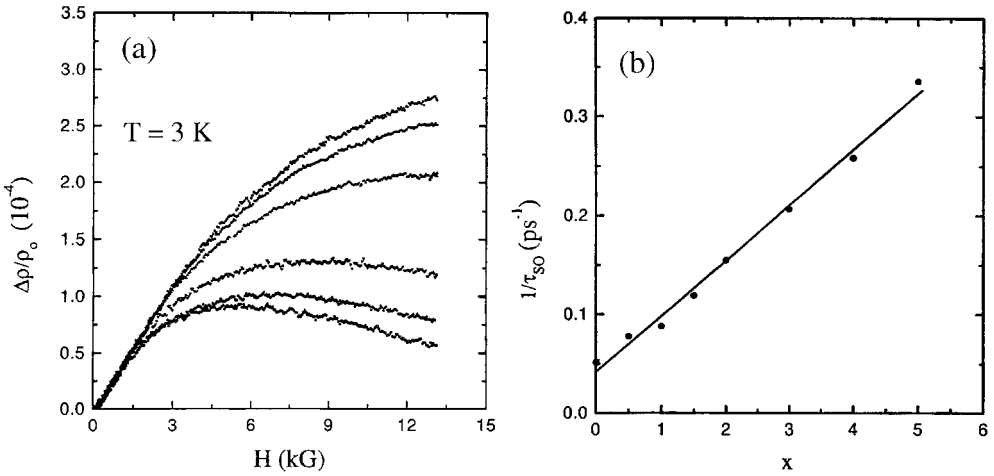

Figure 3. (*a*) Normalized magnetoresistivities $\Delta\rho/\rho^2(0) = [\rho(B) - \rho(0)]/\rho^2(0)$ as a function of magnetic field for three-dimensional $Ti_{73-x}Al_{27}Sn_x$ alloys at 3.0 K and with (from the bottom up) $x \approx 0.5$, 1.0, 1.5, 3.0, 4.0, and 5.0 [81]. (*b*) Spin–orbit scattering rate $1/\tau_{so}$ as a function of x for $Ti_{73-x}Al_{27}Sn_x$ alloys. The straight line is a guide to the eye. This figure was reproduced with permission from [82]. Copyright 1999 by the American Physical Society.

small atomic number $Z = 22$, while Al has an even smaller $Z = 13$. Therefore, the spin–orbit scattering is expected to be moderately weak in this alloy, leaving plenty of room for increasing the spin–orbit scattering rate $1/\tau_{so}$ by 'controlled' doping of heavy atoms. (That the spin–orbit scattering is moderately weak in the parent $Ti_{73}Al_{27}$ phase is evident in the shape of the magnetoresistivity curves shown in figure 2.) This is one of the reasons that Sn is used as the impurity atom, for Sn has an atomic number $Z = 50$. Notice that this $Z = 50$

is sufficiently heavier than that of Ti while it is still not so large as that of, for example, Au ($Z = 79$) or Bi ($Z = 83$). Since it is known that $1/\tau_{so}$ increases rapidly with increasing atomic number as $1/\tau_{so} \propto Z^4$ [83] or Z^5 [47], a small amount of Sn doping will thus, on one hand, significantly increase $1/\tau_{so}$ but, on the other hand, leave other electronic properties of the alloy not appreciably affected. This experiment thus allows a systematic investigation of the effect of spin–orbit scattering from the moderate to the strong limit where $1/\tau_{so} \gg 1/\tau_\phi$.

At any temperature, and for any given alloy composition, values of τ_ϕ and τ_{so} are extracted by fitting the magnetoresistance to the form of equation (3). Because τ_{so} is a temperature-independent material property, τ_ϕ is then the only adjustable parameter in the comparison of the theoretical predictions with the experimental curves measured at different temperatures. In reality, a single value of τ_{so} is used to describe the whole set of magnetoresistivity curves for a given sample, resulting in a fairly reliable estimate of τ_{so}. Thus, the temperature dependence of the magnetoresistivity is totally controlled by the *sole* varying parameter τ_ϕ. If a good number of magnetoresistivity curves are measured at different temperatures, the variation of τ_ϕ with temperature can thus be accurately determined. This, in turn, results in a reliable determination of the exponent of temperature p for the responsible inelastic electron scattering process in question. (It is generally accepted that $1/\tau_i \propto T^p$ over the limited temperature range accessible in a typical experiment.) An accurate determination of the value of p is not only indispensable for identifying the responsible inelastic process but also crucial for a good understanding of the microscopic interactions between the electrons and low-lying excitations.

Figure 3(*b*) shows the extracted spin–orbit scattering rate $1/\tau_{so}$ as a function of the concentration of tin x for the series of $Ti_{73-x}Al_{27}Sn_x$ alloys whose magnetoresistivities are considered in figures 2 and 3(*a*). This figure clearly indicates that the spin–orbit scattering rate increases linearly with x. A linear variation of $1/\tau_{so}$ with the concentration of heavy impurities, at low impurity concentrations, has been established in previous measurements where the level of disorder in the samples was kept fixed [84, 85]. Such linearity provides a convincing consistency check for the established experimental method of sample fabrication and data analysis. It also provides a critical test of the theoretical predictions of equation (3).

Apart from the three-dimensional examples discussed in figures 2 and 3, the reliability and flexibility of the weak-localization studies in extracting values of τ_ϕ can further be illustrated with several other examples, as we now discuss below.

2.2.1. Inelastic scattering times in different dimensions. At liquid-helium temperatures and somewhat higher, inelastic processes (e–ph scattering and e–e scattering) are the most important and dominating sources for the dephasing of conduction electron wave amplitudes. Existing efforts of weak-localization studies in the literature have provided very informative and consistent results in this regard. To illustrate the great success of such studies in extracting τ_i, we discuss in this subsection the measured inelastic electron scattering times in Au–Pd alloys with different dimensionalities. Gold–palladium alloys are well-known prototypical disordered metals, and have been widely used in weak-localization studies over the years [11, 36, 86–91]. As a matter of fact, the first experimental realizations of weak-localization effects in one and two dimensions were performed using small-diameter wires [92] and thin films [93] made of Au–Pd. Three-dimensional weak-localization effects in Au–Pd alloys have also been investigated recently [94]. In studies of this type (one, two, and three dimensions), low-field magnetoresistances are measured at different temperatures and $\tau_\phi(T)$ is extracted. One of the advantages of choosing Au–Pd as the material system is that this metal possesses very strong spin–orbit scattering, and thus, according to the weak-localization predictions, τ_ϕ is the *only* varying parameter in the comparison of theory with experiment, making the extraction of τ_ϕ extremely reliable. (Close inspection of equation (3) reveals that, in the limit of strong

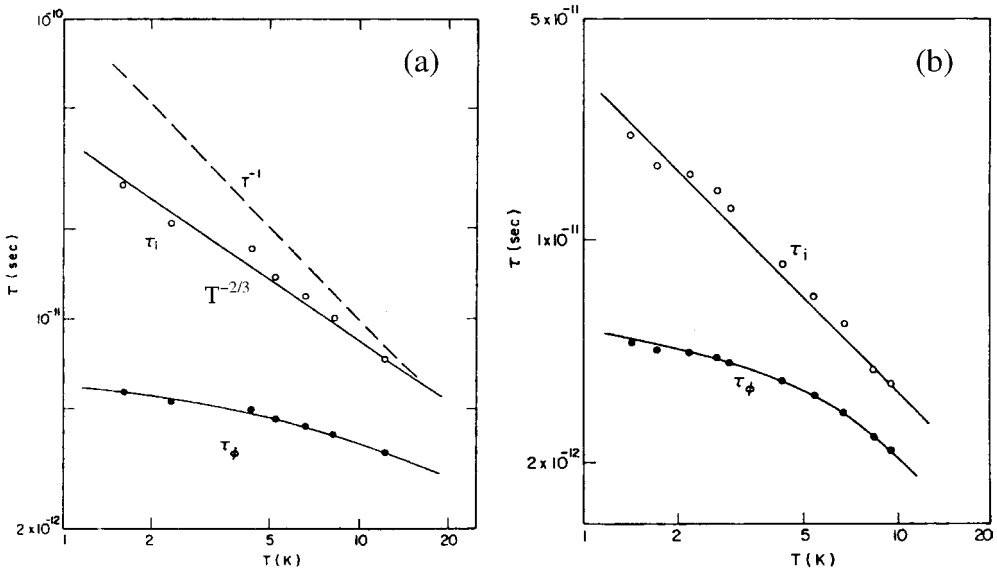

Figure 4. (*a*) The total dephasing time τ_ϕ (closed circles) and the inelastic dephasing time τ_i (open circles) as a function of temperature for a 460 Å diameter Au–Pd wire. The solid line drawn through the data for τ_i shows a $T^{-2/3}$ temperature dependence, while the dashed line is drawn proportional to T^{-1}. The solid line through the data for τ_ϕ is a guide to the eye. (*b*) The total dephasing time τ_ϕ (closed circles) and the inelastic dephasing time τ_i (open circles) as a function of temperature for a 130 Å thick Au–Pd film. The solid curve drawn through the data for τ_i shows a T^{-1} temperature dependence, while the solid curve through the data for τ_ϕ is a guide to the eye. These figures were reproduced with permission from [88]. Copyright 1987 by the American Physical Society.

spin–orbit scattering, the predicted magnetoresistances are insensitive to the value of τ_{so}; see, for example, [1, 3, 4, 7].)

Figures 4(*a*), (*b*), and 5(*a*) show three plots of the variations of τ_ϕ with temperature for Au–Pd small-diameter wires, thin films, and thick films. Inspection of figures 4(*a*), (*b*), and 5(*a*) indicates that, in all three cases, τ_ϕ first increases with decreasing temperature, until the temperature dependence becomes extremely weak at very low temperatures. The increase of τ_ϕ with reducing T at temperatures above a (few) kelvins depends markedly on sample quality, and is associated with the weakening of inelastic processes as the temperature decreases. By comparing the measured $\tau_\phi(T)$ with equation (1), the zero-temperature $1/\tau_\phi^0$ and the temperature-dependent $1/\tau_i$ can be deduced. Then, on the basis of the information obtained about the temperature and disorder dependences of $1/\tau_i$, one can unambiguously identify the relevant inelastic electron processes in question. The values of τ_i extracted in this way for a Au–Pd wire and a Au–Pd film are plotted in figures 4(*a*) and (*b*), respectively. One clearly sees that τ_i possesses different temperature behaviours in different dimensions, namely, $T^{-2/3}$ in one-dimensional wires (figure 4(*a*)) while $\tau_i \propto T^{-1}$ in two-dimensional films (figure 4(*b*)).

In the case of bulk samples (figure 5(*a*)), the measured $\tau_\phi(T)$ is also fitted to equation (1) assuming a single, significant inelastic process, i.e.,

$$\frac{1}{\tau_\phi(T,l)} = \frac{1}{\tau_\phi^0} + A_i(l)T^p, \tag{10}$$

where $A_i(l)$ characterizes the strength of the dominating inelastic electron–low-lying-excitation interaction process, and p is the exponent of temperature for that inelastic scattering

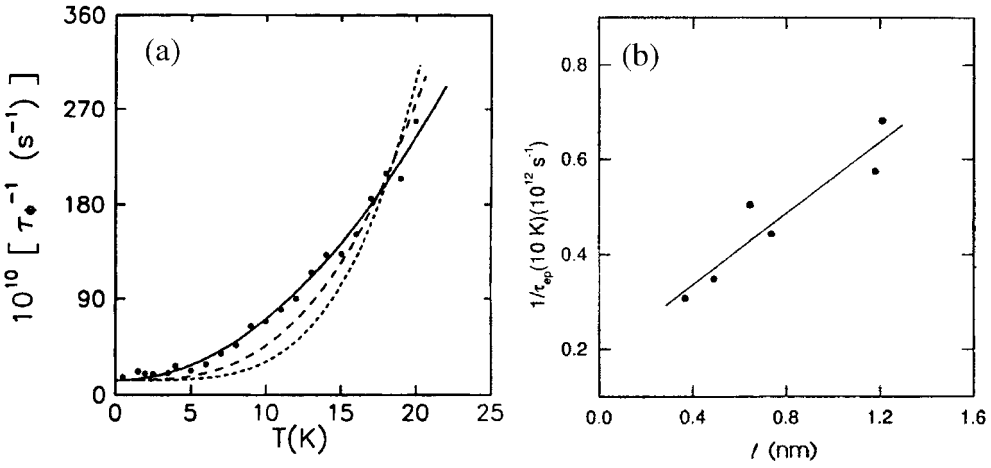

Figure 5. (*a*) The total dephasing rate $1/\tau_\phi$ as a function of temperature for a 5120 Å thick Au–Pd film. The solid, long-dashed, and short-dashed curves are least-squares fits to equation (10) with the temperature exponent p fixed at 2, 3, and 4, respectively. A_i is the fitting parameter, and $1/\tau_\phi^0 = 1.3 \times 10^{11}\ s^{-1}$. (*b*) Variation of the e–ph scattering rate at 10 K, $1/\tau_{ep}(10\ K)$, with electron mean free path l for several three-dimensional $Au_{50}Pd_{50}$ thick films. This figure was reproduced with permission from [94]. Copyright 1998 by the American Physical Society.

rate. Figure 5(*a*) indicates that the measured τ_ϕ in thick Au–Pd can only be described by an exponent $p = 2$. On the other hand, the experimental data on τ_ϕ cannot be described by equation (10) using either $p = 3$ or 4. This observation of an inelastic scattering rate having an exponent of temperature $p = 2$ suggests that, in three dimensions, the relevant inelastic process is due to e–ph scattering. (In lower-dimensional metals, however, it is often necessary to include both e–e scattering and e–ph scattering processes.)

Taken together, the results of figures 4(*a*), (*b*), and 5(*a*) indicate a *systematic change* of p with increasing *sample dimensionality*. This observation is totally expected and understood. It is now known that the exponent of temperature p should be equal to $2/3$ and 1 in one and two dimensions, respectively. Such values of p can be well accounted for by small-energy-transfer e–e scattering which dominates inelastic scattering in reduced dimensions [3, 4, 7]. On the other hand, p should be equal to (or $\gtrsim$) 2 in three dimensions [95,96], because e–ph scattering is the dominating inelastic process in bulk materials [22, 24]. This observation of a clear crossover of the inelastic scattering from the Nyquist e–e interaction to e–ph interaction as the system dimensionality increases demonstrates convincingly the reliability and consistency of the weak-localization studies in inferring τ_ϕ and, thus, τ_i and τ_ϕ^0. It is worthwhile mentioning that the inelastic lifetimes of conduction electrons have also been determined from other experimental methods [97]. The results are in line with those deduced from weak-localization measurements.

2.2.2. Electron–superconducting-fluctuation scattering time. In the case of superconducting samples, superconducting fluctuation effects can contribute to the low-field magnetoresistance, especially when the measurement temperatures approach the superconducting transition temperature T_c of the sample. Then, a marked 'divergence' of $1/\tau_i$ is observed. Physically, what one measures is the transient lifetime of the superconducting fluctuations which are continuously created and annihilated at temperatures just above T_c.

To illustrate the effect of superconducting fluctuations on the magnetoresistivities and the value of τ_i, we compare two dilute superconducting titanium alloys studied in [31]:

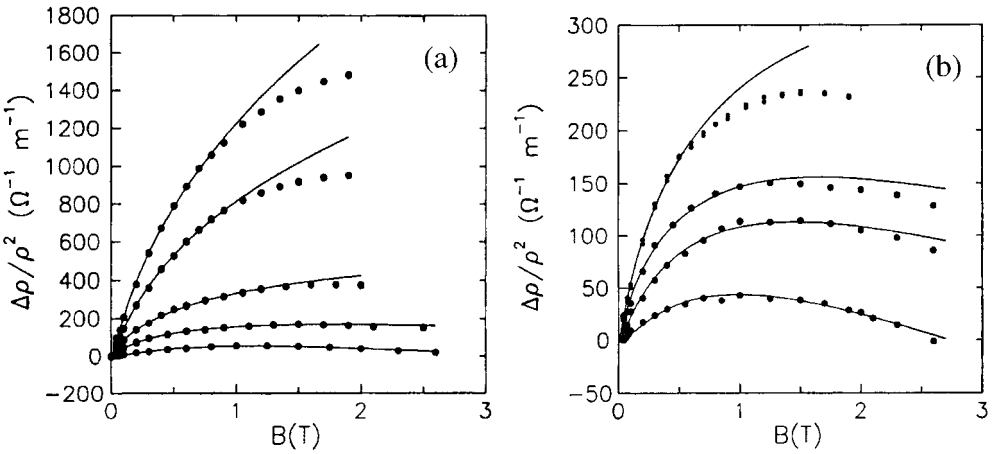

Figure 6. (*a*) Normalized magnetoresistivities $\Delta\rho/\rho^2(0) = [\rho(B) - \rho(0)]/\rho^2(0)$ as a function of magnetic field for three-dimensional disordered superconducting alloys: (*a*) the $Ti_{92.8}Al_{7.15}Co_{0.05}$ alloy at (from the bottom up) 8.00, 3.02, 2.06, 1.85, and 1.70 K; and (*b*) the $Ti_{92.8}Al_{7.2}$ alloy at (from the bottom up) 10.0, 6.00, 3.00, and 1.73 K. The solid curves are the weak-localization predictions of equation (3). This figure was reproduced with permission from [31]. Copyright 1994 by the American Physical Society.

$Ti_{92.8}Al_{7.2}$ and $Ti_{92.8}Al_{7.15}Co_{0.05}$. These two alloys contain similar levels of disorder, with residual resistivities $\rho(10\ \mathrm{K}) \approx 91$ and 94 $\mu\Omega$ cm for the former and the latter, respectively. Previously, it has been found [31, 98] that the addition of a small amount of Co in Ti results in a remarkable increase in T_c from that of pure Ti ($\approx$0.4 K). Therefore, fluctuational superconductivity is markedly enhanced in the Co-doped sample at low temperatures, compared with that in the undoped 'control' sample $Ti_{92.8}Al_{7.2}$. Experimentally, this enhancement is directly manifested in the relatively large low-field magnetoresistivities. Figure 6(*a*) shows the normalized magnetoresistivities $\Delta\rho(B)/\rho^2(0)$ as a function of magnetic field for $Ti_{92.8}Al_{7.15}Co_{0.05}$ at several temperatures. This figure indicates that the magnitudes of $\Delta\rho(B)/\rho^2(0)$ are substantially increased from those in $Ti_{92.8}Al_{7.2}$ (figure 6(*b*)). For example, $\Delta\rho(B)/\rho^2(0)$ at 1.7 K in $Ti_{92.8}Al_{7.15}Co_{0.05}$ is a factor of more than six times larger than the corresponding magnetoresistivity in the parent $Ti_{92.8}Al_{7.2}$. This increase is due to the enhanced superconductivity in this Co-doped alloy. Physically, the magnetoresistivity behaviour with B in figure 6(*a*) is characteristic of the weak-localization and Maki–Thompson superconducting fluctuation effects predicted by equation (3).

Quantitative analysis indicates that, with the addition of a minor amount of Co, both the low-temperature values of the Larkin e–e attraction strength β_{Larkin}, defined in equation (3), and $1/\tau_{\mathrm{i}}$ increase profoundly relative to the corresponding values for $Ti_{92.8}Al_{7.2}$. (On the other hand, the value of τ_{so} remains *unchanged* to within the experimental uncertainties. This is because Co is only slightly heavier than Ti, and since the doping level of Co is extremely low.) In the range of approximately 1.7–4 K, the value of β_{Larkin} in $Ti_{92.8}Al_{7.2}$ shows only a slight increase, while the value in $Ti_{92.8}Al_{7.15}Co_{0.05}$ shows a rapid increase [31]. This rapid increase in β_{Larkin} in the Co-doped sample results in large magnetoresistivities as seen in figure 6(*a*). The value of $\beta_{\mathrm{Larkin}} \approx 5.3$ at 1.7 K for $Ti_{92.8}Al_{7.15}Co_{0.05}$ is a factor $\sim$6.5 higher than that ($\approx$0.8) for $Ti_{92.8}Al_{7.2}$. In short, this experiment, using both the control alloy $Ti_{92.8}Al_{7.2}$ (where the Maki–Thompson contribution is relatively unimportant) and the comparison alloy $Ti_{92.8}Al_{7.15}Co_{0.05}$ (where the Maki–Thompson contribution is significant), demonstrates elegantly the reliability and flexibility of the weak-localization studies.

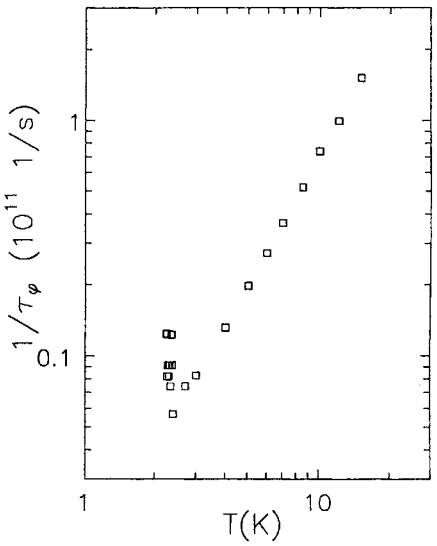

Figure 7. The electron dephasing rate $1/\tau_\phi$ as a function of temperature for a disordered superconducting $Ti_{88}Sn_{12}$ bulk alloy. The superconducting transition temperature T_c for this particular sample is about 2.1 K. This figure was reproduced with permission from [99].

Figure 7 shows the variation of $1/\tau_\phi$ with temperature for a disordered superconducting $Ti_{88}Sn_{12}$ bulk alloy [99]. (In this case, $1/\tau_\phi \approx 1/\tau_i$ in the temperature range of interest.) This figure indicates that $1/\tau_\phi$ (i.e. $1/\tau_i$) possesses a quadratic temperature dependence at temperatures above about 2.5 K, implying the inelastic scattering is due to e–ph relaxation. This figure also shows that $1/\tau_\phi$ (or $1/\tau_i$) exhibits a rapid deviation from the T^2 temperature dependence at temperatures below about 2.3 K; the value of $1/\tau_\phi$ (or $1/\tau_i$) increases abruptly from that as would be extrapolated from the T^2 dependence at higher temperatures. The existence of this 'diverging' behaviour of $1/\tau_\phi$ (or $1/\tau_i$) as the measurement temperature approaches T_c ($\approx$2.1–2.2 K for this particular sample) is understood. Such a pronounced increase in $1/\tau_i$ with decreasing temperature is caused by the increased effectiveness of the e–e interaction in the Cooper channel near T_c. Physically, as the temperature approaches T_c, the inelastic scattering rate $1/\tau_i$ will diverge because of the increasing probability that an electron will meet another electron of nearly opposite momentum and spin and condense into a superconducting fluctuation [3, 7]. A diverging $1/\tau_i$ at temperatures just above T_c has been observed in thin films [68, 100], and thick fibres [101]. Theoretically, the scattering of conduction electrons from superconducting fluctuations has been treated in two dimensions [102]. However, no theoretical prediction is available for three dimensions. A recent discussion on this subject is given by Rosenbaum *et al* [103].

2.2.3. Spin-flip scattering time. Thus far, we have considered mainly the spatial part of the wave amplitude of the conduction electrons, and have largely neglected their spin component. (We have briefly discussed the role of spin–orbit scattering on weak-localization effects in figures 3(*a*) and (*b*).) When the spin degree of freedom of the conduction electrons is taken into consideration, the quantum-interference effects are sensitive to both spin–orbit scattering and magnetic spin–spin scattering. In disordered conductors, spin–orbit scattering can originate from the scattering of conduction electrons off heavy impurity atoms and/or surfaces. On the other hand, spin–spin scattering can originate from scattering of conduction electrons off

magnetic impurity atoms and/or the local moments that might be induced on the surfaces due to oxidation. Systematic measurements of these two kinds of scattering time have advanced greatly over the years [2,47,104–108]. It is now established that both the spin–orbit scattering time τ_{so} and spin–spin scattering time τ_s can be accurately determined from weak-localization measurements. Furthermore, it is observed that the values of τ_{so} (and τ_s) determined from weak-localization studies are *consistent* with those values determined from recent spin-polarized transport measurements [109]. It is also found that the values of τ_{so} based on the weak-localization measurements on thin films [110] are in order-of-magnitude agreement with those extracted from measurements of the electron g-factor distributions in nanometre-scale particles [111]. This consistency of the spin-flip scattering times independently determined from these distinct experiments (i.e., weak-localization, spin-polarized transport, and g-factor distribution studies) is encouraging. It demonstrates the reliability of the weak-localization studies in extracting the values of the electron scattering times.

In quantum-interference studies, we are often involved with (very) dilute magnetic impurities. In the presence of very dilute magnetic impurities, but *without* the Kondo effect, magnetic impurities yield in the Born approximation a temperature-independent dephasing. In this case, the dephasing process does not involve energy exchange between the electron and the 'paramagnetic' environment. On the other hand, the problem of a *single* Kondo impurity is much more sophisticated. On account of the Kondo effect, i.e. the repeated interaction between the conduction electrons and the magnetic impurity, spin-flip processes are strongly enhanced and produce a maximum of dephasing rate at the Kondo temperature T_K [105,106]. Far below T_K, the Fermi-liquid theory of the Kondo effect predicts that the spin-flip scattering disappears and is replaced by an inelastic scattering time proportional to T^{-2}. At zero temperature, the magnetic moment is suppressed (the single Kondo impurity forms a singlet state with the conduction electrons) and neither yields spin-flip scattering, nor acts as a random field. Therefore, the dephasing scattering caused by magnetic impurities can be either scattering of the conduction electrons according to the exchange interaction, $J\boldsymbol{S}\cdot\boldsymbol{s}$, or, at low temperature ($\ll T_K$), an induced inelastic scattering due to the magnetic impurity.

Experiments designed to directly measure magnetic scattering rates have been performed by Bergmann and co-workers [105], and Van Haesendonck *et al* [106]. These elegant experiments provide new insights into the long-standing Kondo problem. Since the magnetic screening of the Kondo impurity extends over distances of the order of $\hbar v_F/k_B T_K$, interaction between the magnetic impurities is non-negligible in real experiments. Consequently, an inelastic scattering time proportional to $T^{-1/2}$, instead of T^{-2}, is measured [105, 112].

In low magnetic fields, the quantum-interference effects are greatly suppressed due to the presence of a finite magnetic spin–spin scattering $1/\tau_s$, as just mentioned. In high magnetic fields of order $g^*\mu_B B \approx k_B T$, there is a saturation of the magnetic moments of the paramagnetic impurities, resulting in a strong decrease in $1/\tau_s$, and thus the dephasing length together with the quantum-interference effects recover their value characteristic of the undoped system. In the case of spin glasses, there are similar effects. Studies in this direction are used as an original probe of the nature of the spin-glass order which is still very controversial [113]. By the same token, studies in this direction might shed light on clarifying the origin(s) of the widely observed saturation of τ_ϕ^0 in experiments (see section 3).

2.3. Universal conductance fluctuations in metals and semiconductors

2.3.1. Universal conductance fluctuations in metal and semiconductor quantum wires. In mesoscopic quantum wires, fabricated on a length scale comparable to the phase-breaking length, another opportunity for extracting estimates for the dephasing time is provided by

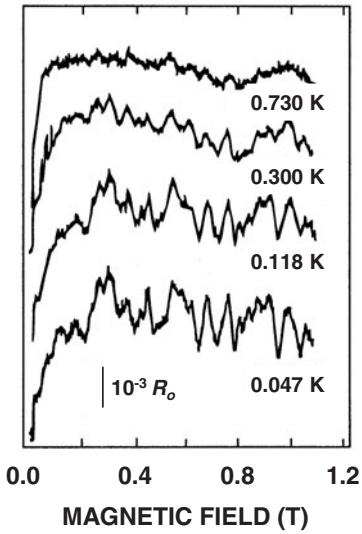

Figure 8. Universal conductance fluctuations in a Au ring at several different temperatures. This figure was reproduced with permission from [114]. Copyright 1987 by the American Physical Society.

the observation of *universal conductance fluctuations* [9, 114, 115]. The fluctuations appear as noise-like structure in the low-temperature magnetoresistance (figure 8), although their fingerprint is found to be highly reproducible as long as the wire is maintained at cryogenic temperatures. Reminiscent of weak localization, these fluctuations also result from a quantum-interference effect, although the nature of this interference is very different to that responsible for weak localization. In particular, the interference process responsible for the fluctuations is *not* restricted to pairs of backscattered trajectories (figure 9). Rather, the idea is that interference between electron partial waves that propagate between the same points via different semiclassical trajectories does *not* average out to zero in these mesoscopic systems. The total phase of these waves rather varies as the magnetic field is varied and it is this process that is reflected directly in the conductance. The detailed *magneto-fingerprint* of the fluctuations is sensitive to the position of *specific* impurities within the wire, in contrast to the case for macroscopic conductors whose conductance typically only depends on the *degree* of disorder in the sample. Fluctuations may alternatively arise by varying the Fermi energy of the carriers, by means of a change to a suitable gate voltage [116], or when the impurity profile in the sample varies with *time*, as can occur when certain defects are able to instantaneously trap or emit carriers [117].

At absolute zero, the amplitude of the conductance fluctuations is predicted to take the *universal* value of order e^2/h, independent of either the degree of disorder or the system size [118, 119]. At non-zero temperatures, however, the presence of decoherence reduces the fluctuation amplitude from its universal value, and this effect may be exploited to obtain an estimate for the dephasing time. For a diffusive quantum wire, the root-mean-square amplitude of the conductance fluctuations is predicted to vary as [115]

$$\delta g_{rms} = \begin{cases} \dfrac{L_T}{L}\sqrt{\dfrac{L_\phi}{L}}, & L_T \ll L_\phi \ll L, \\ \left(\dfrac{L_\phi}{L}\right)^{3/2}, & L_\phi \ll L_T \ll L. \end{cases} \tag{11}$$

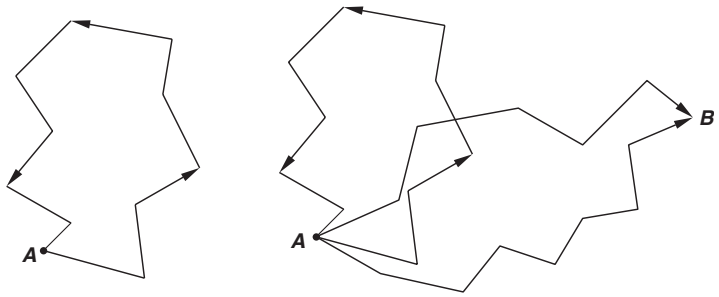

Figure 9. A schematic illustration illustrating the difference between the types of diffusing trajectory that give rise to weak localization (*left*) and universal conductance fluctuations (*right*). Weak localization results from the interference of time-reversed pairs of paths that start from some initial point (A) and diffuse back to this *same* point by undergoing a series of *elastic* scattering events. Universal conductance fluctuations, on the other hand, result from interference involving weak-localization-like trajectories, *as well as* interference between electron partial waves that propagate between *different* points of the sample (A and B), along distinct paths.

In these equations, the conductance fluctuation amplitude is measured in units of e^2/h, and $L_T = \sqrt{D\hbar/k_BT}$ is the thermal diffusion length. This latter quantity essentially defines the length scale over which electron partial waves decohere due to thermal smearing of their energy. According to these relations, thermal smearing and inelastic scattering influence the amplitude of the fluctuations in quite distinct fashions. In particular, when the phase-breaking length is the shorter scale, the effects of thermal smearing are completely cut-off by inelastic scattering. The quantum wire can then be broken into a series of uncorrelated segments, each of length L_ϕ, whose overall fluctuation is described by classical averaging [115]:

$$\delta g_{rms}(L) = \delta g_{rms}(L_\phi)\left(\frac{L_\phi}{L}\right)^{3/2} \approx \frac{e^2}{h}\left(\frac{L_\phi}{L}\right)^{3/2}. \tag{12}$$

In contrast, when the thermal diffusion length is smaller than the phase-breaking length, both inelastic scattering and thermal smearing are effective in reducing the fluctuation amplitude. This situation is unique to one-dimensional conductors, in which the rapid decay of their correlation function ensures that two states with energies differing by more than a *correlation energy* may be treated as statistically independent [115]. This correlation energy is defined as

$$E_c = \frac{\hbar D}{L^2}, \tag{13}$$

and is the energy difference required between two partial waves, such that on diffusing across the wire their accumulated phase change is of order unity. At finite temperatures, the number of independent energies involved in conduction over a single phase-coherent region is therefore [70]

$$N_E = \frac{k_BT}{E_c(L_\phi)} = \left(\frac{L_\phi}{L_T}\right)^2. \tag{14}$$

Due to classical averaging, the amplitude of the fluctuations associated with this region will be reduced by a factor of $N_E^{-1/2}$ from the universal value. The total fluctuation amplitude, measured across the entire length of the wire, will therefore be given by the lower form of equation (11), with additional reduction by a factor of L_T/L_ϕ. Closer inspection shows that this in fact corresponds to the upper form of equation (11).

Experimental investigations of the universal conductance fluctuations are hindered by the fact that, in contrast to the asymptotic behaviour discussed above, most experiments

are performed in a regime where the thermal diffusion and phase-breaking lengths are of *similar* magnitude. Nonetheless, an interpolation formula with an accuracy of approximately 10% has been derived to describe the temperature-dependent decay of the fluctuations in this regime [74]:

$$\delta g = \frac{g_s g_v}{2}\sqrt{\frac{12}{\beta_{\mathrm{UCF}}}}\left(\frac{L_\phi}{L}\right)^{3/2}\left[1+\frac{9}{2\pi}\left(\frac{L_\phi}{L_T}\right)^2\right]^{-1/2}. \tag{15}$$

Here, g_s and g_v are the spin- and valley-degeneracy factors, respectively. The factor β_{UCF} is equal to two in the presence of time-reversal symmetry, but is reduced to one when this symmetry is broken. The influence of time-reversal symmetry enters here since the perturbative calculation of the fluctuation amplitude contains contributions from two distinct impurity scattering processes, the particle–particle and particle–hole ladders [115]. While the amplitudes of these processes are identical at zero magnetic field, the breaking of time-reversal symmetry rapidly quenches the particle–particle contribution, in a similar fashion to that observed in weak localization. This leaves only the contribution from particle–hole diffusion, which is found to be insensitive to magnetic field while the Landau quantization remains unresolved, as a result of which the fluctuations in most metals persist to very high magnetic fields with unaltered characteristics [9]. The same cannot be said for semiconductor systems, however, in which well-defined Landau quantization is achieved at sub-tesla fields, giving rise to dramatic modification of the fluctuation characteristics [120–127]. Nonetheless, over magnetic field ranges where the Landau quantization is not yet resolved, study of the amplitude of the conductance fluctuations has been widely used as a means to determine the dephasing time.

2.3.2. Conductance fluctuations in ballistic quantum dots. While the theories of weak localization and universal conductance fluctuations have been developed for *disordered* conductors, in which electrons undergo diffusive motion in one or more dimensions, recent advances in semiconductor microfabrication technology now allow the realization of ballistic *quantum dots*. These structures are typically realized using the *split-gate technique* [128], in which metal gates with a fine-line pattern defined by electron-beam lithography are deposited on the surface of a high-mobility heterojunction. Application of a negative bias to the gates depletes electrons from underneath them, with the result that current flow from source to drain is forced to occur via the narrow gap defined *between* the gates. Examples of such split-gate quantum dots are shown in figure 10 and consist of a sub-micron-sized central *cavity* that is connected to external reservoirs by means of quantum-point-contact *leads*. These leads are typically configured to support a number of propagating one-dimensional modes, while the size of the central cavity is much smaller than the transport mean free path. Current flow through such dots therefore involves a process in which electrons are injected into the dot and undergo multiple boundary scattering before finally escaping to the reservoirs. At low temperature, phase coherence is maintained over long distances and the magnetoresistance is then found to exhibit reproducible fluctuations (figure 11) [130]. While these fluctuations appear reminiscent of those observed in disordered quantum wires, they are instead understood to result from a magnetic modulation of the interference of *ballistically scattered* electron partial waves within the dot (figure 12) [131]. The dots also typically exhibit a peak in their magnetoresistance, near zero magnetic field, and this has similarly been argued to result from the ballistic analogue of weak localization [132]. The details of both the fluctuations and the zero-field peak have been suggested to depend on the nature of the scattering within the dots (chaotic versus regular), for which reason the study of open dots has attracted much interest as an experimental probe of quantum chaos (for reviews, see [20, 133] and [134]).

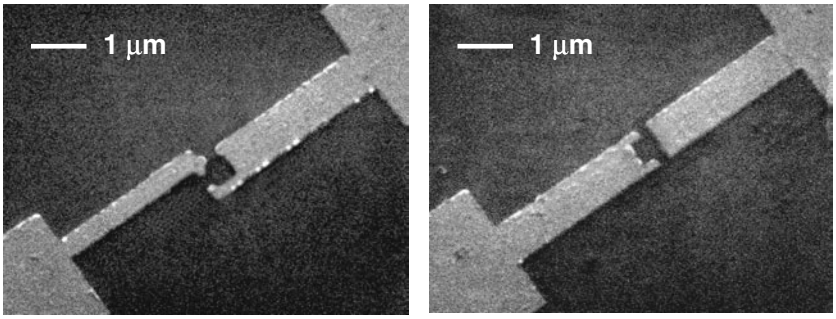

Figure 10. Examples of split-gate quantum dots. The metal gates correspond to the lighter regions and are deposited onto the surface of a GaAs/AlGaAs heterojunction. This figure was reproduced with permission from [129]. Copyright 1999 by the American Physical Society.

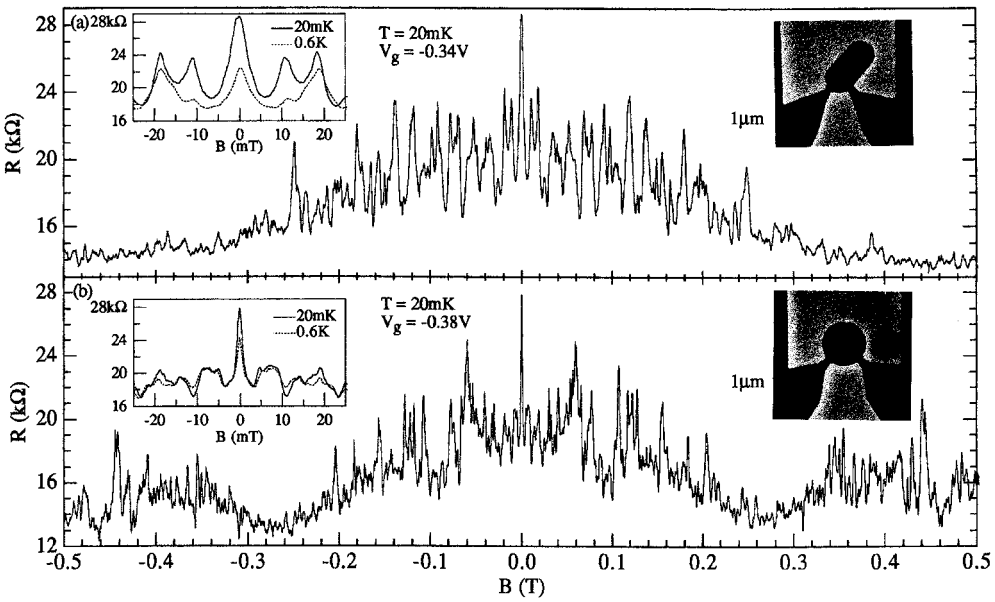

Figure 11. The magnetoresistance of stadium-shaped (top) and circular-shaped dots is found to exhibit pronounced and reproducible fluctuations at low temperatures. This figure was reproduced with permission from [130]. Copyright 1992 by the American Physical Society.

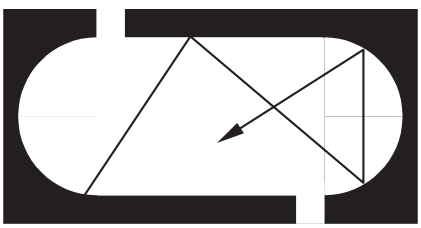

Figure 12. The fluctuations observed in the magnetoconductance of quantum dots are understood to result from a modulation by the magnetic field of interference involving electron partial waves that undergo multiple boundary scattering within the dot.

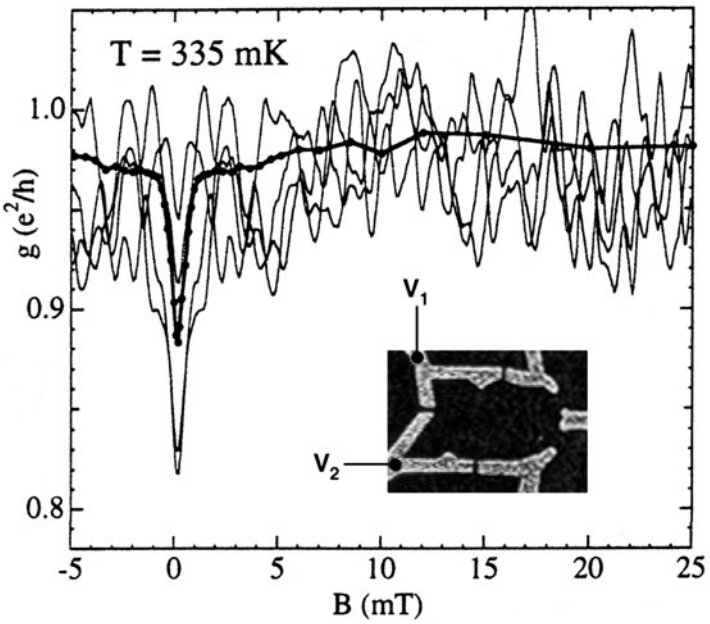

Figure 13. The main figure shows magnetoconductance traces measured in a quantum dot. The four traces shown using thin lines were obtained with different voltages applied to the shape-distorting gates indicated in the inset. The solid line was obtained by *averaging* the results of 47 such measurements to obtain a well-defined resistance peak at zero magnetic field. The inset shows the dot in which the measurements were performed. The total area of this dot is 4 μm^2. This figure was reproduced with permission from [137]. Copyright 1998 by the American Physical Society.

A number of authors have exploited the features in the magnetoconductance of open dots, to extract estimates for the electron dephasing time τ_ϕ. Marcus and co-workers [135–137] extract values for this parameter by assuming that electron motion in the dots may be taken to be fully chaotic (i.e. fully hyperbolic). For such chaotic dots, random-matrix theory predicts a ballistic weak-localization peak at zero magnetic field, whose amplitude is given by [138, 139]

$$\delta g_{WL} = \frac{e^2}{h}\frac{N}{2N + N_\phi}. \tag{16}$$

In this equation, N is the number of propagating modes in the dot leads (this number typically ranges from $\sim$1 to 6 in experiment), while N_ϕ is the number of modes in a fictitious lead that is assumed to couple the dot to a phase-randomizing reservoir [135, 140]. N_ϕ is related to the dephasing time according to

$$N_\phi = \frac{2\pi\hbar}{\tau_\phi \Delta} = \frac{2\pi\hbar}{\Delta}\gamma_\phi. \tag{17}$$

Here, Δ is the average level spacing in the dot and is defined as $\Delta = 2\pi\hbar^2/m^*\mathcal{A}_d$, where $\mathcal{A}_d$ is the area of the dot. In order to extract values for the dephasing time from equation (16), an ensemble of conductance traces is required to compute the amplitude of the weak-localization peak, and in figure 13 we show such an ensemble that was created by varying the voltages applied to the gates identified in the inset to the figure. After averaging over these different traces, a well-defined resistance peak is recovered at zero magnetic field, and from the amplitude of this peak an estimate of the dephasing time may be obtained [137].

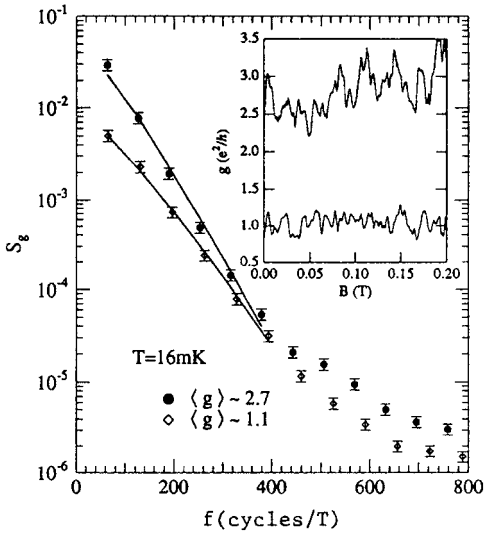

Figure 14. The main panel shows the Fourier power spectrum of the conductance fluctuation traces shown in the inset. Solid lines through the data points correspond to fits to the form of equation (18). The conductance fluctuations shown in the inset were obtained at the same temperature (16 mK), at two different gate voltage values. The dot geometry studied was similar to the stadium structure shown in the inset to figure 11. This figure was reproduced with permission from [135]. Copyright 1993 by the American Physical Society.

In an alternative approach to the above, experimental estimates for the dephasing time have also been obtained from an analysis of the magnetoconductance fluctuations in the dots [135,136]. For fully chaotic transport in the dots, the *power spectrum* of their fluctuations is predicted to vary as [131, 141]

$$S(f_B) = S_0 \mathrm{e}^{-2\pi\alpha h f_B/e}. \tag{18}$$

In this equation, f_B is the *magnetic* frequency (in units of per tesla) and α is a characteristic inverse area, related to the effective escape rate from the dot. This escape rate is broken down into two components, a first due to escape via the two leads, plus a second that represents the effective loss of *coherent* carriers from the dot. The total escape rate is therefore written as

$$\gamma_{eff} = \gamma_\phi + \gamma_{esc}, \tag{19}$$

where γ_{esc} is the rate at which electrons leave the dot via either of its leads. In analogy with equation (17), the escape rate via a lead that supports N modes may be written as

$$\frac{2\pi\hbar}{\Delta} N \tag{20}$$

and, with this definition, the total rate of escape from the dot becomes

$$\gamma_{eff} = \frac{2\pi\hbar}{\Delta}(2N + N_\phi). \tag{21}$$

Since the characteristic inverse area α that appears in equation (18) depends on the presence of coherent electrons in the dot, we may write the following relation:

$$\alpha^2 = \bar{\kappa}(2N + N_\phi), \tag{22}$$

where $\bar{\kappa}$ is a proportionality constant [136]. In figure 14, we show the power spectrum of the conductance fluctuations, measured in the same quantum dot at two gate voltages [135]. The

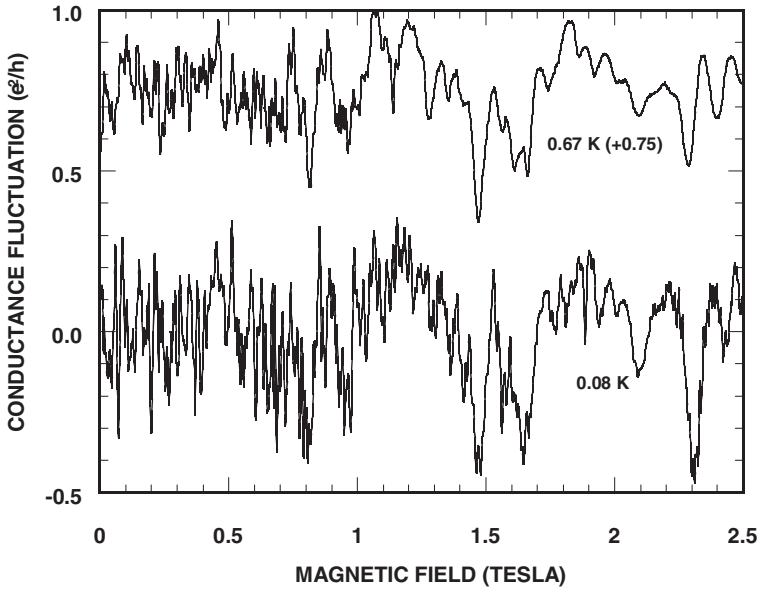

Figure 15. Conductance fluctuations measured in a quantum dot at two distinct temperatures (the higher-temperature trace has been shifted upwards by 0.75 e^2/h for clarity). In both cases, the traces were obtained by subtracting a smoothed polynomial fit from the raw magnetoconductance data. This figure was reproduced with permission from [142]. Copyright 1995 by the American Physical Society.

solid lines that pass through the data are fits to the form of equation (21) and allow the value of α to be determined. By assuming the dephasing time to be *independent* of the number of modes in the leads, the value of $\bar{\kappa}$ may be determined for any dot by plotting the variation of α as a function of the number of modes in the leads. With the values of α and $\bar{\kappa}$ established in this manner, the value of the dephasing time at any temperature may then be extracted [136].

In an alternative approach to those above, Bird and co-workers [142–145] have determined values for the phase-breaking time using a model originally developed to describe the properties of the magnetoconductance fluctuations in quasi-ballistic quantum wires [125]. This approach does not require the assumption of chaotic scattering in the dot but instead determines the dephasing time from the magnetic field dependence of the conductance fluctuations in the edge-state regime. In studies of this type, it is typically found that the basic field scale of the conductance fluctuations increases once the magnetic field is increased such that the cyclotron-orbit size fits within the dot (figure 15). In this regime, fluctuations are thought to arise from interference between different skipping orbits, whose coupling is predominantly generated by scattering in the point contact leads. To compute the characteristic magnetic flux enclosed between these orbits, we consider the area that a single orbit encloses as it skips coherently along the walls of the dot [146]:

$$\mathcal{A}_\phi = \bar{N}\frac{\pi r_c^2}{2} = v_F \tau_\phi r_c, \tag{23}$$

where $\bar{N}$ is the number of bounces the electron makes before losing phase coherence, r_c is the cyclotron radius ($=\hbar k_F/eB$), and v_F is the Fermi velocity. Given this definition, we obtain a

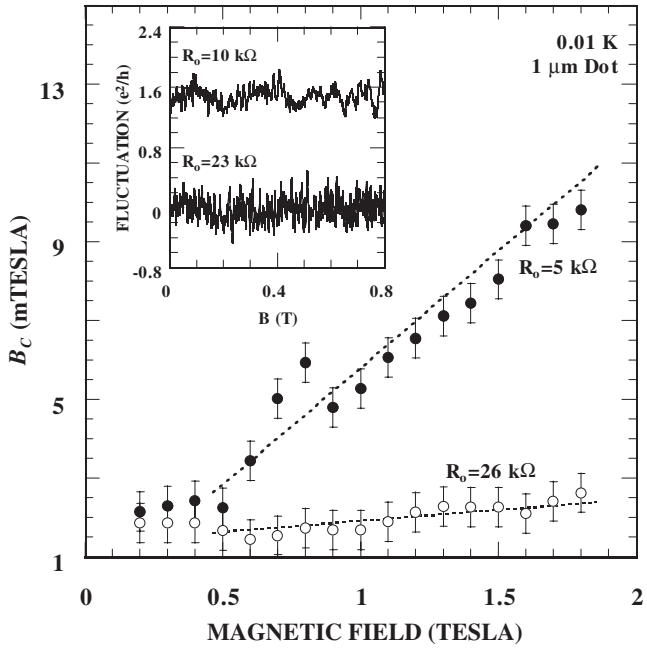

Figure 16. The magnetic field dependence of the correlation field of the conductance fluctuations in a quantum dot. The two different data sets were obtained for different values of the split-gate voltage (R_0 here denotes the zero-field resistance of the dot). This figure was reproduced with permission from [285].

simple expression relating the average period of the fluctuations to the magnetic field:

$$B_c(B) = \frac{\phi_0}{\mathcal{A}_\phi} = \frac{h}{e\mathcal{A}_\phi} = \frac{8\pi^2 m^*}{hk_F^2\tau_\phi}B. \tag{24}$$

In this equation, the field scale B_c is more rigorously defined as the correlation field [115] of the conductance fluctuations, and may be obtained directly from their correlation function. According to equation (24), when the phase-breaking time is independent of magnetic field, the average period of fluctuation should increase as a linear function of the applied field. Such behaviour is indeed found to be typical of experiment (figure 16) and from the slope of the resulting straight-line fit it is possible to use equation (24) to obtain an estimate for the phase-breaking time.

2.4. Reliability of dephasing times extracted from magneto-transport studies

We have discussed in this section the inelastic scattering times in different dimensionalities, the electron–superconducting-fluctuation scattering times in superconductors just above T_c, and the spin-flip scattering times in the presence of local moments. These examples deal with a wide range of different physical phenomena involving very different materials and different dimensionalities. Our discussion should suffice to convey to the reader the reliability, flexibility, and consistency of weak-localization studies in disordered metals. More precisely, the accessibility of explicit weak-localization expressions for the temperature dependence of the resistance and, particularly, the explicit expressions for the magnetoresistance, allow direct comparisons of the theory with experiment. Such quantitative comparison, in turn, has contributed enormously to advances in this area of research. This simultaneous progress,

in both theory and experiment, is rarely found in other areas of research in condensed-matter physics. Indeed, we are now able to obtain very quantitative estimates of the various dephasing times, including the e–ph scattering time τ_{ep}, the critical e–e scattering time τ_{EE}, the Nyquist e–e scattering time τ_{ee}, and the zero-temperature dephasing time τ_ϕ^0. Such information had not been available before the appreciation of weak-localization effects. Quantitative information on the temperature and disorder dependence of the dephasing times can shed light on the underlying mechanisms of the microscopic interactions between electrons and phonons, electrons and electrons, and electrons and other low-lying excitations. Finally, it is worth noting that the weak-localization magnetoresistance can also be used as a probe of magnetic field inhomogeneities on the scale of the phase-breaking length L_ϕ. This direction of research has been carried out to investigate the flux lattice of superconducting films [147][10].

While the study of weak localization and universal conductance fluctuations provides a reliable means of extracting estimates for the dephasing time, the extension of these methods to the study of semiconductor wires can be somewhat more complicated. The long mean free path characteristic of these materials means that the assumption of diffusive transport, a central requirement in the theories of weak localization and conductance fluctuations, may easily be violated. As we have discussed above, in quasi-ballistic quantum wires, it has been suggested that the influence of boundary scattering may be accounted for by modifying the weak-localization theory to account for the effects of flux cancellation [72, 74]. The main effect of this flux cancellation is simply expected to be to enhance the magnetic field required to quench weak localization, as compared to the diffusive case. Similarly, the flux cancellation is expected to lead to an enhancement of the correlation field of the conductance fluctuations in quasi-ballistic quantum wires [74]. The point to note here, however, is that these approaches to quasi-ballistic wires are only expected to remain valid while electron motion *along* the wire can be treated as diffusive. In short wires fabricated from high-mobility semiconductor material [77, 120, 122, 150], this condition may possibly be violated, calling into question the reliability of dephasing times extracted in these structures.

In quantum-dot systems, our understanding of dephasing mechanisms is hindered by a lack of both well-established theories and experiments. The techniques employed by Marcus and co-workers [135–137] provide an analytically elegant approach for extracting dephasing times. The problem with these techniques, however, is that they are based on an assumption of *fully chaotic* electron motion within the dots. An increasing number of studies suggest that fully chaotic dynamics is the exception rather than the rule in such dots [143, 151–156]. These studies rather emphasize the existence of a *mixed* phase space for electron dynamics in the dot, the statistics of which are completely different to those typical of fully chaotic system. A central feature of the chaotic models used to extract estimates for the dephasing time is the assumption of an *exponential* escape process from the dot, characterized by the single escape rate γ_{eff} (equation (19)). For mixed systems, however, the escape process is known to be characterized by a *power-law* form [151, 153], the existence of which violates the assumptions that allow estimates for the dephasing time to be extracted from equation (22). The approach utilized by Bird and co-workers [142–145] also suffers from its own problems, however. While it is clear that this model accounts for the basic behaviour found in experiment, we note from equation (24) that the influence of the magnetic field on the fluctuations is basically *inversely* proportional to the phase-breaking time. This means that the change in the frequency content of

[10] Weak-localization effects in mesoscopic conductors are direct manifestations of the wave nature of the conduction electrons. Shortly after the realization of the underlying physical origin of these effects, similar quantum-interference effects were investigated theoretically and experimentally in classical waves (acoustic waves and electromagnetic waves) [148]. In addition to the enhanced backscattering successfully realized with classical scatterers, coherent scattering of light has very recently been observed in a laser-cooled gas of Rb atoms [149].

the fluctuations is smallest at low temperatures, making it difficult to extract accurate values for the phase-breaking time in this regime. At the same time, while the influence of the magnetic field is most pronounced at higher temperatures, the actual fluctuation signal is weakest here. Nonetheless, in spite of the various problems identified above, we find it interesting to note that *comparable* values for the dephasing time have been obtained using these very different techniques [135–137, 142–145].

3. Dephasing in disordered metals

3.1. Electron–phonon scattering time in disordered metals

The e–ph scattering time τ_{ep} is a physical quantity that determines the most important characteristics of metals and superconductors. For instance, it determines the dephasing time for the electron wavefunction and the cooling time for an electron gas. It also determines the relaxation time for the order parameter in a superconductor. In the case of *clean* metals, the temperature behaviour of τ_{ep} is well established theoretically [157], but *less well* tested experimentally (see below). The e–ph scattering time in the clean limit, τ_{ep}^0, is given by [157]

$$\frac{1}{\tau_{ep}^0} \approx \lambda_{ep}\left(\frac{k_B^3 T^3}{\hbar^3 \omega_D^2}\right) \approx \lambda_{ep}\left(\frac{k_B T^3}{\hbar \theta_D^2}\right), \tag{25}$$

where λ_{ep} is a material-dependent constant that measures the strength of the e–ph coupling, ω_D is the Debye frequency, and θ_D is the Debye temperature. In the presence of strong impurity scattering, however, the situation is less straightforward and still debated. Theoretically, the e–ph interaction in disordered metals has been extensively studied by a number of authors for a few decades now [48], but quite different predictions were made [22, 33, 95, 96, 158–161]. In particular, different values of the exponent of temperature p in $1/\tau_{ep} \propto T^p$, ranging from 2 to 4, have been predicted. Experimentally, the temperature dependence of τ_{ep} reported by various measurements on different material systems are not always in agreement with one another [7, 29]. This issue becomes even more controversial when the dependence of τ_{ep} on disorder is concerned. While theories have predicted distinct disorder dependences of τ_{ep}, due to experimental difficulties, very few measurements in the literature have been able to report a clear dependence of τ_{ep} on the electron elastic mean free path l.

Pippard was the first to theoretically address the problem of the *phonon–electron* interaction in impure metals. In his landmark paper of 1955 [48], he calculated the ultrasonic attenuation (i.e. the phonon decay time) in the presence of disorder. Since, at low temperatures and low frequencies, this decay time is dominated by interaction with electrons, his phonon decay time corresponds to the phonon–electron scattering time, τ_{ph-e}. Therefore, Pippard's result can eventually lead to the theoretical calculation of the *e–ph* scattering time τ_{ep}. For instance, τ_{ep} can be obtained through the energy-balance equation [33, 157]: $C_e/\tau_{ep} = C_{ph}/\tau_{ph-e}$, where C_e and C_{ph} are the specific heats of electrons and phonons, respectively. Pippard found that the longitudinal ultrasonic attenuation coefficient α_L *decreased* monotonically with *decreasing* $q_T l$, where $q_T \approx k_B T/\hbar v_s$ is the wavenumber of thermal phonons, and v_s is the sound velocity. For $q_T l \ll 1$, he reached the conclusion that α_L was smaller than the clean-limit (i.e. $q_T l \gg 1$) result by a factor $q_T l$. The physical origin for this *weakened* phonon–electron interaction is the system's tendency to maintain approximate charge neutrality [48]. This result is now called the Pippard 'ineffectiveness condition' [162], and the physics behind it is understood as follows. (In the following physical picture, we shall translate the original ineffectiveness condition for the case of phonon–electron scattering to the case of e–ph scattering, since the latter is of central interest in the present work.) A finite mean free path l implies that the k-vector of the electron has an uncertainty of magnitude

$\Delta k \sim l^{-1}$. Therefore, if the electron k-vector changes upon scattering by less than Δk, it is as if the initial and final k-vectors are the same within their uncertainty. This is equivalent to the electron not having been scattered at all. Thus, the ineffectiveness condition implies that the low-q_T components of scattering potentials are ineffective in scattering (i.e. they are excluded as a scattering source) when q_T is smaller than l^{-1}. Pippard's result has been confirmed by subsequent microscopic calculations of Tsuneto [163], Schmid [160], and Eisenriegler and co-workers [164]. (For transverse phonons, the result is more complicated, and shows that disorder does increase the transverse ultrasonic attenuation coefficient α_T in certain regimes.)

3.1.1. Measurements of $\tau_{ep}(T, l)$: the importance of three dimensions. The e–ph interaction in impure metals has been calculated by a number of authors [22, 33, 158], with a general consensus having more or less been reached [22, 33, 161]. Experimentally, however, few measurements have successfully provided an overall consistency check of the theoretical predictions. One difficulty in this area of research is the problem of making and comparing samples with significantly different characteristics [165]. Information about the e–ph scattering rate $1/\tau_{ep}$ over a *wide* range of temperature and, particularly, *electron elastic mean free path* l is of prime importance for a stringent test of the current theory for the e–ph interaction in disordered metals.

In the course of studies of quantum-interference effects in disordered systems, weak localization has been extensively investigated in two dimensions, but much less extensively in one and three dimensions. In the case of three dimensions, quantum-interference effects are comparatively small, compared with those in lower dimensions. As a consequence, signal detection is sometimes difficult to carry out with a high degree of accuracy. Furthermore, it is generally not straightforward to make disordered metals *microscopically homogeneous* in the bulk and having a *wide* range of *high* resistivities. (Higher resistivities, i.e. shorter electron mean free paths, give rise to more pronounced quantum-interference effects in bulk materials.) It is only recently that three-dimensional measurements have been performed sufficiently carefully, making possible systematic investigations of the dependence of the electron dephasing time τ_ϕ (τ_{ep}) on *disorder*.

Thus far, most three-dimensional samples used in weak-localization studies have been thick granular films [25–27, 166], doped semiconductors [167, 168], and amorphous metal alloys [29, 30]. In the case of thick granular films, the electronic transport behaviour is generally complicated by the percolating nature of the sample structure, especially when the *macroscopic* disorder of the sample is high. In such systems, an e–ph scattering rate $1/\tau_{ep} \propto T^3$ has often been observed in low-resistance samples, while a *disorder-independent* inelastic scattering rate $1/\tau_{ep} \propto T^2$ has been observed in high-resistance samples, at liquid-helium temperatures [26, 166]. It is conjectured that a disorder-independent $1/\tau_{ep} \propto T^2$ in high-resistance granular samples might actually come from the presence of weakly disordered metal grains. In the case of amorphous metal alloys, although the residual resistivities ρ_0 are often high (hundreds of $\mu\Omega$ cm), it is usually difficult to adjust the value of ρ_0, or l^{-1}, over a reasonably wide range [85, 169]. That is, the atomic arrangement in amorphous metal alloys is already in the limit of strong randomness and, hence, a variation in the constituent concentration will hardly change the value of ρ_0. In some metallic glasses [29], the value of ρ_0 can be adjusted, e.g., by a factor $\sim$2, if the concentration is changed by a large amount, of several tens of per cent. However, the electronic structure and phonon excitation spectra might be totally altered under such circumstances. Therefore, neither such materials are of much use for the experimental investigations of the disorder behaviour of τ_{ep}. In short, a proper selection of material systems, and the fabrication of homogeneous macroscopic samples, remain two major challenges for this direction of experiment.

In studies of quantum-interference effects in disordered systems, it is generally a fashion to focus on 'mesoscopic' samples, whose dimensions are reduced to the smallest possible scale. However, in order to unravel the underlying physics of τ_{ep}, through measurements of its dependences on T and l, it should be pointed out that *three*-dimensional systems are actually more desirable. This is because one often encounters various experimental difficulties in the studies of τ_{ep} in disordered systems, depending largely on the *sample dimensionality*. The major experimental difficulties are discussed below.

(a) In the case of *two*-dimensional samples, there is usually more than one relevant inelastic processes, i.e. e–ph scattering and e–e scattering, of significance in determining the total inelastic scattering time $\tau_{\rm i}$ [7, 161]. Furthermore, the appropriate phonon dimensionality in question depends in a complicated way on the film thickness, the phonon wavelength, the acoustic transparency of the film–substrate interface, etc [7, 170–172]. Besides, experimental data on the sound velocity in thin films (wires) is absent, and the real phonon spectrum is typically unknown (while theory usually assumes the Debye spectrum of phonons). These inevitable complications make it extremely difficult to quantitatively separate τ_{ep} from the total $\tau_{\rm i}$ inferred from quantum-interference measurements. Under such circumstances, one cannot simply rewrite equation (1) in the form of (10) with only one temperature-dependent term. Instead, equation (1) needs to be written in the form

$$\frac{1}{\tau_\phi(T,l)} = \frac{1}{\tau_\phi^0} + A_{ee}T^{p'} + A_{ep}T^p, \tag{26}$$

where $A_{ee}T^{p'}$ is due to the e–e scattering, and $A_{ep}T^p$ is due to the e–ph scattering. Evidently, several free parameters are then involved in any least-squares fits of experimental data to equation (26), leading to appreciable uncertainties in the values of the adjustable parameters. Moreover, it is established that the Nyquist e–e scattering usually dominates over the e–ph scattering in reduced dimensions at a few kelvins and lower, making the extraction of a comparatively small contribution τ_{ep} from the measured τ_ϕ not very reliable.

For a typical speed of sound in metals ($v_s \approx 3000$ m s^{-1}), the most probable wavelength of thermal phonons is $2\pi q_T^{-1} \approx 2\pi\hbar v_s/k_BT \approx 1400\,T^{-1}$ Å (T in kelvins). Therefore, thermal phonons in films with a thickness of several thousands of ångströms will reveal three-dimensional behaviour at liquid-helium temperatures. On the other hand, thermal phonons in films with a thickness of a few hundreds of ångströms or thinner could reveal either two-, three-, or mixed-dimensional behaviour, depending strongly on the acoustic coupling between the film and substrate.

(b) In the case of *three*-dimensional samples, it is established that e–ph scattering is the *sole*, significant inelastic process while e–e scattering is comparatively weak and can be safely ignored [7, 22, 24], i.e. $A_{ee}T^{p'} \ll A_{ep}T^p$. (Generally, $A_{ee}T^{p'}$ becomes compatible with $A_{ep}T^p$ only at sub-mK temperatures.) In practice, however, it is very difficult to fabricate disordered metals *microscopically homogeneous* in bulk and having a *wide* range of *high* impurity resistivities ρ_0, as discussed above. It is only recently that the temperature and disorder dependence of τ_{ep} has been clearly determined in tailor-made polycrystalline alloys [31, 32, 82, 94, 173, 174] (see below).

(c) The issue of whether there exists a phonon confinement effect in lower-dimensional structures is still unclear. Undoubtedly, concerning the temperature dependence, it is necessary for one to understand the 'bulk' behaviour of $1/\tau_{ep} \propto T^p$ before one can unambiguously address the question of whether reducing the sample dimensionality from d to $d-1$ might result in a change in the power-law index p.

For the reasons just discussed, quantitative information on τ_{ep} is very limited in the literature. Recently, Lin and co-workers [31,175] have successfully fabricated series of three-dimensional polycrystalline titanium alloys, such as $Ti_{100-x}(Al, Sn, Ge)_x$, $Ti_{97-x}Sn_3Sc_x$, and $Ti_{73-x}Al_{27}Sn_x$, with the (nominal) impurity concentration x of the order of a few per cent. These polycrystalline disordered alloys are ideal for studies of weak-localization and e–e interaction effects. Compared with other three-dimensional conductors usually employed in this direction of research, bulk dilute titanium alloys are unique and advantageous in several regards. These samples reveal a number of quantitative features of τ_{ep} that were not previously understood, as we now discuss:

(a) Dilute titanium alloys are essentially microscopically homogeneous metal samples having a wide range of, and high, impurity resistivity ρ_0. A wide range of ρ_0 makes feasible a reliable experimental determination of the dependence of τ_{ep} on l. In $Ti_{100-x}(Al, Sn, Ge)_x$ alloys, the measured resistivity ρ_0 increases essentially linearly with increasing x for a wide range of ρ_0, from about 2 to 150 $\mu\Omega$ cm [32, 173]. Such a large variation of ρ_0, by nearly two orders of magnitude, is not always achievable in other materials. The linearity in the variation of ρ_0 with x implies a uniform distribution of the impurity atoms in the Ti host, and ensures that these alloys possess homogeneous composition, and lattice structure, at length scales considerably smaller than L_ϕ.

(b) Dilute doping of a Ti host with various impurity atoms (e.g., Al, Sn, Ge, or Sc) is possible. It is expected that different impurity atoms could affect the phonon excitation spectrum and, probably, the electronic density of states at the Fermi level in different ways, and therefore might cause different temperature and disorder dependences of τ_{ep}. Indeed, it has very recently been proposed that $\tau_{ep}(T, l)$ should critically depend on the extent to which the impurity atoms move (in phase or out of phase) with the lattice atoms [95, 96]. The availability of many different kinds of dilute titanium alloy thus makes these systems ideal for testing current theoretical concepts for the e–ph interaction in disordered metals.

(c) A third advantage is that the most common magnetic atoms, such as Fe, Co, and Ni, do *not* form localized moments in a Ti host [98]. Thus, there is *no* magnetic spin–spin scattering in these titanium alloys, i.e. the magnetic spin–spin scattering rate $1/\tau_s = 0$.

(d) Many dilute titanium alloys exhibit superconductivity, which onsets at temperatures between about 0.5 and 2 K. In practice, such values of T_c are more than adequate for measurements of τ_{ep}. This is because, on one hand, these T_c-values are not too 'high', in the sense that there is still a sufficiently wide temperature window left above T_c where the weak-localization magnetoresistance is measurable. On the other hand, these T_c-values are not too 'low', so the upper critical field, B_{c2}, for each alloy can be conveniently measured using standard cryostats. With B_{c2} being measured [176], the value of the electron diffusion constant D for each alloy can be evaluated through the relation [177]: $D = (4k_B/\pi e)/|\mathrm{d}B_{c2}/\mathrm{d}T|$. As is well known, the value of D is indispensable for computing the value of τ_{ep} from weak-localization studies[11].

The above discussion illustrates that $\tau_{ep}(T, l)$ can be reliably inferred from weak-localization measurements using tailor-made titanium alloys. The measured inelastic scattering time is *not* coupled with either the Nyquist e–e scattering time τ_{ee} or the magnetic spin–spin scattering time τ_s. Such a practice of decoupling different electron scattering times is often

[11] Alternatively, the value of D is often evaluated by measuring the electronic specific heat at liquid-helium temperatures to infer the electronic density of states at the Fermi level, $\nu(0)$. The value of D can then be calculated through the Einstein relation: $\rho_0^{-1} = De^2\nu(0)$, using the measured values of ρ_0 and $\nu(0)$. The values of D deduced from B_{c2}-measurements and specific heat measurements are consistent to within 20% in dilute titanium alloys. Since it is known that $\nu(0)$ *barely* changes with mean free path l in many disordered metals [178], then $D \propto \rho_0^{-1}$ for a given material system.

lacking in other two- or three-dimensional experiments reported in the literature. It should be repeated that such a clear-cut separation of τ_{ep} was achieved by simultaneously taking into consideration both the *sample dimensionality* (which minimizes e–e scattering relative to e–ph scattering in three dimensions) and the *unique sample properties*.

In their experiments, Lin and co-workers have focused on the e–ph interaction in the *dirty limit* of $q_T l \ll 1$. This is the regime that has attracted most theoretical [22, 33, 161] and experimental [171, 179] attention, but the problem is still not very well understood. Apart from this regime, the nature of the e–ph interaction in the presence of intermediate disorder, which lies between the clean limit ($q_T l \gg 1$) and dirty limit, is also of interest. This is a regime where the electron elastic mean free path is of the order of the thermal phonon wavelength, i.e. $q_T l \sim 1$. In fact, it is speculated that many of the samples previously reported in the literature were not yet strongly disordered enough for the e–ph interactions to strictly satisfy the criterion $q_T l \ll 1$, and therefore the predicted T^4 temperature dependence of $1/\tau_{ep}$ was not observed. Instead, most previous measurements dealt with samples having $q_T l \sim 1$. Ptitsina *et al* [180] have recently argued that the theory is in good agreement with experiment in this intermediate region. In any case, it is important to perform systematic studies of τ_{ep} in both the intermediate and dirty limits. Systematic measurements using well-characterized samples with significantly different properties would be very valuable in providing a stringent justification for the current concepts of the e–ph interaction in impure conductors.

3.1.2. Experimental $\tau_{ep}(T, l)$ in the dirty limit. To experimentally test the theory of e–ph interaction in disordered conductors, the most reliable approach is to measure *not only* the dependence on temperature, *but also* the dependence on electron elastic mean free path of τ_{ep}. This could be achieved by employing different kinds of three-dimensional sample containing different degrees of disorder. Useful sample materials include, for example, (binary) alloys whose compositions can be varied from sample to sample, metals and alloys whose atomic arrangement and microstructures can be changed by tuning fabrication conditions, and alloys that possess an intrinsic short electron mean free path of the order of the interatomic spacing. Systematic measurements on such samples can lead to very quantitative information about $\tau_{ep}(T, l)$. Experimental approaches in this direction have been undertaken by, among others, Lin and co-workers and are described below.

(a) *Compositional disorder: dilute titanium alloys.* Using a standard arc-melting method, Lin and co-workers [31,32,173] have recently succeeded in making a series of $Ti_{100-x}Al_x$ and $Ti_{100-x}Sn_x$ alloys that are essentially microscopically homogeneous and have a wide range of high impurity resistivity $\rho_0 \approx 40$–$160\ \mu\Omega$ cm, corresponding to $k_F l \approx 5$–20. Such a wide range of ρ_0 makes feasible a reliable experimental determination of the dependence of τ_{ep} on l, in addition to the dependence on T. Figure 17(a) shows the variations of $1/\tau_{ep}$ with temperature for four $Ti_{100-x}Al_x$ alloys with different concentrations of aluminium x. This figure clearly indicates that $1/\tau_{ep}$ obeys a T^2 law. Moreover, close inspection of figure 17(a) indicates that the magnitude of the scattering rate at a given temperature increases with increasing x. Since $\rho_0 \propto x$ in dilute $Ti_{100-x}Al_x$ alloys [181], $1/\tau_{ep}$ increases with ρ_0. A similar T^2 dependence of $1/\tau_{ep}$ has also been observed in dilute $Ti_{100-x}Sn_x$ alloys with $\rho_0 \gtrsim 100\ \mu\Omega$ cm [32].

Figure 17(b) shows the variation of the measured e–ph scattering rate $1/\tau_{ep}$ at a representative temperature of 10 K with the impurity resistivity ρ_0 for $Ti_{100-x}Al_x$ and $Ti_{100-x}Sn_x$ alloys. This plot clearly indicates a strong disorder dependence of $1/\tau_{ep}(10\ \text{K}) \propto \rho_0 \propto l^{-1}$, i.e. $1/\tau_{ep}$ varies *inversely linearly* with the electron elastic mean free path l. For these $Ti_{100-x}(Al, Sn)_x$ alloys, $q_T l \approx (0.0068$–$0.029)\,T$, where T

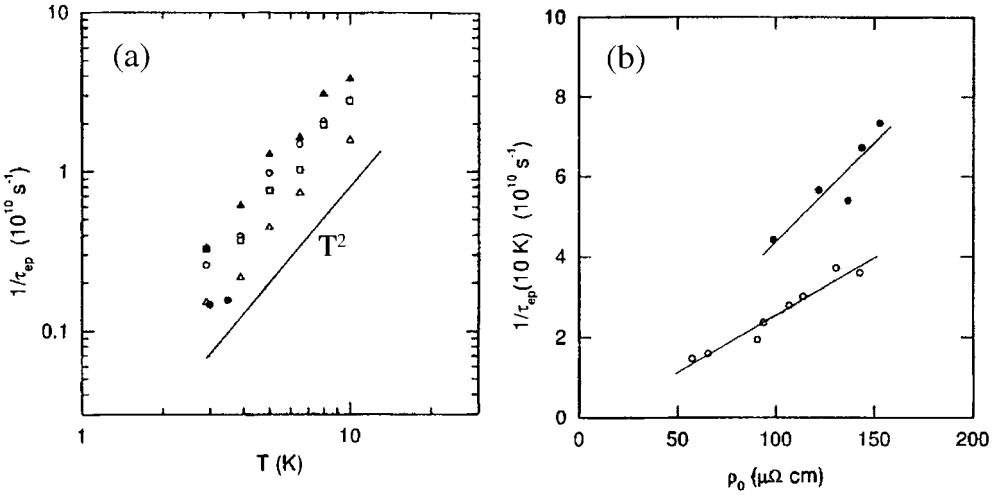

Figure 17. (*a*) Variation of the e–ph scattering rate $1/\tau_{ep}$ with temperature for $Ti_{100-x}Al_x$ alloys with $x \approx 5.3$ (open triangles), 7.2 (solid circles), 8.0 (squares), 10.2 (solid triangles), and 15.0 (open circles). The straight line is drawn proportional to T^2 and is a guide to the eye. (*b*) Variation of the e–ph scattering rate at 10 K, $1/\tau_{ep}(10\ \mathrm{K})$, with impurity resistivity ρ_0 for dilute $Ti_{100-x}Al_x$ (open circles) and $Ti_{100-x}Sn_x$ (solid circles) alloys. The straight solid lines drawn through the data are guides to the eye. This figure was reproduced with permission from [174].

is in kelvins. This value of $q_T l$ suggests that the e–ph interaction is well within the dirty limit at the measurement temperatures.

(b) *Structural disorder: Au–Pd alloys.* Zhong and Lin [94] have recently measured τ_{ep} in a series of three-dimensional $Au_{50}Pd_{50}$ films with a wide range of high residual resistivity $\rho_0 \approx 70$–$230\ \mu\Omega$ cm, corresponding to $k_F l \approx 2.5$–8. Their films were prepared by a standard dc sputtering deposition method; the deposition rate was varied to tune the amount of disorder ρ_0. Unlike in the case of the dilute titanium alloys just discussed, where the level of disorder was controlled by the amount of the doped impurity atoms (Al or Sn), the composition in this case is fixed (i.e. $Au_{50}Pd_{50}$) while the level of disorder is controlled by the structural arrangement of Au and Pd atoms. Therefore, this series of samples has a quality of disorder very different from that in dilute titanium alloys. It is conjectured that the nature of the e–ph interaction, as well as the behaviour of $\tau_{ep}(T, l)$, could be very sensitive to defect and impurity influence [95, 96]. Then, measurements on these two material systems, dilute titanium and Au–Pd alloys, should provide independent and complementary results on $\tau_{ep}(T, l)$.

The measured dephasing time τ_ϕ in one of these Au–Pd films is plotted in figure 5(*a*). Figure 5(*a*) indicates that the total τ_ϕ can only be described by equation (10) with an inelastic scattering rate having an exponent of temperature $p = 2$. On the other hand, the measured τ_ϕ can by no means be described using either $p = 3$ or 4. Figure 5(*b*) shows the e–ph scattering rate $1/\tau_{ep}$ at a representative temperature of 10 K as a function of electron mean free path for several Au–Pd thick films. This figure indicates that $1/\tau_{ep}$ varies *linearly* with l. Very recently, a similar variation of $1/\tau_{ep} \propto T^2 l$ has also been found in three-dimensional $Ag_{40}Pd_{60}$ films [182] and $V_{100-x}Al_x$ alloys [183]. For these Au–Pd alloys, $q_T l \approx (0.024$–$0.078)\ T$, where T is in kelvins. This value of $q_T l$ suggests that the e–ph interaction is well within the dirty limit at measurement temperatures.

(c) *Dirty limit: $Ti_{73}Al_{27}$ alloys.* Apart from measurements in dilute titanium and Au–Pd alloys, there exist a number of experiments which also reported an e–ph scattering rate

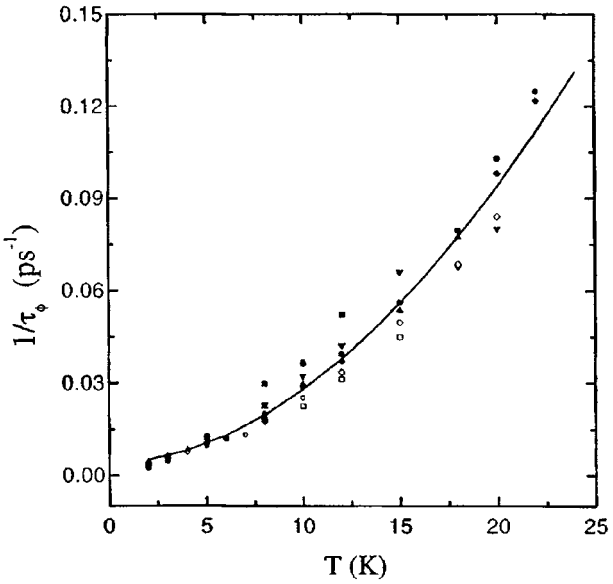

Figure 18. Variation of the electron dephasing rate $1/\tau_\phi$ with temperature for several $Ti_{73-x}Al_{27}Sn_x$ alloys, with $0 \lesssim x \lesssim 5$. Since the measured values of $1/\tau_\phi$ are very similar for all alloys (i.e. x), it is unnecessary to label each symbol with its associated particular alloy. The solid curve is a least-squares fit to equation (10) with the exponent of temperature $p \approx 1.9 \pm 0.2$. This figure was reproduced with permission from [82]. Copyright 1999 by the American Physical Society.

$1/\tau_{ep} \propto T^2$ in various metal films [184]. Theoretically, however, a T^4 law in the dirty limit is predicted, but this is essentially not found in experiments [171, 179]. Since the T^4 temperature dependence is calculated under the disorder criterion of $q_T l \ll 1$, information about the temperature dependence of $1/\tau_{ep}$ in samples having even smaller values of $q_T l$ than *ever* studied is therefore of crucial importance for a critical test of the theory.

With this motivation, Hsu *et al* [82] recently fabricated a series of polycrystalline tin-doped $Ti_{73}Al_{27}$ alloys using a standard arc-melting method. One of the advantages of these alloys is that their impurity resistivities are high ($\approx$225 $\mu\Omega$ cm) and are barely changed upon Sn doping. Such an extremely high value of ρ_0, corresponding to an electron mean free path l of the order of the *interatomic spacing*, put the e–ph interaction in this material much closer to the dirty limit than ever attained in any previous measurements. (Since the electron mean free path in the parent $Ti_{73}Al_{27}$ phase is already of the order of the interatomic spacing, tin doping will thus hardly change ρ_0.) In this case, Hsu *et al* found that their measured $1/\tau_\phi$ can be least-squares fitted with equation (10), resulting in an exponent of temperature $p \approx 1.9 \pm 0.2$ (figure 18). That is, even in this alloy system with a very low value of $q_T l$, the measured $1/\tau_{ep}$ still demonstrates a T^2 law. There is absolutely *no* evidence of a T^4 temperature dependence as expected from the theory. For these $Ti_{73-x}Al_{27}Sn_x$ alloys, $q_T l \approx 0.006\,T$, where T is in kelvins, so the e–ph interaction is *well* within the dirty limit at the measurement temperatures. This experimental result provides very strong evidence that indicates a quadratic temperature dependence of $1/\tau_{ep}$ in disordered conductors.

3.1.3. Comparison with theory.

The dirty limit. Closely related to Pippard's work on ultrasonic attenuation discussed above [48], the problem of the e–ph interaction in impure conductors has been evaluated by

Schmid [160, 185] and Rammer and Schmid [22]. Rammer and Schmid considered impurity atoms that move *in phase* with the other lattice atoms in the long-wavelength limit, namely, their key assumption is that the scattering potential is *completely dragged* by the phonons. (Therefore, the system maintains approximate charge neutrality.) Rammer and Schmid found that there is a subtle compensation between the coupling of the electrons to the 'vibrating' impurities and the interaction of the electrons with the deformed lattice vibrations. As a consequence, the e–ph scattering rate is entirely changed from that in the clean case. For a three-dimensional system in the *dirty* limit, they predict

$$\frac{1}{\tau_{ep}} \approx \lambda_{ep}\left(\frac{k_B T^3}{\hbar\theta_D^2}\right) G(T, l), \tag{27}$$

which differs from equation (25) by the factor $G(T, l)$. For a simple jellium model with a spherical Fermi surface, $G \propto T$ at low temperatures, and decreases as T is increased at high temperatures. In addition, G is a function of the degree of disorder through $k_F l$. Such a *non-monotonic* temperature dependence of G implies that τ_{ep} cannot be described by a simple power law over the entire temperature range, although over the limited range accessible in a typical experiment one would expect to observe an approximate power law with an effective exponent.

Of particular importance in equation (27) is its prediction for the dirty limit of the e–ph interaction. Rammer and Schmid [22] found that the e–ph interaction is *weakened* and given by

$$\frac{1}{\tau_{ep}} \sim (q_T l)\left(\frac{1}{\tau_{ep}^0}\right) \propto T^4 l. \tag{28}$$

This result is consistent with Pippard's conclusion for the longitudinal ultrasonic attenuation coefficient α_L discussed above. This prediction, equation (28), has received wide acceptance from the theoretical community. Moreover, it has been independently confirmed in subsequent calculations by Reizer and Sergeev [33], Belitz [161], and Sergeev and Mitin [95, 96].

Experimentally, the e–ph scattering time in impure metals has previously been measured in many systems. However, the theoretical prediction of equation (28) is essentially *not* found. On the contrary, observation of an e–ph scattering rate $1/\tau_{ep} \propto T^2$ has been reported in both two-dimensional films [184] and three-dimensional samples [82, 94, 173, 183]. Such a result has caused much confusion and controversy on the nature of the e–ph interaction in impure conductors for years. Since the dirty-limit condition of $q_T l \ll 1$ is well satisfied in the recent measurements on dilute titanium and Au–Pd alloys discussed above, the experimental T^2 law thus causes renewed interest in the nature of the e–ph interaction in disordered metals.

Concerning the dependence of τ_{ep} on disorder, a linear dependence of τ_{ep} on l has been found in $Ti_{100-x}(Al, Sn)_x$ alloys [32, 173], but not (yet) in any other materials. On the other hand, an inverse linear dependence of τ_{ep} on l has been found in three-dimensional Au–Pd films [94], Ag–Pd films [182], $V_{100-x}Al_x$ alloys [183], and two-dimensional Nb films [186] and Sb films [187]. The former disorder behaviour of $\tau_{ep} \propto l$ is actually consistent with an earlier theory due to Bergmann [158] and Takayama [159] which considered only the scattering of electrons by impurity vibrations[12]. The latter disorder behaviour of $\tau_{ep} \propto l^{-1}$ is in line with the prediction of the Pippard–Rammer–Schmid theory, equation (28). It is quite surprising that opposite, i.e. linear and inversely linear, dependences of τ_{ep} on l are realized in different disordered metals. These seemingly contradictory results have recently prompted

[12] Recently, however, it was pointed out by Reizer and Sergeev [33] that the calculation of Takayama did not properly subtract the elastic contribution from the total (impurity and phonon) scattering rate, and hence overestimated $1/\tau_{ep}$.

the introduction of new theoretical concepts of the nature of the e–ph interaction in impure conductors [95, 96, 188].

Theoretical expressions for $\tau_{ep}(T, l)$. Equation (28) is derived under the assumption that, in a disordered conductor, the scattering potential of defects and impurities is completely dragged by phonons. Under such a condition, it was found that the e–ph coupling depends substantially on the parameter $q_T l$. If $q_T l < 1$, the e–ph coupling is a factor $q_T l$ weaker than the coupling in the clean limit. (As discussed, this statement is known as the Pippard ineffectiveness condition, i.e. electrons strongly scattering from impurities and defects are ineffective in scattering phonons [48, 162].) In an attempt to resolve the large discrepancies between the theory and experiment on τ_{ep} reported in the literature, Sergeev and Mitin [95,96] have very recently generalized the Pippard–Rammer–Schmid model to take into consideration an additional 'static' (i.e. 'non-vibrating') potential. Largely on the basis of the Rammer–Schmid theory, they introduced an electron mean free path with respect to the static potential, $\mathcal{L}$, in addition to the total electron mean free path l. They found that *even a relatively weak static potential drastically changes the effective e–ph coupling and, thus, the e–ph scattering rate* $1/\tau_{ep}$.

According to Sergeev and Mitin [95,96], the inelastic electron scattering rate of an electron at the Fermi surface due to the interaction with *longitudinal* phonons is given by[13]

$$\frac{1}{\tau_{ep,l}} = \frac{7\pi\zeta(3)}{2}\frac{\beta_l (k_B T)^3}{\hbar^3 (k_F v_l)^2} F_l(q_{T,l} l), \tag{29}$$

where

$$F_l(z) = \frac{2}{7\zeta(3)} \int_0^{k_B\theta_D l/\hbar v_l z} \mathrm{d}x\, \Phi_l(xz)(N(x) + f(x))x^2,$$

and

$$\Phi_l(x) = \frac{2}{\pi}\left[\frac{x \arctan(x)}{x - \arctan(x)} - \left(1 - \frac{l}{\mathcal{L}}\right)\frac{3}{x}\right].$$

$N(x)$ and $f(x)$ are the Bose and Fermi distribution functions, $\Phi_l(x)$ is the Pippard function, and $\zeta(n)$ is the Riemann zeta function. The dimensionless coupling constant responsible for the interaction of electrons with longitudinal phonons is defined by $\beta_l = (2E_F/3)^2(\nu/2\rho_i v_l^2)$, where ν is the electronic density of states, and $\rho_i = n_i M$ is the mass density. In the limiting cases and at $T \ll \theta_D$, equation (29) reduces to

$$\frac{1}{\tau_{ep,l}} = \frac{7\pi\zeta(3)}{2}\frac{\beta_l (k_B T)^3}{\hbar^3 (k_F v_l)^2} \begin{cases} 1, & q_{T,l} l \gg 1 \\ \dfrac{2\pi^3 (q_{T,l} l)}{35\zeta(3)} + \dfrac{3\pi}{7\zeta(3)(q_{T,l}\mathcal{L})} & q_{T,l} l \ll 1. \end{cases} \tag{30}$$

More importantly, the inelastic electron scattering from the vibrating potential generates a new channel of e–ph interaction. Sergeev and Mitin [95, 96] found that this channel is also significantly enhanced in the presence of a static potential. The inelastic electron scattering rate of an electron at the Fermi surface due to the interaction with *transverse* phonons is now given by

$$\frac{1}{\tau_{ep,t}} = \frac{3\pi^2 \beta_t (k_B T)^2}{\hbar^2 (k_F v_t)(k_F l)}\left(1 - \frac{l}{\mathcal{L}}\right) F_t(q_{T,t} l), \tag{31}$$

where

$$F_t(z) = \frac{4}{\pi^2} \int_0^{k_B\theta_D l/\hbar v_t z} \mathrm{d}x\, \Phi_t(xz)(N(x) + f(x))x,$$

[13] In this work we will not attempt to distinguish explicitly between the e–ph inelastic scattering rate and the e–ph energy relaxation rate. These two rates differ only by a numerical factor of order unity [170, 189].

and

$$\Phi_t(x) = 1 + \left(1 - \frac{l}{\mathcal{L}}\right)\left(\frac{3x - 3(x^2+1)\arctan(x)}{2x^3}\right).$$

The dimensionless kinetic constant responsible for the interaction of electrons with transverse phonons is defined by $\beta_t = (2E_F/3)^2(\nu/2\rho_i v_t^2) = \beta_l(v_l/v_t)^2$. In the limiting cases and at $T \ll \theta_D$, equation (31) reduces to

$$\frac{1}{\tau_{ep,t}} = \frac{3\pi^2\beta_t(k_BT)^2}{\hbar^2(k_Fv_t)(k_Fl)}\left(1 - \frac{l}{\mathcal{L}}\right)\begin{cases} 1, & q_{T,t}l \gg 1 \\ \dfrac{l}{\mathcal{L}} + \left(1 - \dfrac{l}{\mathcal{L}}\right)\dfrac{\pi^2(q_{T,t}l)^2}{10} & q_{T,t}l \ll 1. \end{cases} \tag{32}$$

Equations (30) and (32) indicate a *non-single* value of the exponent of temperature, and a *non-monotonic* disorder dependence, of both longitudinal ($\tau_{ep,l}$) and transverse ($\tau_{ep,t}$) e–ph scattering times. The total e–ph scattering rate in the limiting cases is given by the sum of these two contributions.

(a) In *clean* metals ($q_{T,l}l, q_{T,t}l \to \infty$), the total e–ph scattering rate is given by

$$\frac{1}{\tau_{ep}} = \frac{7\pi\zeta(3)}{2}\frac{\beta_l(k_BT)^3}{\hbar^3(k_Fv_l)^2}\left[1 + \frac{6\pi}{7\zeta(3)(q_{T,l}l)}\left(1 - \frac{l}{\mathcal{L}}\right)\left(\frac{v_l}{v_t}\right)^3\right]. \tag{33}$$

The first term is due to the electron–*longitudinal*-phonon interaction while the second term is due to the electron–transverse-phonon interaction. In the limit $q_{T,l}l \to \infty$, the first term dominates the total e–ph scattering rate $1/\tau_{ep}$. This reproduces the classical result of [157], equation (25). For a typical impure metal with $k_F \sim 1.5 \times 10^{10}$ m^{-1}, $v_l \sim 4 \times 10^3$ m s^{-1}, and $\beta_l \sim 0.1$, equation (33) predicts a scattering rate of $1/\tau_{ep} \sim 0.8 \times 10^6\, T^3$ s^{-1} (T in K).

(b) In *disordered* metals and in the *dirty* limit ($q_{T,l}l, q_{T,t}l \ll 1$), the *total* e–ph scattering rate is given by

$$\frac{1}{\tau_{ep}} = \frac{\pi^4(k_BT)^4l\beta_l}{5\hbar^4k_F^2v_l^3}\left[1 + \frac{3}{2}\left(1 - \frac{l}{\mathcal{L}}\right)\left(\frac{v_l}{v_t}\right)^5\right] + \frac{3\pi^2(k_BT)^2\beta_l}{2\hbar^2k_F^2\mathcal{L}v_l}\left[1 + 2\left(1 - \frac{l}{\mathcal{L}}\right)\left(\frac{v_l}{v_t}\right)^3\right]. \tag{34}$$

The asymptotics of equation (34) are as follows.

(i) In the case of pure 'vibrating' scatterers ($\mathcal{L} \to \infty$), equation (34) reproduces the *complete*-drag result of Rammer and Schmid [22], and Reizer and Sergeev [33], i.e. equation (28):

$$\frac{1}{\tau_{ep}} = \frac{\pi^4(k_BT)^4l\beta_l}{5\hbar^4k_F^2v_l^3}\left[1 + \frac{3}{2}\left(\frac{v_l}{v_t}\right)^5\right]. \tag{35}$$

The first term is due to the electron–longitudinal-phonon interaction while the second term is due to the electron–transverse-phonon interaction. Since $v_l/v_t \sim 2$ in typical metals, it is clearly seen that the second term is 1–2 orders of magnitude larger than the first term, i.e. the electron–*transverse*-phonon interaction dominates the total scattering rate $1/\tau_{ep}$ in the dirty limit. For a typical impure metal with $k_F \sim 1.5 \times 10^{10}$ m^{-1}, $v_l \sim 4 \times 10^3$ m s^{-1}, and $\beta_l \sim 0.1$, equation (35) predicts a scattering rate of $1/\tau_{ep} \sim 2 \times 10^{15}\, T^4l$ s^{-1} (in MKS units).

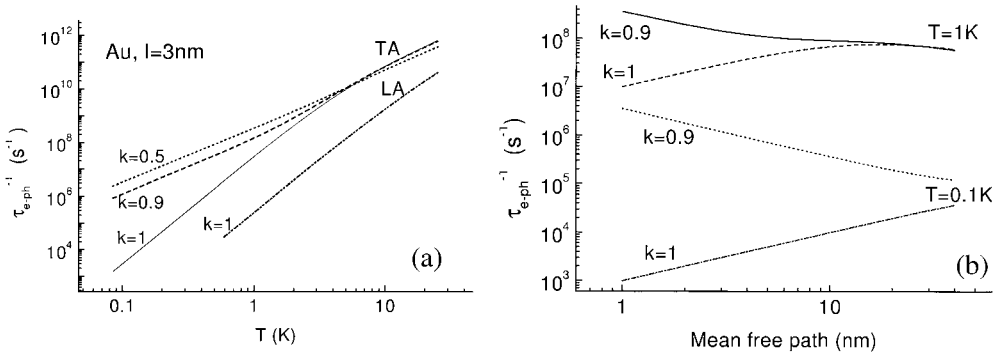

Figure 19. Calculated variation of the e–ph scattering rate $1/\tau_{ep}$ with (*a*) temperature and (*b*) electron mean free path from equation (34), using parameters suitable for disordered Au films: $l = 30$ Å, $v_l = 3200$ m s^{-1}, $v_t = 1200$ m s^{-1}, $v_F = 1.4 \times 10^6$ m s^{-1}, $\beta_l = 0.2$, and $\beta_t = 1.4$. The parameter k $(=1 - l/\mathcal{L}) = 1$ stands for the case of *complete* drag of the scattering potential, while $k < 1$ stands for the case of *incomplete* drag. This figure was reproduced with permission from [95]. Copyright 2000 by the American Physical Society.

(ii) In the case of *incomplete* drag ($\mathcal{L} \ll \infty$; in reality, $1 - l/\mathcal{L}$ will not be much smaller than 1), equation (34) approximates as

$$\frac{1}{\tau_{ep}} = \frac{3\pi^2 (k_B T)^2 \beta_l}{\hbar^2 k_F^2 \mathcal{L} v_l} \left(1 - \frac{l}{\mathcal{L}}\right) \left(\frac{v_l}{v_t}\right)^3. \tag{36}$$

This term is due to interactions between electrons and *transverse* phonons. In particular, this equation predicts an e–ph scattering rate $1/\tau_{ep} \propto T^2 \mathcal{L}^{-1}$. That is, the static potential completely changes the temperature and disorder dependences of $1/\tau_{ep}$ from $T^4 l$ to $T^2 \mathcal{L}^{-1}$. For a typical impure metal with $k_F \sim 1.5 \times 10^{10}$ m^{-1}, $v_l \sim 4 \times 10^3$ m s^{-1}, $\beta_l \sim 0.1$, $v_l/v_t \sim 2$, and $(1 - l/\mathcal{L}) \sim 0.9$, equation (36) predicts a much enhanced scattering rate of $1/\tau_{ep} \sim 0.4\, T^2 \mathcal{L}^{-1}$ s^{-1} (in MKS units).

(c) In disordered metals and in the presence of static scattering potential, it can be shown that transverse phonons dominate the relaxation over a wide range of temperature. In particular, equation (32) indicates that the scattering rate obeys a $T^2 l^{-1}$ law in both asymptotics: $q_{T,t} l \gg 1$ and $q_{T,t} l \ll 1$. At the intermediate temperatures, $q_{T,t} l \sim 1$, the exponent in the temperature dependence is larger than 2.

Figure 19(*a*) shows the theoretical prediction of the temperature dependence of the e–ph scattering rate $1/\tau_{ep}$, equations (29) and (31), for typical Au films with $l = 30$ Å and different values of $k = 1 - l/\mathcal{L}$. This figure clearly illustrates that the electron–transverse-phonon scattering (TA) dominates over electron–longitudinal-phonon scattering (LA). In the case of complete drag of the scattering potential ($k = 1$), the scattering rate $1/\tau_{ep} \propto T^4$ at low temperatures. In the case of the incomplete drag ($k < 1$), the temperature dependence of $1/\tau_{ep}$ changes to T^2 and the scattering rate greatly increases from that in the complete-drag case. Figure 19(*b*) shows the theoretical prediction of the electron mean free path dependence of $1/\tau_{ep}$ for the same Au films as were considered in figure 19(*a*). This figure clearly illustrates that, in the case of complete drag of the scattering potential, the scattering rate $1/\tau_{ep} \propto l$ in the dirty limit (i.e. short mean free paths and low temperatures). On the other hand, in the case of incomplete drag of the scattering potential, and in the dirty limit, the mean free path dependence of $1/\tau_{ep}$ changes to l^{-1} and the scattering rate greatly increases from that in the complete-drag case.

Table 1. The measured temperature dependence of $1/\tau_{ep}(T)$ in representative disordered metals. The sample dimensionality is with respect to the phase-breaking length L_ϕ. The experimental temperature, $T^*_{\rm mea}$, denotes the representative temperature regime where the e–ph scattering was found to be predominant in the measurement. The value of $q_T l \approx k_B T l/\hbar v_s$ in each sample is *calculated* using the average (bulk) speed of sound for that particular metal.

Sample	l (Å)	$T^*_{\rm mea}$ (K)	$q_T l$	$\tau_{ep}^{-1}(T)$	References
Au (1D), Au (2D)	100	(5)[a]–25	3.8–19	T^3	[190]
Cu (2D)[b]	2200	0.025–0.32	0.20–2.6	T^3	[191]
Nb (2D)	12	(5)[a]–20	0.36–1.4[e]	T^3	[192]
Al (2D)	61	1.5–6	0.24–1	T^3	[193]
$Cu_{1-x}O_x$ (3D)	11	1.5–20	0.06–0.8	T^3	[166]
Au (2D)[b]	25.4	0.2–1	0.04–0.19	T^3	[194]
CuCr (3D)[b]	368	0.5–10	0.68–14	T^2	[195]
CuCr (2D)[b]	103	0.5–10	0.19–3.8	T^2	[195]
CuCr (1D)[b]	76	0.5–10	0.14–2.8	T^2	[195]
Au (2D)	39	(5)[a]–20	1.5–5.9	T^2	[196]
W (2D)	38	(5)[a]–30	0.48–2.9	T^2	[197]
Au (2D)[b]	4	0.3–20	0.01–0.6	T^2	[198]
$Ti_{73}Al_{27}$ (3D)	2	(3)[c]–22	0.02–0.15	T^2	[82]
Li (1D)[d]	400	1.6–5.5	1.4–4.8	T^2	[199]
Li (1D)[d]	200	0.1–8	0.044–3.5	T^2	[200]
Hf (2D)[b]	9.4	0.04–0.7	0.0025–0.044[e]	T^4	[179]
Ti (2D)[b]	23	0.1–0.5	0.01–0.05[e]	T^4	[179]
Bi (2D)	25	0.6–1.2	0.11–0.22	T^4	[171]

[a] Below this temperature, the Nyquist electron–electron scattering and/or a 'saturation' of τ_ϕ was predominant, while above around this temperature, e–ph scattering determined the total dephasing.
[b] τ_{ep} was extracted from electron heating measurements. In [198], τ_{ep} was determined using both heating and magnetoresistance measurements; the values determined from these two methods agreed very well with each other.
[c] Much below this temperature, the scattering due to superconducting fluctuations became noticeable, while above around this temperature, e–ph scattering dominated the total dephasing.
[d] Strictly speaking, the inelastic mechanism that leads to the T^2 temperature dependence of the electron scattering rate in Li wires is still not understood. It might be due to e–ph scattering or another yet to be identified inelastic process.
[e] This value of $q_T l$ was calculated using the transverse speed of sound.

The central result of this new Sergeev–Mitin theory is that it can explain (to a certain extent) several experimental features of $1/\tau_{ep}$ that were not understood previously in terms of the standard Pippard–Rammer–Schmid theory [22, 48]. For example, this new theory explains satisfactorily the variation of $1/\tau_{ep} \sim T^2 l^{-1}$ found in $Ti_{100-x}Al_x$ and $Ti_{100-x}Sn_x$ alloys [32, 173]. This theory also provides a qualitative basis for understanding the different disorder behaviours of $1/\tau_{ep}$ found in different alloys. Recently, Lin and co-workers have found that the behaviour of $1/\tau_{ep}(T, l)$ widely varied when different impurity atoms (Al, Sn, Sc, Ge, etc) were gradually introduced into a titanium host [32]. According to this new theory, the total amount of disorder (i.e. ρ_0 in three dimensions and $R_\Box$ in two dimensions) is *not* the only significant factor in establishing the temperature and disorder dependences of $1/\tau_{ep}$. The microscopic properties (e.g. the nature of the imperfections) should also play a critical role. In addition, this theory raises the issue that the clean-limit condition of $q_T l \gg 1$ was *not* satisfied in many existing measurements that reported a seemingly $1/\tau_{ep} \propto T^3$ dependence, and hence they should *not* be explained in terms of electron–longitudinal-phonon scattering. Indeed, tables 1 and 2 indicate that most previous experiments actually dealt with samples falling in the intermediate-disorder regime of $q_T l \sim 1$.

Table 2. Measured temperature and disorder dependences of $1/\tau_{ep}(T,l)$ in representative disordered metals. The sample dimensionality is with respect to the phase-breaking length L_ϕ. The experimental temperature, $T^*_{\rm mea}$, denotes the representative temperature regime where the e–ph scattering was found to be predominant in the measurement. The value of $q_T l \approx k_B T l/\hbar v_s$ in each sample is *calculated* using the average (bulk) speed of sound for that particular metal.

Sample	l (Å)	$T^*_{\rm mea}$ (K)	$q_T l$	$\tau_{ep}^{-1}(T,l)$	References
Mg (2D)	6–19	4–20	0.070–1.1	$T^2 l^0$	[184]
Ag (2D)	12–28	4–20	0.24–2.9	$T^2 l^0$	[184]
Au (2D)	10–65	4–20	0.30–10	$T^2 l^0$	[184]
$Ti_{100-x}Al_x$ (3D)	2.9–7.2	(3)[a]–15	0.023–0.28	$T^2 l^{-1}$	[173]
$Ti_{100-x}Sn_x$ (3D)	2.8–4.2	(3)[a]–15	0.021–0.16	$T^2 l^{-1}$	[32]
$Au_{50}Pd_{50}$ (3D)	3.7–12	(5)[b]–20	0.12–1.6	$T^2 l$	[94]
$V_{100-x}Al_x$ (3D)	1.7–2.5	(4)[a]–20	0.022–0.16	$T^2 l$	[183]
Nb (2D)[c]	8–15	1.5–15	0.05–0.85	$T^2 l$	[186]
Sb (2D)	10–54	(10)[d]–20	0.7–7	$T^2 l$	[187]
$Ti_{100-x}Sn_x$ (3D)	5.9–9.7	(3)[a]–15	0.047–0.38	$T^3 l^{-1}$	[32]
$Ti_{100-x}Ge_x$ (3D)	3.2–8.0	(3)[a]–15	0.025–0.31	$T^{3,4} l^0$	[32]
Sb (2D)[c]	50–500	1.3–4.2	0.43–14	$T^{1.4} l^0$	[172]
Sb (3D)	14–40	(3)[b]–14	0.28–3.7	$T^{2.4} l^0$	[201]

[a] Much below this temperature, the scattering due to superconducting fluctuations became noticeable, while above around this temperature, e–ph scattering dominated the total dephasing.
[b] Much below this temperature, a 'saturation' of τ_ϕ was appreciable, while above around this temperature, e–ph scattering dominated the total dephasing.
[c] τ_{ep} was deduced from electron heating measurements.
[d] Below this temperature, the Nyquist electron–electron scattering and/or a 'saturation' of τ_ϕ was predominant, while above around this temperature, e–ph scattering determined the total dephasing.

The importance of the Umklapp process. Largely inspired by the experimental observations of $1/\tau_{ep} \propto T^2 l^{-1}$ in dilute $Ti_{100-x}Al_x$ and $Ti_{100-x}Sn_x$ alloys [32, 173], Jan *et al* [188] have very recently studied the e–ph interaction in impure metals, focusing particularly on polycrystalline, substitutional alloys. Analysing the $Ti_{100-x}Al_x$ data, they noticed that the alloys showed the property $l^{-1} \propto x$, which implies that $1/\tau_{ep} \propto x$. Jan *et al* therefore suggested that it is the Al-related substitutional disorder that enhances the e–ph interaction. They considered the additional contribution due to the Umklapp process of impurity scattering, which was neglected in all previous nearly free-electron calculations but which is important for the present problem. That is, Jan *et al* included in their full treatment of impurity scattering the Fourier components of the impurity potential at wavevectors of magnitude $\sim O(2\pi/a)$, where a is the lattice constant. They found that, as a result of including the Umklapp process, the scattering rate in the dirty limit $q_T l \ll 1$ is enhanced by disorder due to substitutional impurities and random lattice shift of crystallites. To within a factor of order unity, their result for the e–ph scattering rate in impure polycrystalline metals is given by [188]

$$\frac{1}{\tau_{ep}} \sim \frac{3\pi^2}{4}\frac{(k_B T)^2 \beta_l}{\hbar^2 k_F^2 l v_l}\left[1 + 2\left(\frac{v_l}{v_t}\right)^3\right]. \tag{37}$$

Notably, this equation predicts a temperature and disorder dependence of $1/\tau_{ep} \sim T^2 l^{-1}$ in the dirty limit of $q_T l \ll 1$. For a typical impure metal with $k_F \sim 1.5 \times 10^{10}$ m^{-1}, $v_l \sim 4 \times 10^3$ m s^{-1}, $v_l/v_t \sim 2$, and $\beta_l \sim 0.1$, equation (37) predicts a scattering rate of $1/\tau_{ep} \sim 0.25\, T^2 l^{-1}$ (in MKS units). This theoretical value is in reasonably good agreement with experimental results of figures 17(*a*) and (*b*). It should be noted that the underlying physics of the e–ph interaction invoked by Jan *et al* [188] is entirely different from that investigated

by Sergeev and Mitin [95,96]. Further investigations are needed to clarify the advantages and disadvantages of each theory.

3.1.4. Further discussion of experimental $\tau_{ep}(T, l)$. The temperature and mean free path variations of $\tau_{ep}(T, l)$ depend strongly on the disorder and dimensionality of the sample under study. Whether the e–ph interaction falls in the clean or dirty limit is determined by the parameter $q_T l \approx k_B T l/\hbar v_s$. For typical metals, the average sound velocity lies between about 2000 and 4000 m s^{-1}. Then, $q_T l \approx$ (3.3–6.5) $\times 10^7\, Tl$ (in MKS units), and samples that have an electron mean free path of the order of several tens (hundreds) of ångströms will fall in the intermediate (clean) regime at a few kelvins. To fall safely in the dirty limit at a few kelvins, samples with a mean free path of the order of the interatomic spacing are required. On the other hand, samples with an electron mean free path of several hundreds of ångströms or longer will hardly be in the dirty limit, even at sub-kelvin temperatures.

We have collected the relevant sample parameters (electron mean free path, measurement temperature, $q_T l$) for a number of experiments that have reported temperature and/or mean free path dependences of τ_{ep} in disordered metals and alloys. Table 1 lists those experiments where only the temperature dependence of τ_{ep} was reported, while table 2 lists those experiments where both the temperature and disorder dependence were studied. The important features revealed in these two tables are characterized as follows.

(a) *The T^4 law.* We have discussed that the theoretically expected T^4 temperature dependence of $1/\tau_{ep}$ in the dirty limit has been scarcely seen in experiments. Very recently, using thermal conductance measurements, Gershenson *et al* [179] have found a $1/\tau_{ep} \propto T^4$ dependence in ultrathin disordered superconducting Hf and Ti films between 0.04 and $\lesssim$0.7 K. Their films were deposited by dc magnetron sputtering on sapphire substrates. The dirty-limit condition of $q_T l \ll 1$ was *well* satisfied in their films (see table 1). In addition, the acoustic impedances of Hf and Ti were close to the impedance of the sapphire substrate, so vibrations of the film–substrate interface were expected to be identical to the phonon modes in the film. They found both the magnitude and temperature dependence of the measured τ_{ep} to be in close agreement with the prediction of equation (35). Their result is plotted in figure 20. Essentially for the first time in the literature, this measurement confirms the T^4 temperature dependence expected from theory. Surprisingly, however, close inspection of figure 20 indicates that, at higher temperatures, between about 0.7 and 1 K, the measured power law for the temperature dependence became *slower* than the T^4 law. In the Hf films, a deviation from the T^4 law was already appreciable at 0.7 K where $q_T l \approx 0.04 \ll 1$. Such a noticeable deviation, occurring in a regime where the condition for the dirty limit is well satisfied, is not understood and might signify the incompleteness of the current theory. Previously, a dependence $1/\tau_{ep} \propto T^4$ was found in Bi thin films over a very limited temperature range of 0.6–1.2 K [171].

(b) *The T^2 law.* Experimentally, a quadratic temperature dependence of $1/\tau_{ep}$ is frequently found in weak-localization studies in one-dimensional [199, 200, 202], two-dimensional [84,184,186,197,198,203], and three-dimensional [26,94,204–206] samples. In addition, there exist several measurements of the tunnelling electronic density of states [207] that suggest an Eliashberg function $\alpha^2 F(\omega) \propto \omega$, where ω is the phonon frequency. An Eliashberg function linear in ω implies an inelastic e–ph scattering rate[14] $1/\tau_{ep} \propto T^2$. In a series of carefully designed electron heating measurements on CuCr films of different thickness and width, DiTusa *et al* [195] found a dependence $1/\tau_{ep} \propto T^2$ between 0.5 and 10 K, *independent* of the phonon dimensionality and the level of disorder in the film (see

[14] The temperature dependence of $1/\tau_{ep}$ is determined by the frequency behaviour of the Eliashberg function $\alpha^2 F(\omega)$ through the relation $1/\tau_{ep} = (4\pi/\hbar) \int \mathrm{d}\omega\, [\alpha^2 F(\omega)/\sinh(\hbar\omega/k_B T)]$. In general, an $\alpha^2 F(\omega) \propto \omega^s$ would result in a scattering rate $1/\tau_{ep} \propto T^{s+1}$, where s is a positive integer; see, for example, [208] and [170].

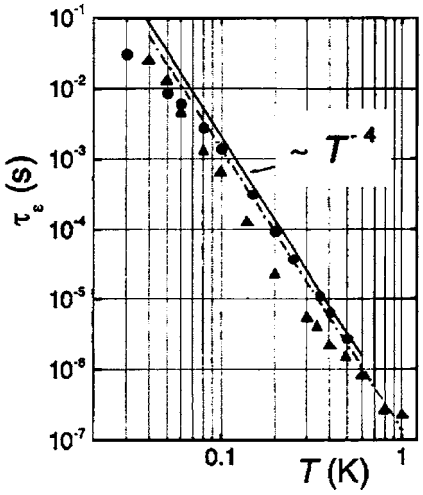

Figure 20. The temperature dependence of the e–ph scattering time (labelled as $\tau_\mathcal{E}$ in the figure) for a 250 Å thick Hf film with $R_\square(1\text{ K}) = 38\ \Omega$ (triangles), and a 200 Å thick Ti film with $R_\square(1\text{ K}) = 14.7\ \Omega$. The dashed and solid lines represent the predictions of equation (35) for Hf and Ti, respectively. This figure was reproduced with permission from [179]. Copyright 2001 by the American Physical Society.

table 1). They concluded that quantization of the phonon spectrum due to the influence of the finite sample dimensions has *no* effect on the temperature dependence of $1/\tau_{ep}$. Interestingly, Trudeau and Cochrane [205] found in a series of paramagnetic amorphous Zr–Fe alloys an inelastic scattering rate $1/\tau_\text{i} \propto T^2$ over the very wide temperature range of 4–77 K. This inelastic rate is probably due to e–ph scattering.

Figure 21 shows the inelastic scattering time τ_i and energy relaxation time $\tau_\mathcal{E}$ as a function of temperature for a 75 Å thick, highly disordered Au film measured by Dorozhkin and Schoepe [198]. The value of τ_i was extracted from weak-localization magnetoresistance measurements, while the value of $\tau_\mathcal{E}$ was extracted from electron heating measurements. It is clearly seen that, above ~5 K, e–ph scattering dominates the dephasing and $1/\tau_\text{i} \approx 1/\tau_{ep} \propto T^2$. On the other hand, below ~5 K, the two-dimensional Nyquist e–e scattering dominates the dephasing and $1/\tau_\text{i} \approx 1/\tau_{ee} \propto T$. Between 0.3 and 2 K, the measured energy relaxation time $\tau_\mathcal{E}$ is *much longer* than the Nyquist dephasing time, and demonstrates a T^{-2} temperature dependence. Most remarkably, the measured $\tau_\mathcal{E}$ clearly coincides with a low-temperature extrapolation of the τ_i data from above 5 K. This proves that e–ph scattering both determines $\tau_\mathcal{E}$ and, at high temperature, limits phase coherence. This figure also illustrates that, at low temperatures, the Nyquist e–e dephasing time is much shorter than the energy relaxation time.

Experimentally, measurements of the electron mean free path dependence of τ_{ep} are much more difficult than studies of the temperature dependence, and there have been few successful measurements on the disorder dependence of $1/\tau_{ep}$ over a wide range of l. Peters and Bergmann [184] found an inelastic scattering rate $1/\tau_{ep}$ that scales with (or, quite close to) T^2 in many quench-condensed metal films, including Mg, Ag, and Au. However, they did *not* observe *any* disorder dependence even when the sample resistivity was varied by more than a factor of ~6 (see table 2). Figure 22 shows a plot of the inelastic scattering field $H_\text{i} = \hbar/4\pi D\tau_\text{i}$ at 9.5 K as a function of low-temperature resistivity for two series of Au thin films measured by Peters and Bergmann [184]. A linear dependence of H_i on ρ is clearly seen in figure 22, implying that τ_i is independent of l. (In this experiment, $1/\tau_\text{i}$ corresponds to $1/\tau_{ep}$.)

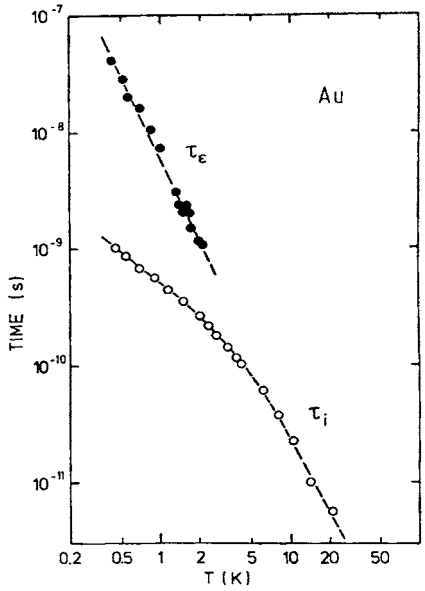

Figure 21. The inelastic scattering time τ_i and energy relaxation time $\tau_\mathcal{E}$ as a function of temperature for a 75 Å thick, highly disordered Au film. τ_i was determined from weak-localization magnetoresistance measurements, while $\tau_\mathcal{E}$ was determined from electron heating measurements. This figure was reproduced with permission from [198].

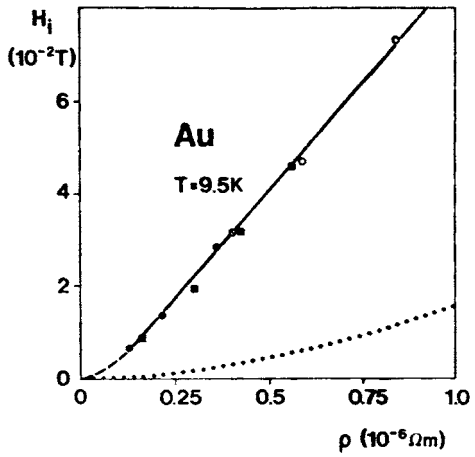

Figure 22. The inelastic scattering field $H_i = \hbar/4\pi D\tau_i$ at 9.5 K for several Au films as a function of the resistivity of the film. The circles denote a series of films deposited in several steps to vary thickness, while the squares denote a series of as-prepared and subsequently annealed films. The dotted curve gives the theoretical prediction for H_i assuming two-dimensional Nyquist electron–electron scattering. The solid curve drawn through the data is a guide to the eye. This figure was reproduced with permission from [184].

Belitz and Sarma [50] have argued that, in thin-film experiments like that shown in figure 22, the extraction of $1/\tau_{ep}$ could be combined with a non-negligible $1/\tau_{ee}$ (equation (26)) and it might also be complicated by a mixed phonon dimensionality [50]. Nevertheless, Bergmann *et al* [170] pointed out that the contribution from the two-dimensional Nyquist e–e scattering

can be clearly separated in their measurements. Therefore, they asserted that the quadratic temperature dependence of $1/\tau_i$ (i.e. $1/\tau_{ep}$) remains a theoretical challenge.

In one-dimensional Li wires at cryogenic temperatures, an inelastic scattering rate $\propto T^2$ was independently observed by Licini *et al* [200] and Moon *et al* [199]. Since in these two experiments the electron mean free path was 200 and 400 Å, respectively, the e–ph interaction in these wires fell in the intermediate-disorder regime of $q_T l \sim 1$. The reason for the observed T^2 dependence of $1/\tau_i$ therefore requires further clarification.

(c) *The $T^2 l$ dependence.* Disordered A15 compounds continue to be an interesting subject in condensed-matter physics due to their unusual normal-state electrical transport properties. However, despite the fair amount of investigation conducted, the e–ph scattering time in superconducting A15 compounds (in the normal state) has not been measured. Very recently, Meikap and Lin [183] have measured τ_{ep} in a series of disordered $V_{100-x}Al_x$ alloys whose composition is close to the superconducting A15 V_3Al compound. Their alloys have an extremely small value of $q_{ph} l \approx (0.005\text{–}0.008)\, T$, where T is in kelvins. They obtained a scattering rate $1/\tau_{ep} \propto T^2 l$. In fact, similar temperature and disorder dependences of $1/\tau_{ep}$ have recently been reported in three-dimensional $Au_{50}Pd_{50}$ [94] and $Ag_{40}Pd_{60}$ [182] films, and two-dimensional Sb [187] and Nb [186] films (see table 2). These observations of a quadratic temperature, and linear mean free path, dependence *cannot* be explained in terms of existing theories [22, 95, 96, 188].

In the case of semiconductor structures, an increasing e–ph scattering rate $1/\tau_{ep}$ with increasing disorder has been observed in GaAs/AlGaAs heterostructures by Mittal *et al* [209] and Chow *et al* [210].

(d) *The T^3 law.* A dependence of the e–ph scattering rate $1/\tau_{ep} \propto T^3$ has been obtained in numerous systems, including one-dimensional [190], two-dimensional [190, 191, 194], and three-dimensional [85, 166, 167, 211] samples. For decades, a measured T^3 temperature dependence has often 'intuitively' been ascribed to energy relaxation due to longitudinal phonons in the *clean* limit. However, for example, inspection of table 1 indicates that this is *rarely* the case. On the contrary, most existing measurements that have reported a T^3 temperature dependence have had a value of $q_T l \sim 1$, instead of $q_T l \gg 1$. According to Sergeev and Mitin [95, 96], such a T^3 temperature dependence actually suggests the intermediate-disorder regime for transverse phonons. It is worth noting that, even in the very widely accepted experiment of Roukes *et al* on Cu films [191], where the mean free path $l \approx 2200$ Å was extremely long and a rate $1/\tau_{ep} \propto T^3$ was found, the condition for the clean limit was *barely* satisfied (see table 1). This was due to the fact that these authors focused their measurements at sub-kelvin temperatures.

(e) *The intermediate-disorder regime.* We have discussed extensively that the experimentally determined values of $1/\tau_{ep}$ are often in disagreement with theoretical predictions in the dirty limit. Since the dependence of $1/\tau_{ep}$ on temperature and disorder is non-monotonic over a wide range of T and l, it is also important to test the theoretical prediction for the intermediate-disorder regime. Lin *et al* [201] have recently measured the e–ph scattering rate $1/\tau_{ep}$ in a series of three-dimensional Sb films. The semi-metal Sb was chosen because its mean free path l is relatively long, compared with that in a normal metal. (The high resistivity in Sb arises mainly from a low carrier concentration, instead of a short mean free path.) Figure 23(a) shows the electron dephasing rate $1/\tau_\phi$ as a function of temperature for two thick Sb films. By comparing the measured $1/\tau_\phi(T)$ with equation (10), the authors found that the inelastic contribution $1/\tau_i \approx 1/\tau_{ep} \propto T^p$ in their samples to be best described with an exponent of temperature $p \approx 2.4$. This value of p is different from that ($p \approx 2$ or 4) expected for the dirty limit. This non-integer temperature exponent was ascribed to the fact that their Sb samples had $q_T l \approx 0.2\, T$ (T in kelvins), and hence these films fell in the

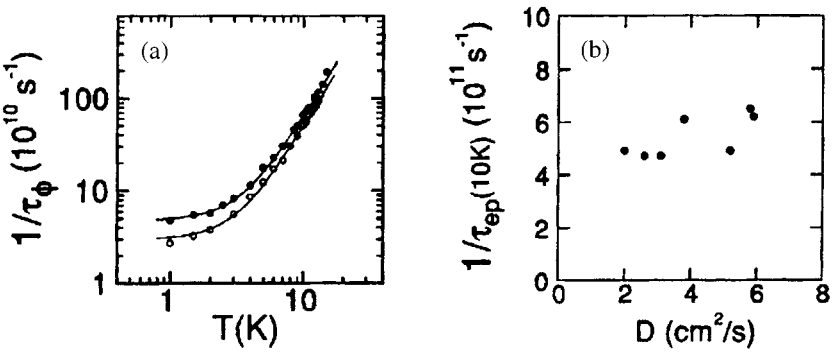

Figure 23. (*a*) Variation of the electron dephasing rate $1/\tau_\phi$ with temperature for two 3000 Å thick Sb films with $\rho_0 = 1130$ (●), and 1650 (○) $\mu\Omega$ cm. The solid curves are least-squares fits to equation (10) with the exponent of temperature $p \approx 2.4$. (*b*) Variation of the e–ph scattering rate at 10 K, $1/\tau_{ep}$(10 K), with diffusion constant D for several Sb thick films having $q_T l \sim 1$. This figure was reproduced with permission from [201]. Copyright 2000 by the American Physical Society.

intermediate-disorder regime with respect to the e–ph interaction. Lin *et al* also found that $1/\tau_{ep}$ is essentially *insensitive* to disorder (figure 23(*b*)), in contrast to the case for the dirty limit where a strong dependence on l is expected. Equations (29) and (31) indeed predict a $1/\tau_{ep}$ insensitive to the mean free path with no unique value of p (which can vary from 2 to 4), in the intermediate-disorder regime. However, Lin *et al* found that the theoretical value was about 3–4 orders of magnitude lower than their experimental value. Their result might suggest the incompleteness of the theory. Apart from the experiment of Lin *et al*, it has been suggested Il'in and co-workers [212] that the theory and experiment were in agreement in NbC thin films in the intermediate regime, over a wide temperature interval.

(f) *Effect of phonon dimensionality.* When one is concerned with low-temperature problems involving thermal phonons, it is important to be sure about the effective phonon dimensionality before a quantitative analysis of $1/\tau_{ep}$ can be made. The thermal phonons are three dimensional if their wavelength q_T^{-1} is shorter than the thickness of the metal film under study. Under the opposite conditions, the thermal phonons are two dimensional. Since $q_T^{-1} \propto T^{-1}$, a dimensional crossover from two dimensional to three dimensional could arise in a given sample on increasing the temperature. For a typical sound velocity of $v_s \approx 3000$ m s^{-1}, the thermal phonon wavelength $2\pi q_T^{-1} \approx 1400\, T^{-1}$ Å. In the case of 'supported' metal films (wires), the problem of the phonon dimensionality is complicated by the acoustic transparency between the film (wire) and the substrate. In connection with the possible variation of phonon dimensionality, there is long-standing interest in whether acoustic phonon confinement might be significant in constricted geometries. Experimental investigations of electron energy relaxation using both metal films [91, 170, 195] and wires [90, 213] have been reported, but the conclusions from these studies are far from clear.

In a series of careful measurements on narrow Al wires and thin films, deposited on oxidized Si substrates, Wind *et al* [214] did not observe any evidence of a phonon-dimensionality effect. Instead, they found that the magnitude and temperature dependence of $1/\tau_{ep}$ ($\propto T^3$) is essentially the same for films and wires. In a series of Au films and wires deposited on GaAs substrates, Friedrichowski and Dumpich [190] also found that both the magnitude and temperature dependence of $1/\tau_{ep}$ ($\propto T^3$) are the same.

The influence of phonon dimensionality on $1/\tau_{ep}$ has also been studied by comparing (constricted) 'supported' and 'free-standing' films. Intuitively, it is expected that phonon

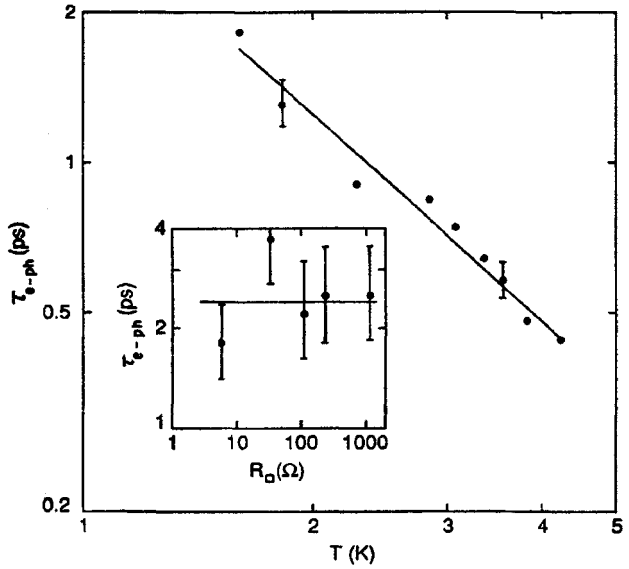

Figure 24. Electron–phonon scattering time as a function of temperature for an Sb thin film with $R_\square = 110\ \Omega$. The solid line is drawn proportional to $T^{-1.35}$. The inset shows the e–ph scattering time at 1.3 K as a function of $R_\square$ for several Sb thin films. This figure was reproduced with permission from [172]. Copyright 1991 by the American Physical Society.

confinement should be pronounced in the case of free-standing structures having free surfaces. DiTusa *et al* [195] have carried out electron heating measurements to determine $1/\tau_{ep}$ in a series of CuCr films. They examined both free-standing and (silicon nitride/silicon) supported films whose thickness and width span lengths comparable to the mean thermal phonon wavelength. As already discussed above, their measured e–ph scattering rate was proportional to T^2, independent of sample configuration (see table 1). In particular, they observed that the quantization of the phonon spectrum, expected from the sample dimensions, has *no* effect on the temperature dependence of $1/\tau_{ep}$. Kwong *et al* [193] have compared the inelastic e–ph scattering rate in several 220 Å thick free-standing Al films with nearly identical films on substrates. Although their films should have been sufficiently thin to modify the three-dimensional spectrum of the thermal phonons, they found *no significant* difference between the e–ph scattering rate in free-standing and supported films. They therefore concluded that the temperature dependence of $1/\tau_{ep}$ ($\propto T^3$) in their thin Al films is *not* strongly affected by the phonon dimensionality.

Applying an electron heating method, Liu and Giordano [172] have measured $1/\tau_{ep}$ in a series of Sb *thin* films in the intermediate regime of disorder. Their films were prepared by thermal evaporation onto glass substrates. They obtained a low value of $p \approx 1.4$ and also found that $1/\tau_{ep}$ was independent of disorder, even when the electron mean free path was changed by a factor of 10. Their observation (figure 24) is in line with the result ($p \approx 2.4$) for Sb thick films studied by Lin *et al* [201]. The temperature dependence reported by Lin *et al* in their thick Sb films can be reconciled with that of Liu and Giordano, if one takes into consideration the effect of phonon dimensionality in Sb. If the thermal phonons are effectively two dimensional in thin films but three dimensional in thick films, then it is straightforward to obtain a value of $p(\approx 2.4)$ that is raised by unity from its corresponding two-dimensional value of 1.4. Taken together, these two results of [172] and [201] suggest that the effect of phonon dimensionality is important in determining the temperature dependence of $1/\tau_{ep}$ in

Sb. (It should be noted that these two independent (but complementary) measurements applied distinct experimental methods, i.e. electron heating and weak-localization magnetoresistance techniques.)

Many of the above-mentioned measurements [172, 190, 193, 195, 201, 214] are focused on metal films and wires having the quantity $q_T l \gtrsim 1$. Apart from the film–substrate mismatch problem, it is not known whether the effect of acoustic phonon dimensionality might depend on the degree of disorder (i.e. $q_T l$) in the sample. Theoretically, the role of phonon dimensionality has often been ignored in the calculations of the e–ph scattering in impure conductors [22,95,96,188]. Further theoretical and experimental studies are needed to clarify the nature of phonon spectrum, speed of sound, and film–substrate interface in reduced-dimensional structures, as well as the effect of phonon dimensionality on the temperature dependence of $1/\tau_{ep}$ in disordered metals.

3.1.5. Comparison with three-dimensional electron–electron scattering time. In this subsection, we evaluate the small-energy-transfer Nyquist e–e scattering time, and compare this time with that expected for e–ph scattering, in typical bulk metals. For e–e scattering, Schmid [215] has given a general expression for the scattering rate in three-dimensional disordered metals, which can be expressed as

$$\frac{1}{\tau_{ee}} = \frac{\pi}{8}\frac{(k_B T)^2}{\hbar E_F} + \frac{\sqrt{3}}{2\hbar\sqrt{E_F}}\frac{(k_B T)^{3/2}}{(k_F l)^{3/2}}. \tag{38}$$

A similar expression has also been derived by Altshuler and Aronov [216]. The first term in equation (38) dominates in the pure case, while the last term dominates in the strong-disorder limit. Using typical values for the relevant parameters in a normal metal: $E_F \approx 5$ eV, and $k_F \approx 1.5\times10^{10}$ m^{-1}, one obtains an e–e scattering rate $1/\tau_{ee} \approx 9\times10^5\, T^2 + 4.7\times10^8\, (T/k_F l)^{3/2}$ s^{-1} (T in kelvins). The e–e scattering rate due to the first term is too small compared with the experimental values in, e.g., figures 5, 17, and 18, although it possesses a T^2 temperature dependence. The second term possesses a $T^{3/2}$ temperature dependence which is not consistent with the experimental results. Moreover, this latter term predicts a scattering rate that is much weaker than the e–ph scattering rate $1/\tau_{ep}(T, l)$. For example, in a disordered metal with $l \approx 10$ Å, this term will become compatible with the prediction of $1/\tau_{ep}$, e.g. equation (36) or (37), only at an extremely low temperature of $\sim$1 mK. Even in a very disordered metal with l being already of the order of the interatomic spacing, this term can become compatible with the prediction of equation (36) or (37) only at $T \lesssim 10$ mK. Therefore, it can be concluded that $1/\tau_i \approx 1/\tau_{ep} \gg 1/\tau_{ee}$ in three-dimensional conductors [24, 32, 94]. (In one or two cases [101,217,218], an inelastic scattering rate $\propto T^{3/2}$ has been reported in bulk measurements, but further studies will be needed to identify the responsible mechanism here.)

3.2. Critical electron–electron scattering time near the mobility edge

Over the years, different inelastic electron processes in three-dimensional impure conductors have been extensively studied. In addition to the e–ph scattering time in weakly disordered metals, the inelastic scattering time in *very low*-diffusivity samples has also been measured. It is often observed that the temperature and disorder dependence of the inelastic scattering rate in such samples is distinct from those discussed thus far. More precisely, an inelastic electron scattering rate (to be denoted by $1/\tau_i = 1/\tau_{EE}$) which is *linear* in temperature and *insensitive* to disorder is observed at liquid-helium temperatures.

Figure 25(*a*) shows the magnetoresistivities for a three-dimensional Sc film measured by Li and Lin [219]. This figure indicates that the weak-localization predictions, equation (3), can

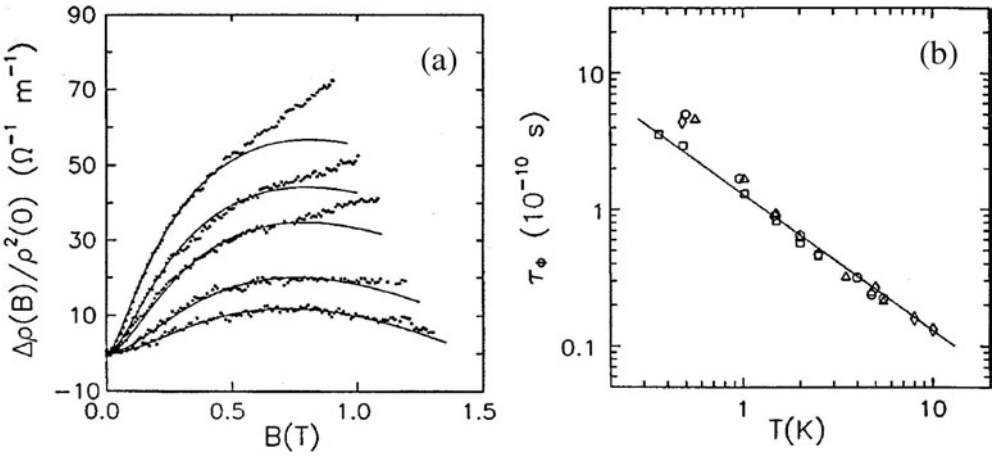

Figure 25. (*a*) Normalized magnetoresistivities $\Delta\rho(B)/\rho^2(0) = [\rho(B) - \rho(0)]/\rho^2(B)$ as a function of magnetic field for a 6310 Å thick Sc film with $\rho_0 = 119\ \mu\Omega$ cm and $D = 0.58\ \mathrm{cm^2\ s^{-1}}$, at (from the top down) 1.02, 1.50, 2.00, 3.50, and 5.50 K. The solid curves are the weak-localization predictions of equation (3). (*b*) Variation of the electron dephasing time τ_ϕ with temperature for Sc thick films with $D \approx 0.25$ (open diamonds), 0.36 (open squares), 0.58 (open triangles), and 0.59 (open circles) $\mathrm{cm^2\ s^{-1}}$. The straight line is given by 1.3×10^{-10} s and is a guide to the eye. This figure was reproduced with permission from [219]. Copyright 1997 by the American Physical Society.

describe well the low-field data, even though the sample has a very low diffusion constant of $D \approx 0.58\ \mathrm{cm^2\ s^{-1}}$. In fact, Altshuler *et al* [41, 220] and Gershenson *et al* [221] have recently demonstrated that the weak-localization theory can describe both the temperature and magnetic field dependences of the resistivity from the weak-localization regime up to the crossover to the strong-localization regime. This result of figure 25(*a*) thus asserts that equation (3) can be used to describe the magnetoresistivities in very low-diffusivity conductors.

The extracted values of τ_ϕ for four Sc thick films measured by Li and Lin are plotted in figure 25(*b*). This figure reveals a *linear* temperature dependence of $1/\tau_\phi \approx 1/\tau_{EE} \propto T$ for well over a decade of temperature from 0.3 to 10 K. This value of the temperature exponent is *significantly smaller* than that ($p \approx 2$–4) established for the e–ph scattering rate in three dimensions. Therefore, e–ph interaction cannot be responsible for the inelastic process in very low-diffusivity bulk conductors. Furthermore, the figure shows that the magnitude of $1/\tau_{EE}$ is *the same* for all films studied, regardless of the difference by a factor of ∼2.4 in the level of disorder in different films. This result is strongly suggestive of a *disorder-insensitive* dephasing mechanism operating in *three-dimensional*, *very low-diffusivity* systems.

Lin *et al* [222] have measured the temperature and mean free path dependences of $\tau_\phi(T, l)$ in a series of metallic, three-dimensional RuO_2 and IrO_2 films. Their samples were polycrystalline and made by RF magnetron sputtering. They studied a number of samples, covering the range of residual resistivity $\rho_0 \approx 160$–$410\ \mu\Omega$ cm, corresponding to the diffusion constant $D \approx 0.29$–$0.75\ \mathrm{cm^2\ s^{-1}}$. They found that their measured $1/\tau_\phi$ could be described well by equation (10) over a wide temperature range of 2–20 K. In particular, only *one* inelastic electron process was needed in their analysis to fully account for the experimental data. Their best fitted values of the exponent of temperature p for the inelastic term for all films are $p \approx 1.14 \pm 0.23$. This value of p strongly implies that the inelastic scattering rate varies *essentially linearly* with temperature in these metallic oxides. Moreover, Lin *et al* found that, at a given temperature of 10 K, the magnitude of the inelastic rate for all samples varied only between (6–9) $\times\ 10^{10}\ \mathrm{s^{-1}}$ even though the resistivities and, hence, the diffusion constants

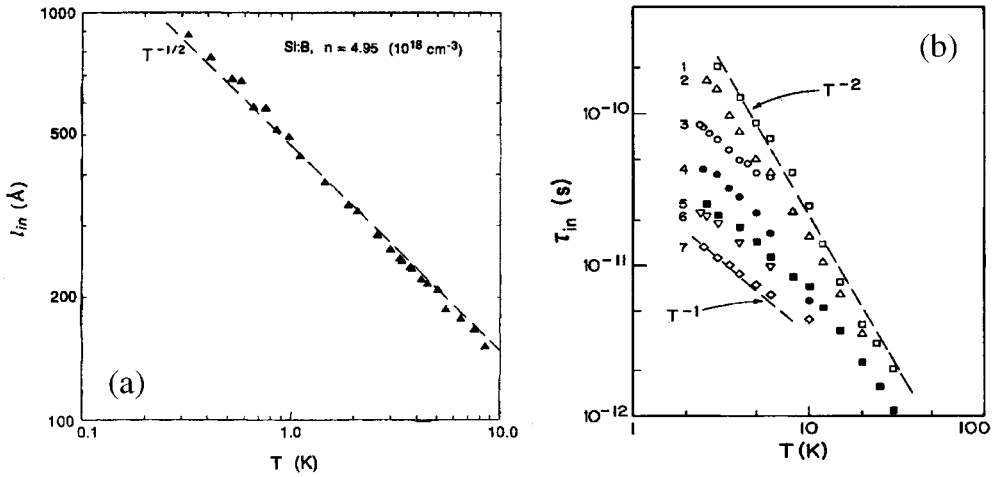

Figure 26. (*a*) Inelastic diffusion length $l_{\rm in} = \sqrt{D\tau_{\rm in}}$ as a function of temperature for a p-type Si:B bulk sample with a carrier concentration $n = 1.22\,n_c$ (n_c is the critical concentration for the metal–insulator transition). The line denotes slope -0.5, or $l_{\rm in} \propto T^{-1/2}$. This figure was reproduced with permission from [223]. (*b*) Inelastic scattering time as a function of temperature for 1 μm thick granular Al films with room temperature resistivities (from 1 to 7) 290, 520, 940, 1640, 2190, 3530, and 5800 $\mu\Omega$ cm. The solid lines drawn proportional to T^{-2} and T^{-1}, respectively, are guides to the eye. This figure was reproduced with permission from [25]. Copyright 1984 by the American Physical Society.

differed by a factor of 2.6. This latter result strongly suggests that the responsible inelastic process is *essentially insensitive* to disorder. A disorder-independent behaviour implies a non-e–ph scattering origin. If e–ph interaction were the predominant inelastic process, a noticeable dependence of the inelastic scattering rate on D should have been observed.

In the case of *three*-dimensional samples, observation of a dependence of the inelastic scattering rate (i.e. $1/\tau_{EE}$) linear in temperature has been reported in thick granular aluminium films [25], doped semiconductors [223, 224], and heavily doped conjugated polymers [225], on the metallic side of the metal–insulator transition. For instance, figure 26(*a*) shows the variation of the inelastic diffusion length $l_{\rm in} = \sqrt{D\tau_{\rm in}}$ with temperature for a p-type Si:B bulk sample which is reasonably close to the transition [223]. This figure reveals a very clear linear T variation of the inelastic electron scattering rate between 0.3 and 10 K. Recently, these observations have been attributed to e–e scattering in disordered conductors near a mobility edge. Theoretically, Belitz and Wysokinski [34] have calculated the inelastic quasiparticle lifetime due to Coulomb interaction in disordered bulk metals. Their calculation is perturbative with respect to the screened Coulomb interaction, but for an arbitrary disorder. They found that the inelastic e–e scattering is very sensitive to the 'critical' current dynamics in systems near the Anderson transition (while the current dynamics is 'diffusive' in the weakly disordered regime). In particular, they observed a linear temperature dependence of the inelastic scattering rate. They also predicted that the inelastic scattering rate should be disorder independent. Their predictions (the temperature as well as the disorder dependences) are in line with these experimental results discussed above. Quantitatively, the experimental value of the inelastic scattering rate observed in figure 25(*b*) is comparable with the theoretical predictions of Belitz and Wysokinski.

Strictly speaking, in applying the Belitz–Wysokinski theory to experiment, one should note that it may not be totally indisputable. According to their theory, a linear T dependence of the inelastic e–e scattering rate should be realized only in strongly disordered metals in

the vicinity of the metal–insulator transition. In particular, the prediction of a disorder-independent inelastic scattering time holds only in the extremely disordered regime. In the experiments performed on polycrystalline Sc [219], RuO_2, and IrO_2 [222] thick films, the transport is probably still not close enough to the mobility edge. Typically, a resistivity of a few thousand $\mu\Omega$ cm is what one would assume to be needed in order to be in the quantum-critical state, for which the Belitz–Wysokinski theory is applicable. For example, Mui *et al* have found a scattering rate $1/\tau_i \approx 1/\tau_{EE} \propto T$ in a series of granular Al thick films for which $\rho(300\ \mathrm{K}) \approx 2000$–$6000\ \mu\Omega$ cm (see figure 26(*b*)). On the other hand, as far as the *microscopic* disorder is concerned, one should realize that the polycrystalline (Sc, RuO_2, and IrO_2) thick films studied by Lin *et al* are far more homogeneous than granular, thick Al, films. In high-resistivity granular films where a linear temperature dependence of $1/\tau_i \approx 1/\tau_{EE}$ is observed, most of the resistivities are actually contributed from the grain boundaries while the metal grains might only be weakly disordered. Then, it is conjectured that the criterion for the applicability of the Belitz–Wysokinski theory might be less stringent than originally evaluated. In short, we can say that the Belitz–Wysokinski theory is the *most* (and only) plausible *existing* theory that contains the fundamental attributes (i.e. independence from disorder and a linear T dependence) seen in the experimental data shown in figures 25(*b*), 26(*a*), and (*b*)[15].

It should be stressed that the linear temperature dependence of the inelastic scattering rate discussed in this subsection is *not* due to the more familiar Nyquist e–e process in two dimensions. Here, we are concerned with samples that are *strongly* disordered and *three dimensional* with regard to the phase-breaking length L_ϕ. The *two-dimensional* Nyquist e–e process usually operates in *weakly* disordered thin films where an exponent $p = 1$ is firmly established [1, 2, 7].

Crossover from e–ph scattering to critical electron–electron scattering. From our discussions of inelastic scattering in three dimensions, we have learned that e–ph scattering dominates the dephasing in the weakly disordered regime while critical e–e scattering dominates the dephasing in the strongly disordered regime. These two inelastic processes have been observed, respectively, in many different disordered metals and semiconductors. It is thus interesting to consider whether these two dephasing processes can be seen in a *single* material system, if the level of disorder in that material can be varied sufficiently. Experimentally, several measurements have been performed in this direction. Mui *et al* [25] have studied a series of three-dimensional granular Al films with room temperature resistivities varying between 300 and 6000 $\mu\Omega$ cm. Their results for the inelastic electron scattering times are plotted in figure 26(*b*). This figure exhibits that for the samples with the lowest resistivities (samples 1 and 2) τ_i is approximately proportional to T^{-2}. Samples with higher resistivities have a weaker dependence on temperature, except near the highest measurement temperatures where their magnitude of τ_i and its temperature dependence tend to the same values for the low-resistivity specimens. These observations are very suggestive of a crossover from e–ph scattering to critical e–e scattering as the specimens approach the mobility edge. Very recently, a crossover of the inelastic scattering from e–ph to critical e–e scattering has also been reported by Lin *et al* [228] in a series of three-dimensional Cu_xGe_{100-x} films. Therefore, it is established, both theoretically and experimentally, that the inelastic electron process in impure conductors switches from the e–ph dephasing to the critical e–e dephasing as the level of disorder increases and the system approaches the mobility edge.

[15] In this subsection, we have focused our discussion on the theoretical prediction and experimental situation of the critical e–e scattering in very low-diffusivity conductors. However, it may be noted that a linear T dependence of the inelastic rate has also been predicted due to scattering of the electrons from the two-level tunnelling modes [226]. One of the difficulties with this theory is that, while it is established that tunnelling modes are predominant in metallic glasses, their existence in disordered metals is still not much explored [227].

3.3. Saturation of the dephasing time at very low temperatures

The electron dephasing time τ_ϕ is one of the most important quantities governing quantum-interference phenomena. Recently, the behaviour of the dephasing time near zero temperature, $\tau_\phi^0 = \tau_\phi(T \to 0)$, has attracted vigorous experimental [11–13, 37–39, 53, 144, 229–231] and theoretical [14, 15, 41, 42, 44, 232–240] attention. One of the central themes of this renewed interest is concerned with whether τ_ϕ^0 should reach a finite or an infinite value as $T \to 0$. The connection of the τ_ϕ^0 behaviour with fundamental condensed-matter physics problems, such as the validity of the Fermi-liquid picture [58], the possibility of the occurrence of a quantum phase transition, and also the feasibility of quantum computing, has been intensively addressed [241]. There are also works suggesting that a saturation of τ_ϕ^0 might explain the long-standing persistent current problem in metals [242, 243]. Conventionally, it is accepted that τ_ϕ^0 should reach an infinite value in the presence of only e–e and e–ph scattering. However, several recent careful measurements, performed on different mesoscopic conductors, have revealed that τ_ϕ^0 depends only very weakly on temperature, if at all, when the temperature is sufficiently low. There is *no generally* accepted process of electron–low-energy-excitation interaction that can satisfactorily explain the experimentally observed saturation of τ_ϕ^0. Furthermore, measurements have demonstrated that Joule heating, external microwave noise, and very dilute magnetic impurities *cannot* be the dominant source for the finite value of τ_ϕ^0 found in the experiments. Therefore, the microscopic origin(s) for the widely observed 'saturation' behaviour of τ_ϕ^0 remain undetermined.

Recently, Mohanty *et al* [12] have examined the dependence of τ_ϕ on temperature for many different samples over a wide range of temperature. Their observations are shown in figure 27[16]. This figure indicates that a saturation of τ_ϕ^0 occurs in both one- and two-dimensional metal and semiconductor mesoscopic structures. In spite of the very different sample properties, the saturated time for all samples seems to fall in the range of $\sim 10^{-12}$–10^{-8} s. The temperature at which the saturation first occurs depends on the sample material, the microscopic quality of the microstructures, and the sample geometry, etc. It can range from anywhere from a few tenths of a kelvin to several kelvins [244, 245]. Roughly, the lower the dephasing time, the higher the onset temperature. This observation of Mohanty *et al* immediately triggered many experimental and theoretical groups asking whether the saturation might be universal in all material (polycrystalline metal, amorphous metal, and MBE-grown semiconductor, etc) systems and all dimensions.

In this subsection, we focus our discussion mainly on the experimental aspects of this problem. We survey existing proposals for the observed saturation of τ_ϕ^0 as well as recent systematic efforts aimed at testing these proposals. Several early measurements of τ_ϕ in different metals down to about 0.1 K are also surveyed. (Experimental data on τ_ϕ in mesoscopic metals below 0.1 K were extremely limited before the recent renewed interest in the saturation problem.)

3.3.1. Electron heating and related effects. In weak-localization studies, the saturation of τ_ϕ^0 is inferred from the low-field magnetoresistance, which does *not* increase as fast as expected with decreasing temperature. As an illustration of this effect, figure 28 shows a plot of the magnetoresistance of a Au–Pd thick film at four different temperatures. The solid curve is a least-squares fit to the three-dimensional weak-localization theory, equation (3), at 6 K. A good fit is obtained in this case and, thus, the value of $\tau_\phi(6\ \mathrm{K})$ is accurately determined. Similarly good agreement between theory and experiment is obtained at all the other temperatures. However, in order to illustrate the 'unexpectedly weak' temperature

[16] It should be noted that, in the two-dimensional Au films (closed diamonds) shown in this figure, the lowest electron temperature achieved in the measurement was 20 mK [112].

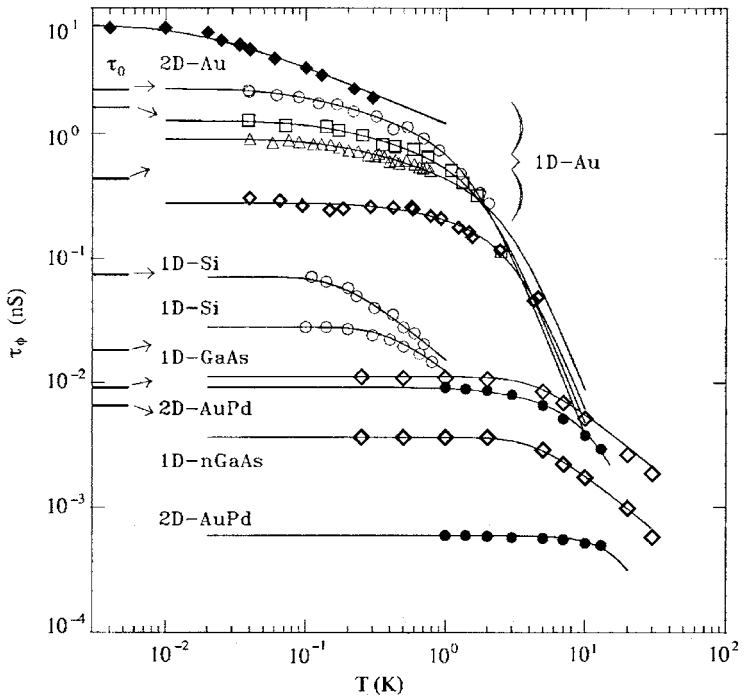

Figure 27. Temperature dependences of the electron dephasing time τ_ϕ in one- and two-dimensional Au, one-dimensional Si and GaAs, and two-dimensional Au–Pd experiments. This figure was reproduced with permission from [245].

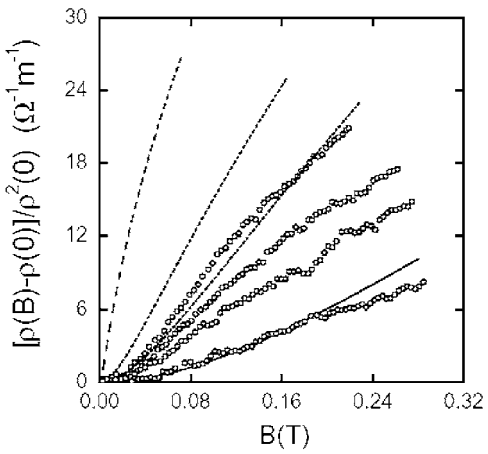

Figure 28. Normalized magnetoresistivities $\Delta\rho/\rho^2(0) = [\rho(B) - \rho(0)]/\rho^2(0)$ as a function of magnetic field at (from the top down) 0.6, 2.0, 3.0, and 6.0 K for a 4900 Å thick Au–Pd film with $\rho_0 = 473\ \mu\Omega$ cm. The solid curve is a least-squares fit to the weak-localization prediction, equation (3), at 6 K. The dashed curves are the predictions of equation (3) at (from the top down) 0.6, 2.0, and 3.0 K, assuming $1/\tau_\phi^0 = 0$ and $1/\tau_\phi \approx 1/\tau_{ep} = A_{ep}T^2$, where A_{ep} is determined from the fit at 6 K.

dependence of the magnetoresistance as $T \to 0$, the least-squares fits at 0.6, 2, and 3 K are not shown in figure 28. Instead, the dashed curves plotted are the 'extrapolated' three-

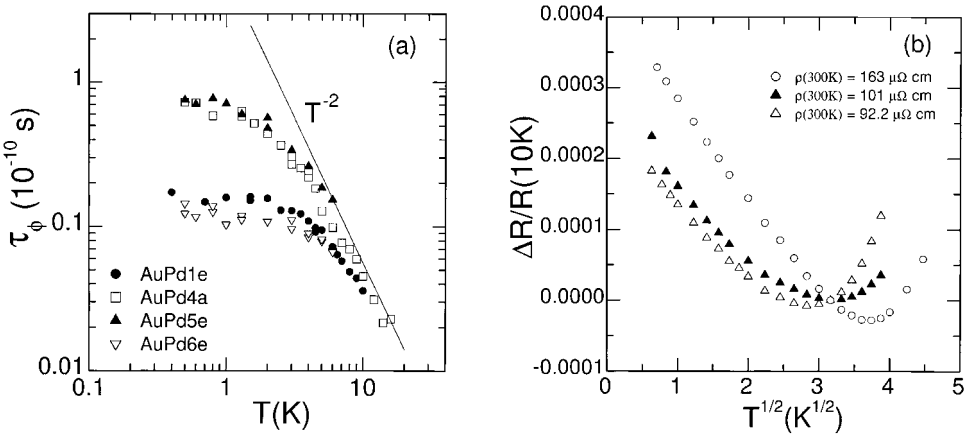

Figure 29. (*a*) Electron dephasing time τ_ϕ as a function of temperature for 6000 Å thick Au–Pd films with $\rho_0 = 124$ (Au–Pd1e), 467 (Au–Pd4a), 473 (Au–Pd5e), and 115 (Au–Pd6e) $\mu\Omega$ cm. The solid line is drawn proportional to T^2 and is a guide to the eye. (*b*) Normalized resistance $\Delta R/R(T) = [R(T) - R(10\text{ K})]/R$ (10 K) as a function of $\sqrt{T}$ for three Au–Pd thick films. This figure was reproduced with permission from [246].

dimensional weak-localization predictions at (from the top down) 0.6, 2, and 3 K, assuming that the electron dephasing is *totally* determined by e–ph scattering (i.e., $1/\tau_\phi \approx 1/\tau_{ep} = A_{ep}T^2$, where the constant A_{ep} is already given by the least-squares fit at 6 K). This figure clearly indicates that the observed temperature dependence of the magnetoresistance is *much weaker* than the theoretical prediction, implying a dephasing process that varies much more slowly than the expected T^2 law. In other words, the term $1/\tau_\phi^0$ is not zero in this case. It should be stressed that the temperature-insensitive magnetoresistance at low temperatures is found in a temperature regime where the electron gas is *in thermal equilibrium* with the phonons, i.e. the weak dependence is *not* caused by hot-electron effects, due to either the measurement current or external noise. This assertion is confirmed by the observation of a $\sqrt{T}$ rise of the resistivity with decreasing temperature down to the lowest measurement temperatures [246]. For instance, figure 29(*a*) shows the measured τ_ϕ as a function of temperature for four as-sputtered Au–Pd thick films. Comparing with figure 29(*b*), one sees clearly that the 'saturation' of τ_ϕ^0 is observed in a temperature regime where the sample resistance varies as $-\sqrt{T}$ all the way down to the lowest measurement temperature. This $-\sqrt{T}$ dependence of the resistance is well described by the three-dimensional e–e interaction theory [3]. The absence of heating effects has also been demonstrated in other studies of the saturation [11–13, 229, 247], where the sample resistance was shown to vary continuously down to very low temperatures. (For example, in the case of one-dimensional wires, the resistance was shown to increase proportionally to $1/\sqrt{T}$ all the way down to the lowest measurement temperatures [12]. The $1/\sqrt{T}$ dependence is due to one-dimensional e–e interaction effects [3].) For comparison, in the case of quasi-ballistic GaAs/AlGaAs quantum wires, Bird *et al* [122] have extracted estimates for the dephasing length from the amplitude of the universal conductance fluctuations. They found that the dephasing length remained independent of temperature below 1 K, even though the amplitude of the fluctuations themselves increased by a factor of 4 over the same range (see section 4 and figure 43).

Dephasing by high-frequency noise. Altshuler *et al* [49] have considered the dephasing of electron wave amplitudes by non-equilibrium high-frequency electromagnetic noise. They have argued that the microwave noise can already be large enough to cause dephasing, while still too

small to cause significant Joule heating of the conduction electrons. The reason for this was argued to be the presence of small-energy-transfer ($\delta\mathcal{E} \ll k_B T$), quasielastic, scattering. The phase change associated with $\delta\mathcal{E}$ accumulates with time while energy does not. Numerical evaluation of the relative strength among the dephasing power of microwaves, the cooling power of e–ph scattering, and the cooling power of electron out-diffusion into cold leads has been discussed by Altshuler *et al* [41] and Gershenson [24]. Careful experimental measurements have recently been designed to test these predictions. These experiments [230, 244, 248] explicitly demonstrated that direct dephasing due to radiation could not be the cause of the widely observed saturation. By studying Au wires exposed to an externally applied high-frequency noise, Webb *et al* [244] found that there was heating in their wires by the high-frequency noise, before it affected dephasing, i.e. *electron heating preceded dephasing by high-frequency noise*. From studying semiconductor open quantum dots in the presence of deliberately introduced high-frequency noise, Huibers *et al* [230] also reached a similar conclusion.

Burke *et al* [248] have very recently investigated the effect of externally applied *broadband* Nyquist noise on the intrinsic dephasing rate of electrons in two-dimensional GaAs/AlGaAs heterojunctions at low temperatures. Their experiment was based on the idea that the Nyquist dephasing is equivalent to the interaction of an electron with the fluctuating electromagnetic field produced by all the other electrons in the system [49]. Therefore, it was argued that applying a fluctuating electric field from an external circuit should affect the dephasing time in the same way as the fluctuating electric field produced by the sample itself. Surprisingly, however, Burke *et al* found *no major* change in the measured τ_ϕ even when their sample was subject to *large-amplitude*, externally applied, voltage fluctuations. At the same time, they also found that there was no significant change in the resistance at zero magnetic field, indicating heating to be unimportant. This measurement therefore clearly demonstrated that a broadband fluctuating electric field with a high amplitude has a *negligible* effect on dephasing. This result strongly suggests that the effect of microwave noise on electron heating and dephasing requires further theoretical clarification. It should be noted that this observation was also in contrast with the result obtained when the sample is subject to a constant-amplitude, single-frequency field. In the latter case, a suppression of weak localization (and thus, τ_ϕ) was found [244, 249]. It was suspected [248] that the effect of heating and the electric-field-induced dephasing was mingled in the latter case.

From measurements on superconductor/normal devices that were extremely sensitive to the presence of ac electromagnetic fields, Ovadyahu [43] recently argued that no evidence could be found for dephasing due to high-frequency noise. In another fairly quantitative study by Lin and Kao [13], concerned with three-dimensional polycrystalline metals, this microwave-induced dephasing picture fails as well. While Altshuler *et al* predicted a variation of the dephasing time $\tau_\phi^0 \propto D^{-1/3}$ in the most effective frequency range ($\sim 1/\tau_\phi^0$), a recent experiment by Lin and Kao found a distinct dependence of $\tau_\phi^0 \propto D^{-\alpha}$, with α close to or slightly larger than 1.

Non-equilibrium dephasing. Ovadyahu [43] has explored the possibility of *non-equilibrium* dephasing at low temperatures, using low-carrier-concentration In_2O_{3-x} and In_2O_{3-x}:Au thin films. He found that, when the bias voltage exceeds some particular value, the low-field magnetoresistance and τ_ϕ^0 can appear to saturate while the sample resistance continues to increase as $T \to 0$. On the basis of this observation, Ovadyahu argued that the bias voltage or the measuring electric field $\mathcal{F}$ affects dephasing more than heating (or, equivalently, the bias voltage or the measuring electric field affects the magnetoresistance more than it affects the resistance). Thus, it may not be sufficient to rely on $R(T)$ as a 'thermometer' and Ovadyahu instead emphasized that such a procedure is justified only in thermal equilibrium. The criterion

for ensuring thermal equilibrium is given by $e\mathcal{F}L_{\mathcal{E}} \ll k_B T$, where $L_{\mathcal{E}} = \sqrt{D\tau_{\mathcal{E}}}$ is the energy relaxation length [43]. In the case of diffusive In_2O_{3-x} films with a *low* carrier concentration ($\lesssim 10^{20}$ cm^{-3}), $L_{\mathcal{E}}$ can reach a very large value, of about 100 μm at low temperatures. (It was noted [43] that the excess electron energy was not directly relaxed through e–ph interaction in these samples.) Therefore, the equilibrium criterion might not be met if the biasing electric field is not extremely small. On the other hand, in the case of three-dimensional disordered metals, the energy relaxation is due to strong e–ph scattering and $L_{\mathcal{E}}$ is several orders of magnitude shorter than that in In_2O_{3-x}. Thus, the equilibrium criterion can be more readily satisfied in the metal samples studied in, e.g., [13] and [246].

To summarize, in this subsection, we have shown that hot-electron effects *cannot* satisfactorily explain the widely observed saturation of τ_ϕ^0 in the experiments.

3.3.2. Magnetic impurities: spin–spin scattering. Over the years, the saturation behaviour of τ_ϕ^0 has often been ascribed to a finite spin–spin scattering rate, due to the presence of a tiny amount of magnetic impurity in the sample. Such a finite scattering rate will eventually dominate over the relevant inelastic scattering in the limit of sufficiently low temperatures, equation (1). This idea of magnetic-scattering-induced dephasing immediately became widely accepted since the discovery of weak-localization effects two decades ago. On the experimental side, it is conceived that a metal mesoscopic structure can readily be contaminated with a low level (e.g. a few ppm) of magnetic impurities. Apart from possible contamination during sample fabrication and the measurement processes, oxidation of metal surfaces might also give rise to (para)magnetic moments [107, 250]. On the theoretical side, the calculation of Hikami *et al* [46] has greatly shaped the current understanding of the effect of spin-flip scattering on the weak-localization magnetoresistance. According to Hikami *et al*, magnetic scattering can lead to decoherence between the two time-reversed wave amplitudes traversing a closed loop, resulting in a suppression of weak-localization, and related quantum-interference, effects. Generally, the spin–spin scattering time τ_s is taken to be essentially independent of temperature, compared with the relatively strongly temperature-dependent e–ph and e–e scattering times. With this understanding, it is natural to interpret any saturated τ_ϕ^0 measured in the experiments[17] in terms of a finite τ_s.

In addition to many early studies that often attributed the observed saturation behaviour of τ_ϕ^0 to spin–spin scattering, there are some recent studies that also argue in favour of the role of magnetic impurities. In particular, the Saclay–MSU group [38, 39] has measured both the energy exchange rate between quasiparticles and the dephasing time of quasiparticles in several noble-metal Cu, Au, and Ag narrow wires. They found in one Ag wire (650 Å wide) and one Au wire (800 Å wide) that τ_ϕ varies as $T^{-2/3}$ down to 40 mK. (The $T^{-2/3}$ variation is expected from one-dimensional Nyquist e–e scattering, equation (45).) Comparing these two complementary measurements, they concluded that a saturation of τ_ϕ occurs only in wires that contain a small amount of magnetic impurity. In those wires where they found no anomalous energy exchange, they also found *no* sign of saturation in the dephasing time (down to 40 mK). In Cu wires (even made from a very pure source), the Saclay–MSU group *always* observed a saturation of τ_ϕ^0. They ascribed such saturation behaviour to the presence of paramagnetic oxides on the surfaces [252]. Figure 30 shows the variation of τ_ϕ with temperature for several Cu, Ag, and Au wires measured by the Saclay–MSU group.

The Saclay–MSU group has measured the electron distribution function $f(E)$ in their metal wires driven out of equilibrium by biased currents. Their experimental results have

[17] Apart from magnetic spin–spin scattering, the effect of zero-point fluctuations of impurity atoms (the scatterers) on dephasing has also been investigated in the literature [251]. However, it is found that such an effect will be absorbed in the renormalization of the static (i.e. time-independent) potential, leading to zero dephasing.

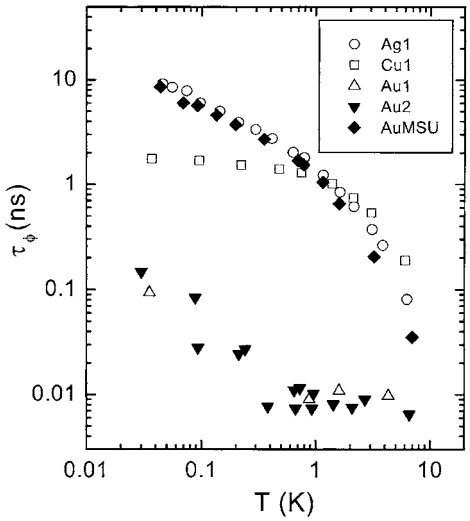

Figure 30. Electron dephasing time τ_ϕ as a function of temperature for several Cu, Ag, and Au wires. The τ_ϕ in Ag1 and AuMSU wires shows a $T^{-2/3}$ temperature dependence down to 40 mK. The Cu wire shows a saturation of τ_ϕ below 1 K. The τ_ϕ in Au1 and Au2 wires shows a rapid increase with decreasing temperature below 0.4 K, while it is insensitive to temperature between 0.5 and 10 K. This figure was reproduced with permission from [39].

triggered several theoretical studies [16, 40, 253] of the inference of one-channel and two-channel Kondo effects on the energy relaxation and dephasing rates. Very recently, they have also performed measurements of Aharonov–Bohm oscillations in small rings (in the presence of a high magnetic field), hoping to better clarify the role of magnetic impurities in dephasing [254]. It should be noted that the metal wires studied by the Saclay–MSU group are relatively clean, with a diffusion constant $D \approx 100$–$200\ \mathrm{cm}^2\ \mathrm{s}^{-1}$ [255]. In terms of their width, the wires are a factor of 10–20 wider than the narrowest wires (50 Å wide) studied by Natelson *et al* [11] to be discussed below.

Proposal for non-magnetic origin. In contrast to the conclusion reached by the Saclay–MSU group discussed above, Mohanty *et al* [12] have tested and argued for a non-magnetic origin for the saturation behaviour of τ_ϕ^0. Mohanty *et al* first studied very pure Au wires (containing less than 1 ppm of magnetic impurities), finding that there was always a saturation of τ_ϕ^0 (the one-dimensional Au wires shown in figure 27). From these measurements, they realized that both the value of τ_ϕ^0 and the onset temperature of saturation could be tuned by adjusting the sample parameters such as the wire length, resistance, and diffusion constant. To explore this idea, Webb *et al* [244, 245] reported further measurements on several carefully fabricated Au wires, whose onset temperature of saturation was indeed pushed down to very low temperatures. Figure 31 shows the variations of τ_ϕ with temperature for three of their Au wires. This figure reveals that τ_ϕ keeps increasing with decreasing temperature all the way down to 40 mK. Despite this temperature-dependent behaviour, Webb *et al* argued that τ_ϕ^0 *should still saturate* in these wires[18] at a temperature $\ll$40 mK.

To clarify the effect of magnetic scattering on τ_ϕ, Webb *et al* [12, 245] ion implanted several ppm of Fe impurities in their pure Au wires. They found that τ_ϕ decreased by more than an order of magnitude upon adding these impurities, but remained temperature dependent

[18] Very recently, a measurement on an Au wire was performed down to 35 mK by Dikin *et al* [256]. A saturation of τ_ϕ^0 was observed at the lowest temperatures, but the reason for this was not discussed.

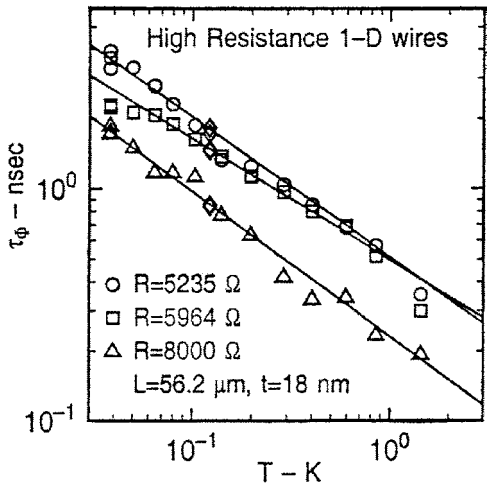

Figure 31. Electron dephasing time τ_ϕ as a function of temperature for three high-resistance Au wires. This figure was reproduced with permission from [244].

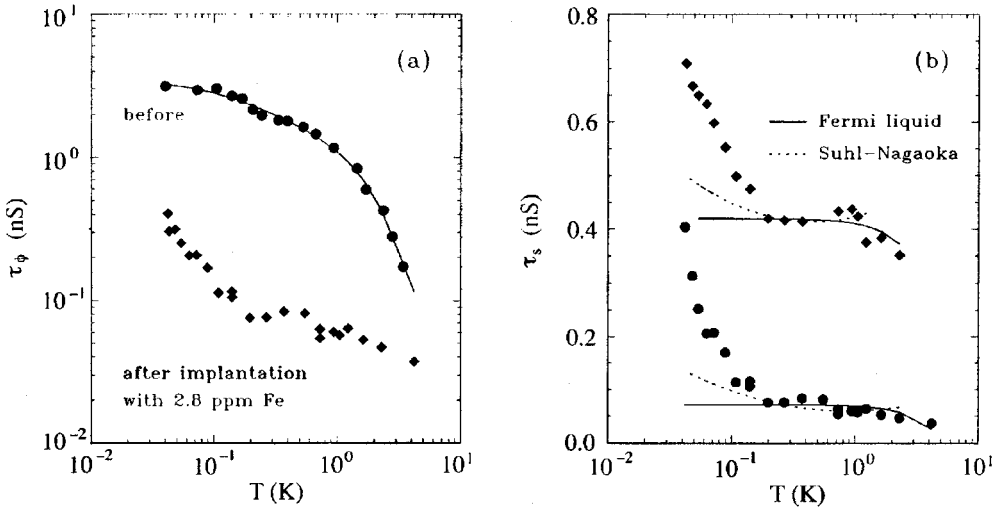

Figure 32. (*a*) The temperature dependence of the dephasing time τ_ϕ of a Au wire before and after implantation of 2.8 ppm of Fe. (*b*) The temperature dependence of the spin-flip scattering time τ_s for the same wire as shown in (*a*) and an Au wire with 7.8 ppm of Fe (top). This figure was reproduced with permission from [245].

down to 40 mK (figure 32). Therefore, they concluded that the saturation behaviour of τ_ϕ^0 observed in pure Au wires, and in those samples shown in figure 27, *cannot* be due to magnetic scattering[19]. In addition, they pointed out that saturation behaviour of τ_ϕ^0 is also often observed in semiconductor mesoscopic structures (see section 4). Since such structures are thought to contain only the smallest concentration of magnetic impurities, they concluded that the widely

[19] For Fe impurities in Au, the Kondo temperature T_K is known to be about 0.3 K. Therefore, it has been pointed out that, for such a 'high' T_K, Fe impurities cannot cause a saturation of τ_ϕ below about 100 mK ($\ll T_K$). It has also been argued that, if there exist other magnetic impurities with a much lower T_K ($\ll$0.3 K), then the associated spin–spin scattering would persist down to very low temperatures, causing a saturation in the measurement. We thank N O Birge for pointing out this argument to us.

observed saturation must be universal, and cannot be simply due to magnetic scattering. It should be noted that the sample properties of the Au wires studied by Webb and co-workers were essentially similar to those studied by the Saclay–MSU group discussed above. However, entirely contradictory conclusions regarding the low-temperature behaviour of τ_ϕ^0 were reached by these two groups.

The contradicting conclusions of the Saclay–MSU group and Webb *et al* illustrate well the subtlety and complexity of 'the saturation problem'. First, it is *not* a trivial experimental task to unambiguously determine the influence of magnetic scattering on τ_ϕ^0, because the level of magnetic contamination is probably so low that it cannot be readily detected with state-of-the-art material-analysis techniques. Secondly, since there are no known physical properties that are more sensitive to spin-flip scattering than the dephasing process, the problem of whether there is a tiny amount of magnetic contamination in the sample, thus, cannot be verified with other complementary measurements. (Very recently, it was proposed that the influence of a tiny amount of magnetic impurities may be detected by studying Aharonov–Bohm oscillations as a function of magnetic field [254].) The situation becomes even more serious when *lower-dimensional* systems are considered. In the case of low-dimensional structures, surface effects due to interfaces, substrates, and paramagnetic oxidation are likely to be non-negligible. Then, it is not straightforward to ascribe the observed saturation behaviour of τ_ϕ^0 to either intrinsic material properties or surface effects. On the other hand, this kind of ambiguity does *not* occur in carefully designed *three-dimensional* experiments. Indeed, systematic measurements of bulk samples covering a *wide* range of material properties might prove to be a powerful probe of the underlying physics of zero-temperature dephasing.

3.3.3. Systematic measurements and indications of non-magnetic origin. To resolve the underlying physics of τ_ϕ^0, the usual experimental approach of measuring the inelastic electron processes via temperature-dependent magnetoresistance studies is not very useful. In the case of inelastic scattering, the microscopic physics of the relevant electron–low-energy-excitation interactions is extracted through the measured variation of the scattering time with temperature. However, in the case of τ_ϕ^0, there is only a very weak, or no, temperature dependence involved. It is then desirable to seek variations of τ_ϕ^0 with the material characteristics of the samples, such as the amount of disorder [13], the sample geometry [11], and the effect of annealing [246]. Systematic information about the influence of material characteristics on τ_ϕ^0 should shed new light on the origins of the zero-temperature dephasing mechanism. In this subsection, we therefore discuss a few experimental measurements which have provided systematic information on τ_ϕ^0, over a *wide* range of sample properties.

Two-dimensional polycrystalline metal films. As discussed just above, an explanation for the saturation behaviour of τ_ϕ^0 based on magnetic scattering cannot be easily discerned experimentally. This experimental difficulty results in several groups insisting on the presence of magnetic impurities in the sample as the origin of saturation. In our opinion, this problem might be resolved by studying *a series of* samples covering a sufficiently wide range of sample properties. For instance, Lin and Giordano [36] performed systematic measurements of τ_ϕ^0 on a number of evaporated and sputtered films. Figure 33(*a*) shows a plot of τ_ϕ as a function of temperature for several two-dimensional Au–Pd films. This figure indicates that every film shows evidence for a saturation of τ_ϕ at low temperatures. The onset temperature of this saturation also depends on the sample (but is not well defined). Comparing with equation (1), the value of τ_ϕ^0 for each sample can be determined. Figure 33(*b*) shows the variation of their experimental τ_ϕ^0 (labelled as τ_s in the figure) as a function of sheet resistance (or resistance per square) $R_\square$ for a series of sputtered and two evaporated Au–Pd thin films. In the literature in

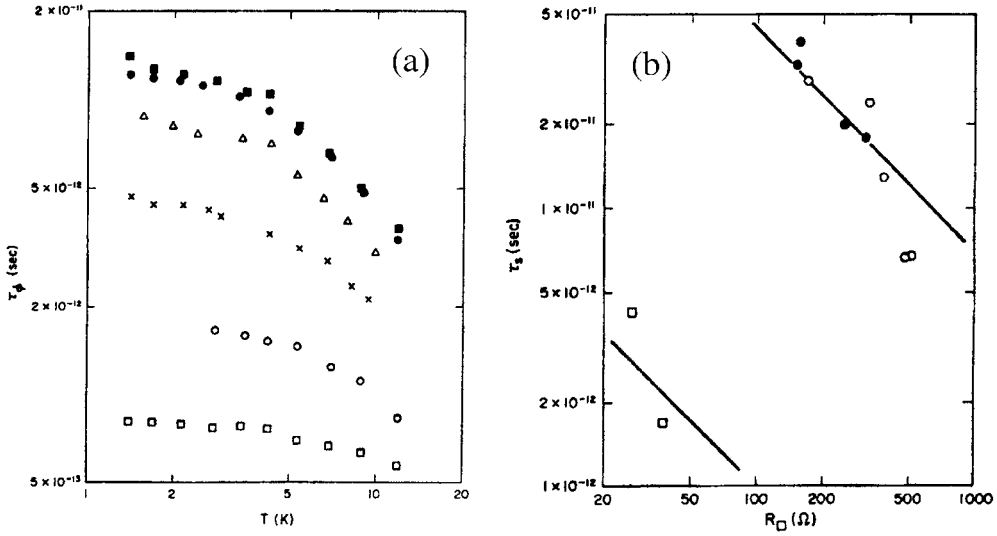

Figure 33. (*a*) Variation of the dephasing time τ_ϕ with temperature for several Au–Pd thin films: a sputtered, annealed film with $R_\square = 157\ \Omega$ (closed squares); a sputtered, annealed film with $R_\square = 153\ \Omega$ (closed circles); a sputtered, as-prepared film with $R_\square = 327\ \Omega$ (open triangles); a sputtered, as-prepared film with $R_\square = 381\ \Omega$ (crosses); an evaporated film with $R_\square = 27\ \Omega$ (open circles); an evaporated film with $R_\square = 38\ \Omega$ (open squares). (*b*) The magnitude of the 'saturated' dephasing time τ_ϕ^0 (labelled as τ_s in the figure) for several Au–Pd thin films: sputtered, as-prepared films (open circles); sputtered, annealed films (closed circles); and evaporated films (open squares). The solid lines are drawn proportional to $R_\square^{-1}$ and are guides to the eye. These figures were reproduced with permission from [36]. Copyright 1987 by the American Physical Society.

the 1980s, the saturated dephasing time was most often ascribed to spin–spin scattering and denoted by τ_s. However, on the basis of the result of figure 33(*b*), Lin and Giordano pointed out that magnetic scattering could *not* be the mechanism responsible. In particular, this figure indicates that τ_ϕ^0 (τ_s) varies approximately as $R_\square^{-1}$, where $R_\square = \rho_0/t \propto t^{-1}$, and t is the film thickness. This is quite surprising since magnetic scattering should be a 'bulk' property, and therefore not depend on t. (The effect of disorder on magnetic scattering and the Kondo effect will be discussed below.)

One might argue that if the spin–spin scattering occurred predominantly at the surface of the film, then τ_s (i.e. τ_ϕ^0) should also vary as $R_\square^{-1}$, since surface scattering would become more important as t is decreased. This speculation had been examined by Lin and Giordano. They pointed out that, in figure 33(*b*), their annealed sputtered films also fall on the same common curve as their as-prepared sputtered samples (i.e. the effect of annealing is to reduce $R_\square$ and increase τ_ϕ^0). Since annealing changes $R_\square$ but not t, these results are thus *not* consistent with an explanation involving surface scattering. While many of their samples were prepared on glass substrates, Lin and Giordano also studied several samples with quartz substrates, with the idea that perhaps the spin–spin scattering was due to magnetic impurities in the glass. However, their samples on glass and quartz substrates displayed quite similar behaviour. Since the quartz substrates contained far fewer (magnetic) impurities, this suggests that scattering from the substrate did not contribute significantly to the spin–spin scattering. From these observations, they concluded that *the observed saturation of* τ_ϕ^0 *cannot be explained in terms of magnetic scattering*. They suggested that there might be some other, hitherto *unidentified* source of electron dephasing which is both temperature independent and also dependent on the value of $R_\square$. They further suggested that the strength of the impurity scattering which is

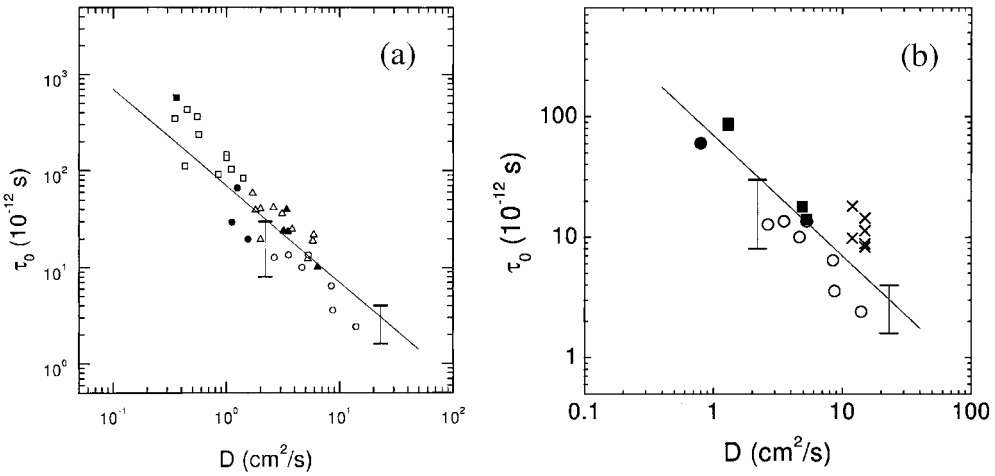

Figure 34. (*a*) Variation of the 'saturated' dephasing time τ_ϕ^0 (labelled as τ_0 in the figure) with diffusion constant for numerous three-dimensional polycrystalline metals: dc sputtered $Au_{50}Pd_{50}$ (circles), dc and/or RF sputtered $Ag_{40}Pd_{60}$ (squares), dc sputtered Sb (triangles), thermal-evaporation-deposited Au_xAl (solid triangles), thermal-evaporation-deposited $Sc_{85}Ag_{15}$ (solid squares), and arc-melted $V_{100-x}Al_x$ (solid circles). The two vertical bars at $D \approx 2.2$ and 23 $cm^2\ s^{-1}$ represent the experimental values of τ_ϕ^0 for dc sputtered and thermally evaporated polycrystalline Au–Pd thin films, respectively, taken from [36]. The solid line is drawn proportional to D^{-1} and is a guide to the eye. This figure was reproduced with permission from [13]. (*b*) Variation of the 'saturated' dephasing time τ_ϕ^0 (labelled as τ_0 in the figure) with D for polycrystalline Au–Pd samples taken from several independent experiments: circles [13], closed squares [246], crosses [11], closed circle [245], and vertical bars [36]. The solid line is drawn proportional to D^{-1} and is a guide to the eye.

responsible for τ_ϕ^0 could be very sensitive to the *metallurgical properties* of the films, which are in turn a function of both thickness and annealing, etc. Since it is accepted that TLS are closely associated with the presence of dynamical defects in the microstructures in the sample, their observation of a sensitive, metallurgical-property, influence on τ_ϕ^0 has recently inspired several theoretical studies of the interaction between electrons and TLS [14, 15].

Three-dimensional polycrystalline metals. Lin and Kao [13] have recently studied the electron dephasing times τ_ϕ in numerous *three*-dimensional *polycrystalline* disordered metals. Their samples were made of various materials, using various fabrication techniques (see the description in the caption to figure 34(*a*)). Since one of the major issues in this direction of research is to study whether or not there might exist a universal saturation behaviour of τ_ϕ^0, the use of many kinds of sample with distinct characteristics is highly desirable. Any behaviour of τ_ϕ^0 common to all these materials, if found, should bear important information on the nature of the zero-temperature dephasing. Regardless of the very different preparation and measurement conditions, the authors found in numerous normal metals that there is a saturation of τ_ϕ at sufficiently low temperatures and that τ_ϕ^0 in every sample can be determined according to equation (1). Most surprisingly, they found that their experimental τ_ϕ^0 varied with the diffusion constant D with a simple power law as

$$\tau_\phi^0 \propto D^{-\alpha}, \qquad \alpha \gtrsim 1 \tag{39}$$

where the exponent α *is close to or slightly larger than 1*.

Figure 34(*a*) shows the variation of τ_ϕ^0 with D measured by Lin and Kao. This figure indicates that the values of τ_ϕ^0 for all samples fall essentially on a universal dependence. Particularly, it reveals that all that matters in determining the value of τ_ϕ^0 is the diffusion

constant, regardless of the distinct material characteristics (e.g., electronic structure) of the various samples. This figure covers about *two decades* of D from 0.1 to 10 cm^2 s^{-1}, corresponding to the quantity $k_F l$ ranging from of order unity to of order 10. This observation of $\tau_\phi^0 \propto D^{-\alpha}$ ($\alpha \gtrsim 1$) is totally unexpected. Such a scaling behaviour cannot be coincidental and deserves a full explanation. This result implies that the saturation behaviour, e.g. the functional form of τ_ϕ^0 with respect to disorder, might be universal for a given dimensionality and a given kind of sample (e.g. polycrystalline) structure, while it might *not* be universal over different dimensionalities and different sample structures. On the contrary, it is often conjectured that τ_ϕ^0 should increase with *reducing* disorder, *at least* in one and two dimensions [12,229]. Until now, it has *not* been known exactly how differently τ_ϕ^0 should behave in different dimensionalities and in different sample structures. For comparison, the experimental τ_ϕ^0 in the as-prepared Au–Pd thin films considered in figure 33(b) are also indicated in figure 34(a) by the two vertical bars. It should be noted that these Au–Pd thin films have short electron mean free paths and are three dimensional with regard to Boltzmann transport.

The result of figure 34(a) argues against the role of magnetic scattering as the dominant dephasing process in three-dimensional polycrystalline metals as $T \to 0$. This is asserted since the numerous samples considered in figure 34(a) were made from very different high-purity sources, using very different fabrication techniques such as thermal-flash deposition, dc and RF sputtering, and the arc-melting method. The measurements were also performed at very different times over a period of more than four years. It is hard to conceive that spin-flip scattering due to 'unintentional' magnetic contamination could have caused the 'systematic' variation given by equation (39). If magnetic scattering were responsible for the measured τ_ϕ^0 in figure 34(a), then the unintentional magnetic impurity concentration n_m must vary *randomly* from sample to sample, and therefore one should expect a *random* τ_ϕ^0 ($\propto n_m^{-1}$), independent of disorder or the diffusion constant D. Moreover, any spin–spin scattering that might result from surface effects such as interfaces, substrates, and paramagnetic surface oxidation, should be largely minimized in these three-dimensional samples (while surface effects could be significantly more important in lower-dimensional systems). Therefore, the result of figure 34(a) cannot be simply explained in terms of magnetic scattering.

Figure 34(b) shows the measured τ_ϕ^0 (labelled as τ_0 in the figure) as a function of D for polycrystalline Au–Pd samples taken from five existing experiments. Au–Pd is known as a prototypical disordered metal and has been widely used to make films and wires for quantum-interference studies [11, 36, 183, 245, 246]. As a result of the *short* electron mean free path, all of the wire and film samples studied in figure 34(b) were *three* dimensional with respect to Boltzmann transport. Therefore, it is justified to compare together the variation of τ_ϕ^0 with D in the same plot. This figure indicates that τ_ϕ^0 follows closely the relation established by equation (39). Since the five experiments considered in figure 34(b) were carried out in different laboratories over a period of 15 years, this experimental observation of $\tau_\phi^0 \propto D^{-\alpha}$ is strongly indicative of an intrinsic material property. The observed saturation behaviour of τ_ϕ^0 can *by no means* be due to *random* contamination of magnetic impurities[20].

The observation of figure 34(a) is still not understood. Nevertheless, this result unambiguously indicates that the saturation of τ_ϕ^0 in this case is certainly *not* due to microwave

[20] One should notice that it is not always justified to compare the disorder behaviour of τ_ϕ^0 over thin and thick films and narrow wires made of a same material such as in figure 34(b). A comparison is only meaningful if the electron mean free path is short and surface scattering is unimportant. One should also bear in mind that while D is used to characterize the level of disorder in three dimensions, the relevant parameter is $R_\square$ in two dimensions. These two parameters, D and $R_\square$, are not entirely equivalent. The molar concentrations of Au and Pd in different experiments reported in the literature are sometimes slightly different. However, for the discussion here, there is no need to distinguish the exact compositions of the various samples used in different experiments.

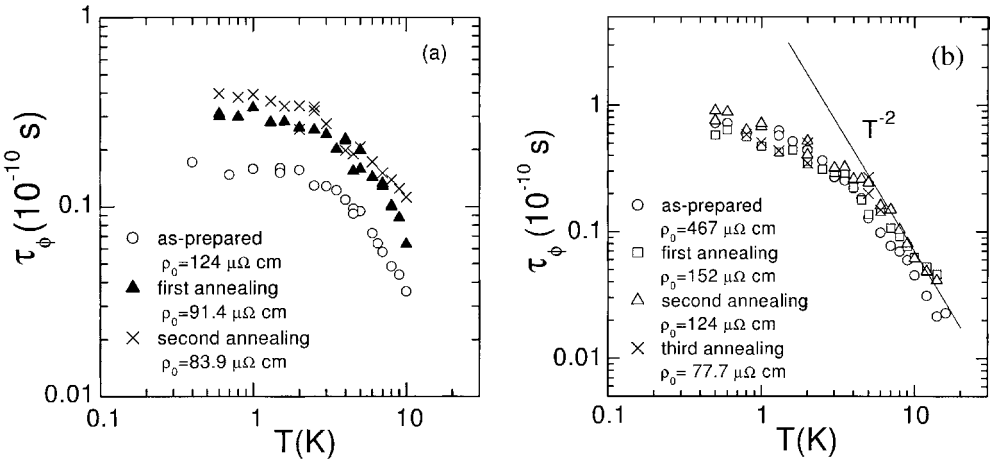

Figure 35. Electron dephasing time τ_ϕ as a function of temperature for (*a*) a 'moderately' disordered and (*b*) a 'strongly' disordered, Au–Pd thick film before and after thermal annealing. The solid line in (*b*) is drawn proportional to T^{-2} and is a guide to the eye. This figure was reproduced with permission from [246].

noises, because microwave dephasing should result in a $\tau_\phi^0 \propto D^{-1/3}$ dependence in three dimensions [49]. This observation of an essentially inverse linear dependence of τ_ϕ^0 on D rather implies an approximately 'constant' saturated dephasing length of $\sqrt{D\tau_\phi^0} \sim 1000$ Å in all samples. This in turn might imply that the more relevant quantity that governs the underlying physics of electron dephasing near zero temperature is the decoherence length $\sqrt{D\tau_\phi^0}$, or the decoherence volume $(D\tau_\phi^0)^{d/2}$ in d dimensions, instead of the dephasing time τ_ϕ^0 itself. It should also be noted that the observation of an increasing τ_ϕ^0 with decreasing D in figure 34(*a*) is not an isolated case. In fact, a similar but less quantitative behaviour has been observed by Noguchi *et al* [229] in GaAs/AlGaAs quantum wires. In their *high*-mobility GaAs/AlGaAs quantum wires, Noguchi *et al* found that τ_ϕ^0 *increased* with increasing Fermi energy E_F. In contrast, in their *low*-mobility wires, they found that τ_ϕ^0 *decreases* with increasing E_F (see section 4 and figures 42 and 44). Since D varies essentially linearly with E_F, their result concerning low-mobility wires is in line with the observation of figure 34(*a*). These observations may suggest that the behaviour of the zero-temperature dephasing can differ substantially between *clean* and *dirty* conductors.

Effect of thermal annealing: three-dimensional polycrystalline metals. The effect of thermal annealing on three-dimensional polycrystalline metals has been studied very recently. Lin *et al* [246] have performed systematic measurements of τ_ϕ on several series of *as-sputtered* and subsequently *annealed* Au–Pd and Sb thick films. Such controlled annealing measurements are crucial for testing theoretical models of dephasing that invoke the role of magnetic scattering and dynamical defects. Figure 35(*a*) shows a plot of the variation of τ_ϕ with temperature for one of the as-prepared and subsequently annealed Au–Pd thick film studied by Lin *et al*. This figure clearly indicates that τ_ϕ is increased by annealing. This effect is similar to that in metal thin films, figures 33(*a*) and (*b*). At first glance, it appears that this observation is easily explained. Suppose that annealing results in the rearrangement of lattice atoms and a relaxation of grain boundaries, thereby making the film less disordered. Because TLS are closely associated with defects in the microstructures, their number concentration, n_{TLS}, is

therefore reduced by annealing. (Theoretically, the low-energy excitations of the dynamical defects are usually modelled by TLS.) Assuming that dynamical defects are effective scatterers as $T \rightarrow 0$, one can then understand figure 35(a) in terms of a TLS picture, i.e. $\tau_\phi^0 \propto n_{\rm TLS}^{-1}$. However, it is impossible to perform a quantitative comparison of the experiment with TLS theories [14, 15]. The difficulties lie in the facts that

(i) the number concentration $n_{\rm TLS}$ in a particular sample is not known,
(ii) the strength of coupling between conduction electrons and a TLS is poorly understood, and
(iii) the dynamical properties of real defects (impurities, grain boundaries, etc) are even less clear.

Moreover, as is to be discussed below, further measurements of Lin *et al* indicate that the nature of low-temperature dephasing in polycrystalline metals is not so straightforward. They found that the effect of annealing on τ_ϕ is distinctly different in 'strongly' disordered metals. (The film considered in figure 35(a) is referred to as 'moderately' disordered since it has $\rho_0 \approx 120\ \mu\Omega$ cm before annealing, while the film considered in figure 35(b) is referred to as strongly disordered since it has $\rho_0 \approx 500\ \mu\Omega$ cm before annealing.)

In addition to the moderately disordered samples, Lin *et al* have also carried out measurements on Au–Pd thick films containing much higher levels of disorder. Surprisingly, they discovered that annealing has a *negligible* effect on τ_ϕ in *strongly* disordered Au–Pd thick films. Figure 35(b) shows the variation of τ_ϕ with temperature for a strongly disordered Au–Pd thick film. This figure clearly demonstrates that the values of τ_ϕ for the as-prepared and annealed samples are essentially the same, even though the resistance and hence the diffusion constant D are changed by the annealing by a factor of more than 6. The absence of an appreciable annealing effect in this case implies that, in addition to the usual TLS addressed above, strongly disordered films also contain other defects that cannot be readily cured by annealing. This ineffectiveness of thermal annealing might suggest that there are two kinds of TLS. On the other hand, it might also suggest that, despite a large effort in this direction, no real defects of any nature have dynamical properties which can explain the saturation of τ_ϕ^0 found in the experiments. Inspection of the large discrepancy in figures 35(a) and (b) strongly indicates that low-temperature dephasing is very sensitive to the microstructures under study[21].

We return to the issue of magnetic scattering. The result of figures 35(a) and (b) indicates that magnetic scattering should play a subdominant role, if any, in inducing the saturation of τ_ϕ^0. The reasons are given as follows:

(i) Suppose that there is a low level of magnetic contamination in the as-sputtered film. Upon annealing, the magnetic impurity concentration n_m should be left unchanged. If the original saturation in the as-sputtered sample is caused by spin–spin scattering, one should then expect the same value of τ_ϕ^0 ($\propto n_m^{-1}$) after annealing. However, the result of figure 35(a) indicates an increased τ_ϕ^0 with annealing, which is in disagreement with this assumption.
(ii) Blachly and Giordano [259] have found that the Kondo effect is very *sensitive* to disorder, namely that increasing disorder suppresses the Kondo effect. Along these lines, if the original saturation of τ_ϕ^0 found in figure 35(b) were really due to magnetic scattering, one should then argue that thermal annealing that suppresses disorder should enhance the Kondo effect. Therefore, a decreased τ_ϕ^0 should be expected with thermal annealing.

[21] Recent calculations [257] have indicated that the number concentration $n_{\rm TLS}$ needed to give the right order of magnitude for the dephasing time is significantly larger than what is found in real disordered metals. In terms of the proposal of two-channel Kondo interaction as an origin for the saturation of dephasing, an estimate of the value of the Kondo temperature is given in [258].

Since the measured τ_ϕ^0 does not change, even when the sample resistivity is reduced by a factor of more than 6 by annealing, figure 35(*b*) cannot be reconciled with a magnetic scattering scenario (especially if the effect of disorder is taken into account).

This picture of a weakened Kondo effect with increasing disorder is also incompatible with the result for the moderately disordered film considered in figure 35(*a*), where an increased, instead of a decreased, τ_ϕ^0 is found after annealing. Above all, systematic annealing measurements in both two-dimensional (figure 33(*b*)) and three-dimensional (figure 35) samples *cannot* be reconciled with magnetic scattering being responsible for the zero-temperature dephasing time found in the experiments.

It is worth noting that the saturation problem can be addressed better in three-dimensional, rather than lower-dimensional, structures. This is because of the increased contrast between the saturation and the strong dependence of $\tau_i(T)$ in three dimensions. In three dimensions, $1/\tau_i \approx 1/\tau_{ep} \propto T^p$, with $p \gtrsim 2$. Such a temperature variation is much stronger than the dominating $p = 2/3$ in one dimension and the $p = 1$ in two dimensions. (It is known that, in lower dimensions, $1/\tau_i \approx 1/\tau_{ee}$ at a few kelvins and lower.) For instance, inspection of the solid line, which is drawn proportional to T^{-2}, in figure 35(*b*) clearly reveals that the measured τ_ϕ^0 at 0.5 K is *already more than one order of magnitude* lower than would be extrapolated from the measured τ_{ep} at a few kelvins. Such a large discrepancy cannot simply be ascribed to experimental uncertainty. In contrast, in one-dimensional wires, the dominating inelastic dephasing time obeys a much weaker $T^{-2/3}$ variation, as already mentioned. In this case, any discrepancy between the measured and extrapolated values of τ_ϕ^0 would be much less dramatic in the attainable range of temperature, rendering less clear cut discrimination of the presence or not of a saturation[22] of τ_ϕ^0 as $T \to 0$.

3.3.4. Effect of sample geometry. Natelson *et al* [11] have investigated the saturation problem using thin films and narrow wires made from polycrystalline Au–Pd. The *only* parameter that was varied in their experiment was the *sample geometry* and their results are plotted in figure 36. In the 5 nm wires, they found $\tau_\phi \propto T^{-2/3}$ down to 80 mK, consistent with one-dimensional Nyquist e–e scattering. In wide films, the e–e scattering theory predicts a stronger variation, $\tau_\phi \propto T^{-1}$. However, Natelson *et al* found a very weak temperature dependence in their 1100 and 1250 nm wide films, signifying a saturation of τ_ϕ^0. This figure suggests that the sample geometry alone can be essential for the saturation behaviour of τ_ϕ^0. Natelson *et al* proposed that this observation provides a new constraint on theoretical models of saturation phenomena. They also suggested that their result for the 5 nm wires allows examination of quantum-interference phenomena in the new, molecular-length scale, while their result for wide films is consistent with that observed previously by Lin and Giordano [36].

Taken together, figure 36, along with the observation of a pronounced $\sqrt{D\tau_\phi^0} \sim 1000$ Å in three-dimensional polycrystalline metals, figure 34(*a*), seem to point to a coherent empirical picture of a more pronounced saturation of τ_ϕ^0 with increasing (higher) dimension in polycrystalline metals. This observation deserves further investigation. It is worth noting that in the 5 nm wires of Natelson *et al*, the reported L_ϕ (80 mK) is only ~1250 Å, corresponding to $D \approx 14$ cm^2 s^{-1}, and $\tau_\phi(80\text{ mK}) \approx 1.1 \times 10^{-11}$ s. This value of $L_\phi(80\text{ mK})$ is not inconsistent with the scaling relation established in figures 34(*a*) and (*b*). Such a comparison should be meaningful since the wires and films studied by Natelson *et al* had short electron

[22] There is another advantage of using bulk samples in the studies of τ_ϕ^0. Compared with the fabrication of one-dimensional wires, the preparation of three-dimensional samples usually does not require sophisticated lithographic processing, thereby greatly minimizing any (magnetic) contamination that might eventually act like a spin flipper at low temperatures.

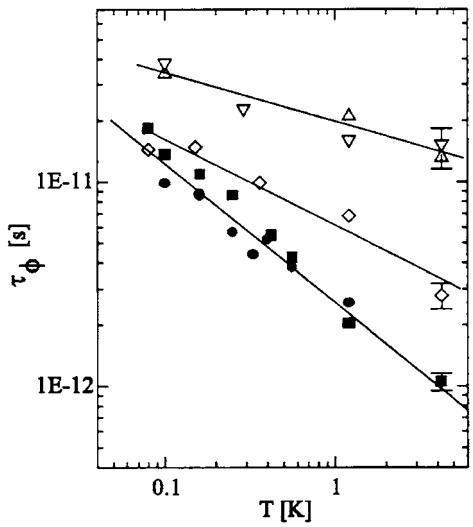

Figure 36. Electron dephasing time τ_ϕ as a function of temperature for wide and narrow Au–Pd thin films with thickness of 7.5 nm and various width of 5 (closed symbols), 200 (diamonds), 1100 (inverse triangles), and 1250 (triangles) nm. This figure was reproduced with permission from [11]. Copyright 2001 by the American Physical Society.

mean free paths and were three dimensional with regard to Boltzmann transport. In any case, it is important to notice that the dephasing time in the 5 nm wires studied by Natelson *et al* was greatly suppressed according to the relation $\tau_{ee} \propto W^{2/3}$, where W is the width of the wire (see equation (45)). Due to this sample-geometry suppression, their experimental value of τ_ϕ was still very short, even at 80 mK. It would be of great interest to carry out measurements on these wires down to lower temperatures. It would be also of decisive importance to extend their measurements to very narrow wires made of other metals, such as Cu, Ag, or Au.

Experimentally, saturation of τ_ϕ^0 has been observed in several metal wires [87, 200, 256] and rings [260–262] about 50–100 nm wide. This width is generally already small enough for the samples to exhibit one-dimensional quantum-interference effects at low temperatures. However, this width is a factor of more than ten times larger than that of the narrowest wires studied by Natelson *et al*. The result of Natelson *et al* seems to suggest that the characteristic length scale that determines the saturation behaviour of τ_ϕ^0 is significantly different from the more familiar phase-breaking length L_ϕ which determines quantum-interference effects.

3.3.5. Earlier low-temperature measurements of τ_ϕ. While we have extensively discussed the experimental observation of a finite τ_ϕ^0 as $T \to 0$ in several measurements, it should be noted that there are several two- and three-dimensional experiments[23] which do not display a clear signature of saturation down to 0.1 K. We notice that, before the recent renewed interest in the saturation problem, experimental data on τ_ϕ below 0.1 K were extremely limited in the literature. We briefly summarize these measurements below and list the values of the relevant parameters in table 3.

[23] In the case of one dimension, besides the recent works on narrow wires by the Saclay–MSU group [38, 39] and Natelson *et al* [11], Echternach *et al* [55] have measured τ_ϕ in 900 Å wide Au wires made by thermal evaporation. They found the expected $\tau_\phi \propto T^{-2/3}$ between 0.1 and 5 K. They obtained $\tau_\phi(0.1\ \mathrm{K}) \approx 0.3$ ns and $L_\phi(0.1\ K) \approx 2\ \mu$m. Since the sample parameters of this wire are similar to those of Mohanty *et al* [12] and Gougam *et al* [38], it would be necessary to perform measurements down to below 0.1 K in order to clarify whether there might be a saturation.

Table 3. Values of relevant parameters for available experiments which show no signature of saturation down to about 0.1 K or lower. The thicknesses t of three-dimensional films are listed for comparison with the measured phase-breaking length $L_\phi(T_{\min})$. $T_{\min}$ is the lowest measurement temperature in the experiment.

Sample	t (μm)	D (cm^2 s^{-1})	$T_{\min}$ (mK)	$\tau_\phi(T_{\min})$ (ns)	$L_\phi(T_{\min})$ (μm)	Reference
1D Ag		120	40	10	11	[38]
1D Au		110	40	10	10	[39]
1D Au–Pd		12	80	0.014	0.13	[11]
1D Au		135	100	0.3	2.0	[55]
2D Au		12	100	7.5	3.0	[194]
2D Bi		10–20	100	0.2–0.8	0.45–1.3	[250]
2D Bi		10	100	0.2	0.45	[218]
2D Mg		3.9	100	12	2.2	[263]
3D Bi	0.20	0.6	100	10	0.77	[26]
3D Bi	0.40	0.6	100	10	0.77	[26]
3D Bi	0.70	33	50	0.45	1.2	[27]
3D $Cu_{1-x}O_x$	1.0	6	1500	10	2.4	[166]
3D $Cu_{0.9}Ge_{0.1}$	300 [a]	—	3000	4.5	—	[211]
1D Au		—	0.04	2–4	—	[244]
2D Au		135	0.04	60	28	[245]

[a] This $Cu_{0.9}Ge_{0.1}$ sample was a drawn wire and, in this case, t refers to the diameter of the wire. The resistivity and diffusion constant for this sample were not available.

Two-dimensional films. Komori *et al* [250, 264] have measured τ_ϕ between 0.1 and 10 K in several Bi thin films about 100 Å thick. Their films were prepared by thermal-flash deposition in a *moderate* vacuum of 10^{-6} Torr onto glass substrates held at room temperature. Their films had a high sheet resistance $R_\square(4\ \mathrm{K}) \sim 1000\ \Omega$, corresponding to a residual resistivity $\rho_0 \sim 1000\ \mu\Omega$ cm. Their results are plotted in figure 37(a). Between 0.1 and 2 K, they found $\tau_\phi \propto T^{-1}$ which is due to two-dimensional Nyquist e–e scattering, while above 3 K they found $\tau_\phi \propto T^{-2}$ which was ascribed to e–ph scattering. Figure 37(a) indicates that the value of τ_ϕ increases with increasing D (see the caption to figure 37 for the values of D). The absence of saturation of τ_ϕ in this experiment was ascribed by Komori *et al* to a very high Kondo temperature such that no magnetic impurity could be formed in Bi. They obtained phase-breaking lengths $L_\phi(0.1\ \mathrm{K}) \approx 0.45$–$1.3\ \mu$m for the various films studied.

Beutler and Giordano [218] have studied a 270 Å thick Bi film made by dc sputtering onto a liquid-nitrogen-cooled glass substrate. They found no saturation of τ_ϕ down to 0.1 K. Between 0.1 and 5 K, they observed $\tau_\phi \propto T^{-3/2}$ which was ascribed to three-dimensional e–e scattering. It is not understood why the *three*-dimensional inelastic Nyquist process is observed in a *two*-dimensional (with regard to quantum-interference transport) film. They obtained a phase-breaking length $L_\phi(0.1\ \mathrm{K}) \approx 0.5\ \mu$m.

White *et al* [263] have measured τ_ϕ in a 400 Å thick Mg film which was evaporated onto a glass substrate held at 4.2 K. Between 0.1 and 10 K, they found that $\tau_\phi \propto T^{-1}$ which was ascribed to two-dimensional e–e scattering. They obtained a phase-breaking length $L_\phi(0.1\ \mathrm{K}) \approx 2\ \mu$m.

For a 110 Å thick Au film made by evaporation onto an oxidized Si wafer held at room temperature, Bozler and co-workers [194] reported $\tau_\phi \propto T^{-1}$ between 0.1 and 1 K, which was ascribed to two-dimensional e–e scattering. They obtained a phase-breaking length $L_\phi(0.1\ \mathrm{K}) \approx 2.9\ \mu$m.

It would be of great interest to perform measurements down to lower temperatures to check whether the temperature dependence of τ_ϕ in the above-mentioned metal thin films remains as

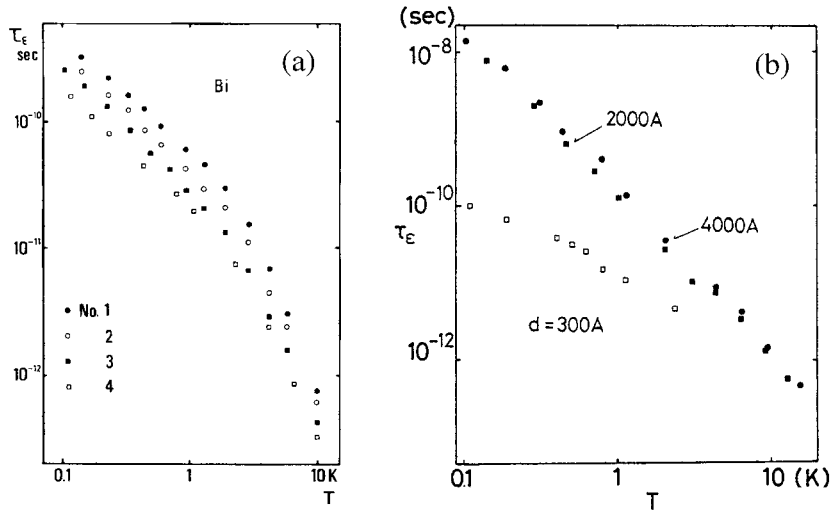

Figure 37. (a) Electron dephasing time τ_ϕ (labelled as $\tau_\mathcal{E}$ in the figure) as a function of temperature for four Bi thin films with diffusion constant (film thickness) = 20 (120), 16 (110), 12 (97), and 10 (91) $cm^2\ s^{-1}$ (Å), respectively, for No 1, 2, 3, and 4. This figure was reproduced with permission from [250]. (*b*) Electron dephasing time τ_ϕ (labelled as $\tau_\mathcal{E}$ in the figure) as a function of temperature for three Bi films with thickness of 300, 2000, and 4000 Å. The 300 Å thick film is two dimensional and in it $\tau_\phi \propto T^{-1}$, while the 2000 and 4000 Å thick films are three dimensional and in them $\tau_\phi \propto T^{-2}$. This figure was reproduced with permission from [26].

expected from the e–e scattering theory. It is also of importance to ask why Bi (and Mg) reveal a *much less* pronounced signature of saturation than other metals. This is particularly intriguing since Bi (and Mg) are highly oxidizable compared with other metals, and such oxidation could result in serious inhomogeneities in the microstructure of the sample. Furthermore, it should be noted that in those experiments mentioned above, the samples were made only in a typical, but not extremely high, vacuum. They were deposited only on typical glass substrates, rather than much purer quartz substrates. It would be worth exploring why the saturation behaviour of τ_ϕ^0 is much less evident, or even absent, under such circumstances of 'minimal precaution'.

In an elaborate effort to extend electrical transport measurements to very low temperatures, Mueller *et al* [112] have succeeded in cooling a 76 Å thick amorphous Au film down to 20 mK. Above 20 mK, they observed a logarithmic variation of the resistance with temperature, while below 20 mK they found *no* change in either the resistance or magnetoresistance curves, confirming that the lowest electron temperature was about 20 mK. The logarithmic temperature variation of the resistance is due to two-dimensional weak-localization and e–e interaction effects [1,3,4]. More strikingly, they observed an inelastic electron dephasing rate $1/\tau_\phi \propto T^{1/2}$ between 20 and 300 mK. Mueller *et al* interpreted their result in terms of electron scattering by magnetic impurities. They further explained that their measured magnetic scattering rate was not due to single-Kondo-impurity behaviour, but intimately connected with impurity–impurity interactions [105]. They obtained a phase-breaking length $L_\phi(20\ \text{mK}) \approx 3\ \mu\text{m}$.

Three-dimensional films. Komori *et al* [26] have measured τ_ϕ in 2000 and 4000 Å thick Bi films. Their films were prepared by repeating many times thermal-flash deposition and subsequent oxidation of a small amount of Bi on glass substrates. The structure of their films was composed of small particles of Bi (which had an average diameter of ~40 Å) coupled through a thin oxide. They found a $\tau_\phi \propto T^{-2}$ dependence between 0.1 and 20 K, which was

ascribed to e–ph scattering. They obtained a phase-breaking time $\tau_\phi(0.1\ \mathrm{K}) \approx 1 \times 10^{-8}$ s, independent of film thickness. Their results are plotted in figure 37(*b*).

Koike *et al* [27] have measured τ_ϕ in a 7000 Å thick granular Bi film made by evaporation in the presence of an oxygen atmosphere. The grain size of the film was ∼380 Å, and the resistivity was $\rho(4\ \mathrm{K}) \approx 2800\ \mu\Omega\,\mathrm{cm}$. They found a $\tau_\phi \propto T^{-3/2}$ dependence between 0.05 and 5 K, which was ascribed to three-dimensional e–e scattering. They obtained a dephasing time $\tau_\phi(50\ \mathrm{mK}) \approx 4.5 \times 10^{-10}$ s, corresponding to a dephasing length $L_\phi(50\ \mathrm{mK}) \sim 1.2\ \mu\mathrm{m}$. However, it should be pointed out that, in the same experiment, a clear indication of a saturation of τ_ϕ^0 was found in another 7000 Å thick Bi film with a slightly higher resistivity of $\rho(4\ \mathrm{K}) \approx 3800\ \mu\Omega\,\mathrm{cm}$. In particular, the saturation in that film occurred only at $T \lesssim 0.1$ K, but *not* at a temperature above 0.1 K. This result poses the serious question of whether the dephasing time in Bi samples might keep increasing as $T \to 0$. To the best of our knowledge, this is the only Bi sample in the literature on which measurements have been made down to a temperature below 0.1 K.

Aronov *et al* [166] have measured τ_ϕ in a 1 μm thick granular $Cu_{1-x}O_x$ film made by RF sputtering in a dilute oxygen atmosphere onto a glass substrate. Between 1.5 and 20 K, they found a $\tau_\phi \propto T^{-3}$ dependence which was ascribed to e–ph scattering. They obtained a phase-breaking length $L_\phi(1.5\ \mathrm{K}) \approx 2.5\ \mu\mathrm{m}$. Unfortunately, no data were reported for the lower-temperature regime ($\lesssim$1.5 K) where a stringent test of the saturation problem is critically needed.

It should be noted that, in each of the three-dimensional experiments [26, 27, 166] just discussed, the sample thickness was exceeded by the decoherence length L_ϕ measured at the lowest temperature. That is, while three-dimensional weak-localization theory was applied at all temperatures, these films should have been treated as *two* dimensional with regard to weak-localization effects at sufficiently low temperatures. A more self-consistent analysis of these measurements is therefore desirable[24].

Eschner *et al* [211] have studied a drawn, high-resistivity $Cu_{0.9}Ge_{0.1}$ wire of 0.3 mm diameter. They found a $\tau_\phi \propto T^{-3}$ dependence between about 3 and 70 K, which can be accounted for by e–ph scattering. Unfortunately, no data in the more relevant lower-temperature regime for the saturation problem were reported. Measurements on these samples down to much lower temperatures would be crucial for clarifying the saturation problem in three dimensions.

An alternative interpretation. As discussed, Webb *et al* [244] have measured τ_ϕ in carefully tailor-made Au wires and films. They found no sign of saturation in certain samples down to 40 mK (figure 31). However, they argued that this was because the saturation in these samples had been pushed down to lower, experimentally inaccessible, temperatures. In another experiment, they were able to demonstrate a Au thin film which has an extremely long dephasing time $\tau_\phi(40\ \mathrm{mK}) \approx 60$ ns (which is about a factor of 10 longer than ever reported in a mesoscopic system), corresponding to a dephasing length $L_\phi(40\ \mathrm{mK}) \approx 28\ \mu\mathrm{m}$ [245]. However, they proposed that a saturation of τ_ϕ should be still present in this film, but that it should occur only at ∼1 mK. Webb *et al* have suggested that the independent single-electron picture will not hold in most mesoscopic systems at such low temperatures, and that the saturation of τ_ϕ^0 as $T \to 0$ is intrinsic [58, 245].

[24] In the case of measurements on one-dimensional wires down to very low temperatures, another problem can arise in the comparison of weak-localization theory and experiment. While the weak-localization theory assumes an ensemble average, in the experiment this average might be far from complete, especially when the inferred decoherence length is of order several μm long. This situation can become serious in measurements where the wires were not made sufficiently long.

4. Dephasing in semiconductor mesoscopic structures

In this section, we review the results of experimental studies of dephasing in mesoscopic, semiconductor quantum wires and dots. We first of all briefly review the different theoretical predictions for electron dephasing due to e–e scattering in wires and films, after which we consider the results of experimental studies of dephasing in dirty and quasi-ballistic quantum wires. These studies demonstrate that, at temperatures below 10–20 K, the dominant dephasing mechanism is due to e–e, rather than e–ph, scattering. Two contributions to this scattering are identified, involving small, and large, energy transfer. While these results can be well understood within the framework of established theories, an unexpected finding in many experiments is that, at temperatures below a kelvin or so, a 'saturation' of the dephasing time occurs, reminiscent of that discussed above (section 3) for metallic mesoscopic systems. A similar saturation is also found to occur in transport studies of ballistic quantum dots, as we also review in this section. Finally, we consider the results of a smaller group of experiments, which use a variety of different approaches to extract estimates for the dephasing time in ballistic, two-dimensional-electron-gas systems. An interesting finding here is evidence for a massive enhancement of the phase-breaking length, observed in the quantum-Hall regime where current flows via edge states.

4.1. Electron interactions and dephasing in dirty wires and films: a theoretical overview

In section 3 it was shown that, in three-dimensional systems, the e–ph interaction provides the dominant mechanism for dephasing, with the e–e interaction being much less effective. In lower dimensions, such as in thin films and quantum wires, in contrast, we will see that the experimental results are consistent with the dominant source of dephasing as arising from e–e interactions. We will furthermore see that, dependent on the range of temperature, these interactions may involve either small, or large, energy transfer. Before discussing the results of these studies, however, we first provide a brief overview of the different theoretical predictions for dephasing due to e–e scattering in dirty films and wires.

In any discussion of dephasing due to e–e scattering, it is important to distinguish between the manner in which the phase of the wavefunction, and the electron energy, are randomized by means of the Coulomb interaction. Our starting point for this discussion is the conceptual framework of Fermi-liquid theory, in which it is typical to calculate the timescale over which the *excess* energy of a quasiparticle, excited beyond the Fermi level, is relaxed by means of the electron interaction. In three dimensions, and in the absence of disorder, it is well known that the quasiparticle lifetime, due to this interaction *alone*, scales with temperature as [265]

$$\frac{1}{\tau_{\mathrm{i},ee}} \sim \frac{1}{\hbar}\frac{(k_B T)^2}{E_F}, \tag{40}$$

where the expression above is accurate to within a numerical prefactor of order unity. (For the sake of consistency, in this section we will use the notation $\tau_{\mathrm{i},ee}$ to represent the inelastic lifetime due to e–e scattering and τ_{ee} to denote the dephasing time due to this scattering.) In lower dimensions, and, in particular, in the presence of disorder, the variation of the inelastic lifetime with temperature is considerably more complicated. Giuliani and Quinn [266] used a perturbative approach to calculate to inelastic Coulomb lifetime of an electron in a *clean* two-dimensional electron gas and obtained the result

$$\frac{1}{\tau_{\mathrm{i},ee}} = -\frac{E_F}{2\pi\hbar}\left(\frac{k_B T}{E_F}\right)^2\left[\ln\left(\frac{k_B T}{E_F}\right) - \ln\left(\frac{Q_{TF}}{k_F}\right) - \ln 2 - 1\right]. \tag{41}$$

Here, $Q_{TF} = 2m^*e^2/\epsilon\hbar^2$ is the two-dimensional Thomas–Fermi screening wavevector and equation (41) is expected to be valid at low temperatures, where the thermal energy is much smaller than the Fermi energy. As can be seen from this equation, a $T^2 \ln T$ variation of the inelastic lifetime is expected in the clean-metal limit, and evidence for this dephasing mechanism has been found in non-equilibrium transport studies of high-mobility two-dimensional-electron-gas systems [267], as we discuss in more detail below. A very different functional dependence on temperature is obtained when the influence of disorder is taken into account, however [54, 215, 268, 269]. Physically, an important effect of the disorder is to introduce strong spatial correlations among eigenstates that are nearby in energy, thereby modifying the nature of the e–e interaction. Abrahams *et al* [268] computed the inelastic lifetime in dirty metals due to electron scattering and found that, in two dimensions, the variation of $1/\tau_{i,ee}$ is modified to a $T \ln T$ form, while in other dimensions a $T^{d/2}$ variation is expected. While these authors evaluated the inelastic time from the self-energy of the one-particle electron Green function, in later work Fukuyama and Abrahams [269] computed the lifetime of the particle–particle diffusion propagator in the momentum representation. They also found that, in the presence of disorder, the relaxation rate in two dimensions is modified to a $T \ln T$ form, and their results may be summarized as

$$\frac{1}{\tau_{i,ee}} = \frac{\pi}{2}\frac{(k_BT)^2}{\hbar E_F}\ln\left(\frac{E_F}{k_BT}\right), \qquad k_BT\tau > \hbar \tag{42}$$

$$\frac{1}{\tau_{i,ee}} = \frac{k_BT}{2E_F\tau}\ln\left[\frac{4(E_F\tau)^2 D\kappa^2}{\hbar k_BT}\right], \qquad k_BT\tau < \hbar. \tag{43}$$

Here, κ is the effective inverse screening length and, within the Thomas–Fermi approximation, $\kappa = 1/Q_{TF}$. D is the diffusion constant. Equation (42) is the result for the clean-metal limit ($E_F\tau/\hbar \to \infty$), while equation (43) shows the modification that arises in the dirty-metal limit.

While the various calculations described above yield expressions for the inelastic lifetime due to electron scattering, it is important to realize that they are *not* necessarily equivalent to a calculation of the dephasing time *per se*. In particular, as was pointed out by Altshuler *et al* [35], at low temperatures it is possible that e–e scattering events may destroy the electron phase without relaxing its excess energy. This process of dephasing via multiple-scattering events, each involving *small energy* transfer, is known as *Nyquist dephasing*, since it can essentially be viewed as arising from thermal fluctuations in the background electromagnetic field, generated by the ensemble of electrons [35]. At temperatures where this Nyquist mechanism is effective, τ_{ee} and $\tau_{i,ee}$ are thus quite distinct from each other. Altshuler *et al* have computed the temperature dependence of the dephasing time due to this mechanism and find the following results for two and one dimensions, respectively:

$$\frac{1}{\tau_{ee}} = \frac{k_BT}{2\pi\nu(0)D\hbar^2}\ln(\pi\nu(0)D\hbar), \tag{44}$$

$$\frac{1}{\tau_{ee}} = \left[\frac{k_BT}{\sqrt{D}W\nu(0)\hbar^2}\right]^{2/3}. \tag{45}$$

In these expressions, $\nu(0)$ is the density of states at the Fermi level and W is the width of a one-dimensional channel. As is usual in discussions for weak localization, the transition from one- to two-dimensional behaviour is taken to occur once the phase-breaking length becomes *shorter* than the channel width. Early experimental confirmation of this Nyquist mechanism were given in studies of dirty-metal wires [87, 214].

Having introduced the various predictions for the dephasing, and energy relaxation, rates due to e–e scattering in dirty-metal systems, we now compare these forms with the results of experimental studies of semiconductor quantum wires.

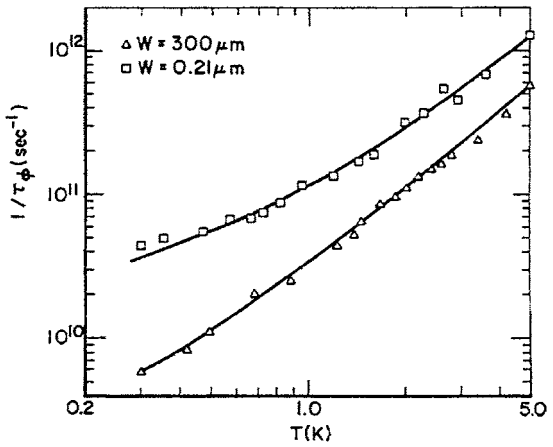

Figure 38. The temperature dependence of the dephasing rate, determined from measurements of the weak-localization magnetoresistance, in a two-dimensional electron gas (triangles) and a narrow quantum wire (squares). Both samples were realized in a GaAs/AlGaAs heterojunction. This figure was reproduced with permission from [71]. Copyright 1987 by the American Physical Society.

4.2. Dephasing in dirty and quasi-ballistic quantum wires

A thorough study of the origins of low-temperature dephasing in diffusive quantum wires was undertaken by Choi *et al* [71], who extracted values for the dephasing time from the weak-localization magnetoresistance of GaAs/AlGaAs quantum wires. The results of their analysis are shown in figure 38, in which the temperature-dependent variation of the dephasing rate is plotted for a narrow channel of effective width 0.21 μm, and is compared to the corresponding variation obtained in measurements of a two-dimensional Hall-bar structure. For both the two-dimensional sample, and the narrow wire, the authors found the variation of the dephasing time with temperature to be well described as a *combination* of e–e scattering rates, involving small *and* large energy transfer. For a quasi-one-dimensional wire, the combined dephasing rate due to these mechanisms may be written as

$$\frac{1}{\tau_\phi} = \frac{\pi}{2}\frac{(k_BT)^2}{\hbar E_F}\ln\left(\frac{E_F}{k_BT}\right) + \left[\frac{k_BT}{\sqrt{D}W\nu(0)\hbar^2}\right]^{2/3}. \tag{46}$$

The first term on the right-hand side of this equation is just the *inelastic* electron scattering rate due to e–e scattering, obtained by Fukuyama and Abrahams [269] for *clean*, *two-dimensional*, metals (equation (42)). That is, this term represents the rate at which e–e scattering occurs with large energy transfer. The second term in equation (46) is the Nyquist rate for e–e scattering with small energy transfer, as calculated by Altshuler *et al* [35] in the dirty-metal regime. The solid curve through the narrow-channel data of figure 38 is a least-squares fit to the form

$$\frac{1}{\tau_\phi} = \bar{A}T^2 + \bar{B}T^{2/3}, \tag{47}$$

and the values of the fitting coefficients ($\bar{A} = 4.23\times10^{10}$ s^{-1} K^{-2}, $\bar{B} = 7.25\times10^{10}$ s^{-1} K$^{-2/3}$) were found to be in reasonable agreement with the predictions of equation (46). These values indicate that, at temperatures of order a kelvin, the Nyquist mechanism dominates dephasing, while at higher temperatures, large-energy-transfer e–e scattering becomes dominant. This basic scenario of temperature-dependent e–e scattering has subsequently been confirmed

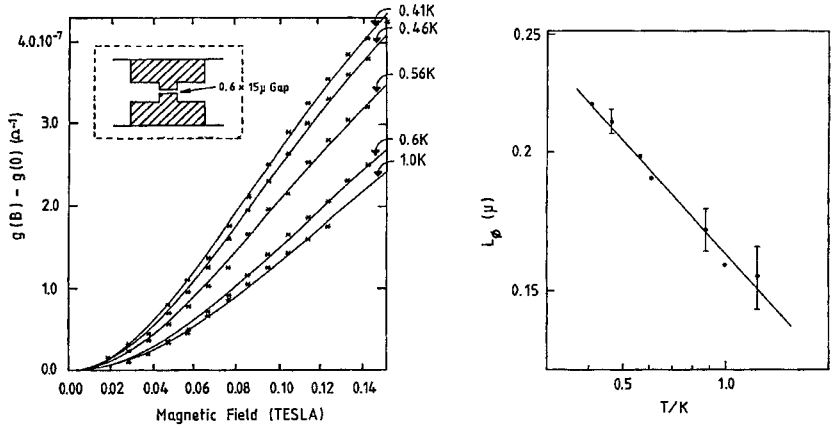

Figure 39. The left-hand panel shows the positive magnetoconductance at series of temperatures, for the split-gate quantum wire shown in the inset. Solid lines represent the result of fits to one-dimensional weak-localization theory. The extracted phase-breaking length and its variation with temperature are shown in the right-hand panel. The solid line represents a $T^{-1/3}$ power-law variation. This figure was reproduced with permission from [128]. Copyright 1986 by the American Physical Society.

in a number of different studies. Thornton and co-workers used the weak-localization magnetoresistance [128], and the amplitude of the universal conductance fluctuations [270], to determine the temperature dependence of the dephasing time in narrow GaAs/AlGaAs channels. The transport in these structures was quasi-ballistic in nature, although the authors used the corresponding diffusive theories [54, 115] for weak localization and universal conductance fluctuations to extract the dephasing time. In either approach, the temperature dependence of the extracted dephasing time was found to be well described by invoking the Nyquist mechanism alone (figure 39). This result is not necessarily inconsistent with the findings of figure 38, since Thornton and co-workers focused on the low-temperature range, where Choi *et al* also found the Nyquist term to be dominant. The Nyquist term has also been observed in studies of narrow Si MOSFETs [271], in which estimates for the dephasing time were extracted from the weak-localization magnetoresistance. In these diffusive structures, a crossover to one-dimensional Nyquist scattering was observed at temperatures below a kelvin. In other studies of quasi-ballistic GaAs/AlGaAs quantum wires, the combined scattering rate of equation (46) was found to give reasonable agreement with the results of experiment at temperatures exceeding 30 K, suggesting that e–e scattering can remain the dominant source of dephasing at temperatures as high as these [121]. In a somewhat different approach, evidence for e–e scattering with small and large energy transfers has been found in quasi-ballistic GaAs/AlGaAs rings, in which the temperature-dependent decay of the Aharonov–Bohm oscillations was exploited as a means to extract the dephasing time [272]. In another noteworthy study by Linke *et al*, the dephasing of equilibrium and non-equilibrium electrons in a quasi-ballistic GaAs/AlGaAs quantum wire was investigated [273]. Interestingly, these authors found the temperature dependence of the dephasing time of *equilibrium* electrons to be consistent with the Nyquist mechanism, over the entire temperature range from 0.3 to 10 K. In *non-equilibrium* studies, however, a variable dc voltage was superimposed on top of the small ac measuring bias, and was found to give rise to a suppression of weak localization. In order to account for this suppression, it was found necessary to assume that e–e scattering involves only *large energy* transfer, in contrast to the finding of the equilibrium studies.

The various studies discussed above provide a consistent picture, in which the dephasing of electrons at low temperatures (<30 K) is understood to be dominated by the contribution of e–e scattering. A common finding of many experiments is that, at temperatures above a few kelvins, this scattering is dominated by large energy transfer, as expected for clean metals [269]. At lower temperatures, however, coherence is typically lost through a series of quasielastic events, in which electrons scatter from noise-like fluctuations in the electromagnetic environment [35]. A very different picture of dephasing was obtained in the study by de Graaf *et al* [274], however. These authors studied the magnetoresistance of a short, narrow, constriction formed in a Si MOSFET by a multi-gate technique. A weak-localization peak was observed in the vicinity of zero magnetic field and was used to extract estimates for the dephasing time. The short length of this channel (<1 μm) required the authors to use the modified expression for the weak-localization magnetoresistance, developed by Chandrasekhar *et al* [78], to determine the dephasing time. The results of their analysis are indicated in figure 40, in which the temperature-dependent variation of the dephasing time in a narrow constriction (open circles) is compared to that obtained for the two-dimensional electron gas of the MOSFET (filled triangles). The data for the constriction were suggested to be consistent with the predicted form for the dephasing length due to e–e scattering in *one* dimension with *large* energy transfer [268, 275]:

$$L_\phi = \left[\frac{\pi W \nu(0)\hbar D}{a\sqrt{2}} L_T\right]^{1/2} \propto T^{-1/4}, \tag{48}$$

where L_T is the thermal coherence length. While some evidence for a $T^{-1/4}$ variation was found in much earlier studies of one-dimensional MOSFETs [275], it is very difficult in experiment to clearly distinguish this power-law dependence from that expected for one-dimensional Nyquist dephasing. Indeed, in figure 40 we have added the dashed line to indicate a $T^{-1/3}$ variation of the dephasing length. Given the scatter in this figure, one might argue that this variation is in fact consistent with the experimental data.

A common feature of *all* theories for e–e scattering in mesoscopic systems, regardless of their specific assumptions, is that they predict an *infinite* dephasing time in the limit of *zero* temperature. As a number of experiments have now demonstrated, however, a 'saturation' of the dephasing time may occur at low temperatures, implying the existence of a *finite* dephasing rate on extrapolation to absolute zero. One of the earliest observations of such saturation was reported by Choi *et al* [71], in their studies of short, wet-etched wires (figure 41). These authors extracted values for the dephasing time from weak-localization studies and found clear evidence for saturation once the phase-breaking length becomes comparable to the length of the wire. This behaviour is easily understood within the framework of theory, however, and can be attributed to a transition to zero-dimensional weak localization [276]. The basic idea is that, as the zero-dimensional limit is approached, the phase-breaking length that appears in the various weak-localization expressions should be replaced with the *effective* length scale [71]:

$$\frac{1}{L_{eff}^2} = \frac{1}{L_\phi^2} + \frac{4\pi^2}{L^2}. \tag{49}$$

Equation (49) clearly shows that, once L_ϕ becomes comparable to $L/2\pi$, such zero-dimensional effects are expected to become important [276]. Indeed, by comparing the effective length extracted from the weak-localization magnetoresistance of the short wire to the phase-breaking length determined at the same temperature in a two-dimensional Hall bar, equation (49) has been used to extract estimates for the total length of the wire, and these values were found to be in good agreement with its known lithographic dimensions [71].

In contrast to the experiment of Choi *et al* discussed above, saturation of the phase-breaking length on scales much *shorter* than $L/2\pi$ has also been observed in a number of

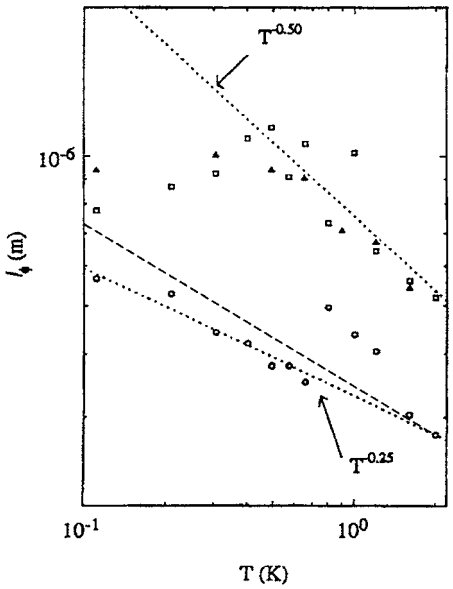

Figure 40. Variation of the phase-breaking length with temperature in a narrow-channel Si MOSFET. The solid triangles represent the results of experiments performed on the two-dimensional electron gas of the MOSFET, while the open circles represent the result obtained with the narrow channel formed. The open squares correspond to the results of fits to the phase-breaking length in two dimensions. The dotted lines show the indicated power-law variations, while the dashed line has been added by us and indicates a variation of $L_\phi \propto T^{-1/3}$. This figure was reproduced with permission from [274]. Copyright 1992 by the American Physical Society.

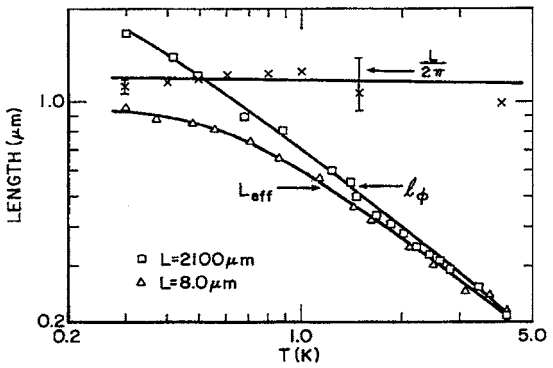

Figure 41. L_{eff} from a short channel (open triangles) and L_ϕ from a long channel (open squares). The crosses indicate values of the quantity $L/2\pi$, obtained from the data using equation (49). This figure was reproduced with permission from [71]. Copyright 1987 by the American Physical Society.

experiments and *cannot* be explained in terms of a dimensional crossover. This observation strongly suggests that the saturation itself does not result from the influence of the leads on coherence in the wire, but is rather associated with dephasing processes that arise *within* the wire itself. One of the earliest reports of such saturation was provided by Ikoma and co-workers [77], who later undertook the most extensive study of this effect [229]. In this latter report, these authors extracted values for the dephasing time from weak-localization

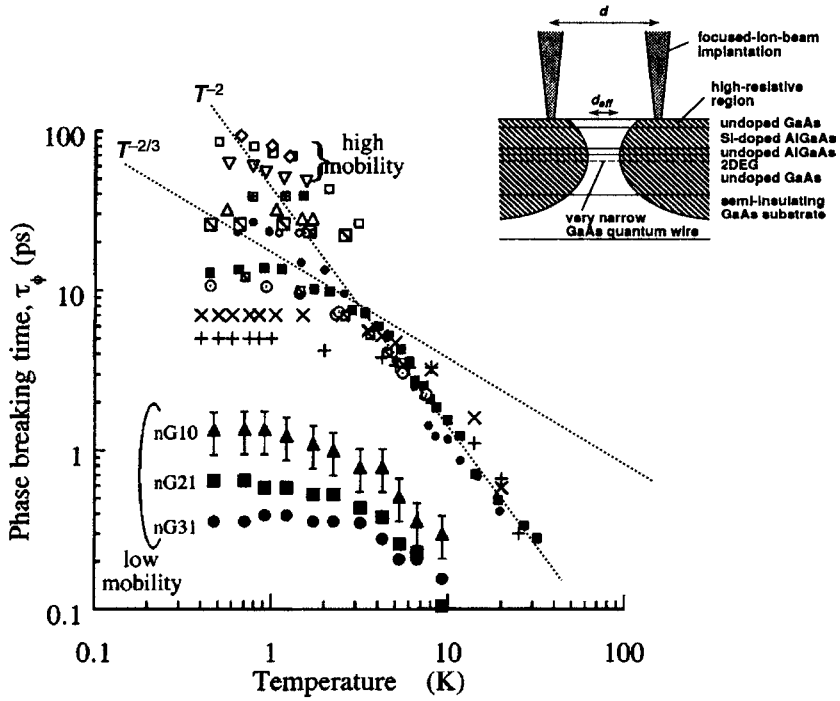

Figure 42. The temperature dependence of the dephasing time in a number of different GaAs/AlGaAs quantum wires. Open symbols denote split-gate quantum wires while filled ones correspond to those realized by focused ion-beam implantation. This figure was reproduced with permission from [229]. Copyright 1996 by the American Institute of Physics.

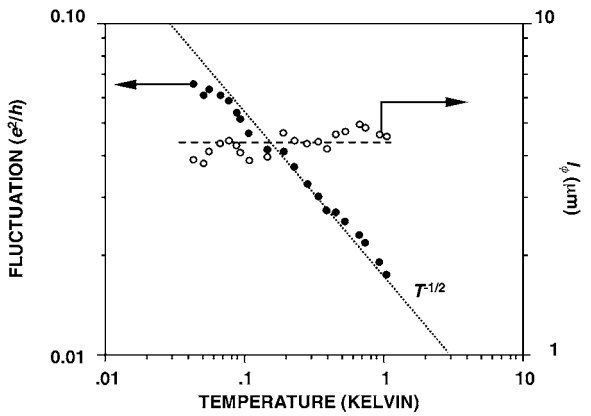

Figure 43. The open circles denote the value of the phase-breaking length, obtained from an analysis of the conductance fluctuation amplitude (filled circles) in a GaAs/AlGaAs quantum wire. This figure was reproduced with permission from [122].

studies of quasi-ballistic GaAs/AlGaAs quantum wires, realized by both focused ion-beam implantation and the split-gate technique. The wires were fabricated in heterojunctions with a variety of different spacer-layer thicknesses and the results of their study are summarized in figure 42. In almost all of the samples, a saturation of the dephasing time is found at

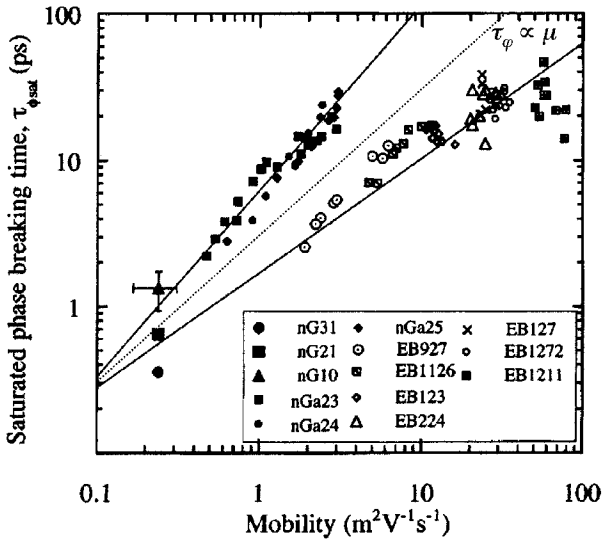

Figure 44. The dependence of the 'saturated' dephasing time on mobility in a number of different GaAs/AlGaAs quantum wires. Open symbols denote split-gate quantum wires while filled ones correspond to those realized by focused ion-beam implantation. This figure was adapted with permission from [229]. Copyright 1996 by the American Institute of Physics.

low temperatures, while at higher temperatures, up to 30 K, the data appear consistent with dephasing due to large-energy-transfer e–e scattering. By varying the drive current used in the magnetoresistance measurements over more than two orders of magnitude, the authors were able to establish that the saturation is not caused by the increased importance of Joule heating at low temperatures [77]. This result is consistent with the findings of Bird *et al* [122], who extracted estimates for the phase-breaking length from the amplitude of the conductance fluctuations observed in quasi-ballistic, wet-etched, GaAs/AlGaAs quantum wires. These authors found that the phase-breaking length remained independent of temperature below a kelvin, even though the amplitude of the fluctuations themselves increased by a factor of four over the same range (figure 43). The temperature dependence of the fluctuations in this figure is understood to result *solely* from the corresponding variation of L_T. We point out here that the physical significance of the phase-breaking and thermal diffusion lengths has been discussed by Lee *et al* [115]. These authors point out that the phase-breaking length may be viewed as the length scale over which the phase of the electron is destroyed through its *dynamic* interactions with its environment, while the thermal diffusion length describes a *static* dephasing, which arises due to the thermal smearing of the electron energy. For the data shown in figure 43, the $T^{-1/2}$ variation of the fluctuation amplitude is consistent with a temperature-independent L_ϕ in equation (15), in which case the temperature dependence of the fluctuations arises solely from the variation of L_T alone. From figure 42, it is apparent that the saturated value of the dephasing time increases with increasing mobility (that is, with increasing spacer-layer thickness), a trend that was also noted in the study by Bird *et al* [122]. In figure 44, the variation of the saturated dephasing time with mobility is summarized for both ion-beam implanted and split-gate wires [229]. While there is clearly a consistent difference between the two types of wire, we see from this figure that the saturated value of τ_ϕ scales approximately with mobility as $\tau_\phi \propto \mu$ (for high-mobility samples).

Subsequent to the observations of Hiramoto *et al* [77], a low-temperature saturation of the dephasing time was reported by a number of different authors. A deviation from the expected Nyquist scattering rate was observed by Pooke *et al* [271] in narrow Si MOSFETs, once the temperature was lowered below 0.3 K. Fukai *et al* [150] studied the weak-localization magnetoresistance of quasi-ballistic, on-facet, GaAs/AlGaAs quantum wires, grown by selective molecular-beam epitaxy. These authors found a transition from a Nyquist-consistent, to a saturated, dephasing time at temperatures below 0.4 K, simultaneous with the emergence of a *positive* term in the weak-field magnetoresistance. Since the latter effect is indicative of spin–orbit scattering in semiconductors [277], Fukai *et al* argued that the observed saturation of the dephasing time could be attributed to the increased importance of spin–orbit scattering at low temperatures. Aihara *et al* [278] used reactive-ion etching to fabricate quasi-ballistic, GaAs/AlGaAs heterojunction rings, and determined the dephasing time from the temperature-dependent decay of the Aharonov–Bohm oscillations. At temperature above a few kelvins, the dephasing time showed the T^{-2} variation expected for dephasing in clean metals [269]. At lower temperatures, however, a saturation was found. In the study discussed earlier by de Graaf *et al* [274], a saturation of the dephasing time was actually found in the *two-dimensional* electron gas of the MOSFET at temperatures below 0.5 K (figure 40). Furthermore, for the narrow-channel data of figure 40, if we assume that the variation of the phase-breaking length is closer to a $T^{-2/3}$ variation, the dephasing time of this structure shows possible evidence for saturation at temperatures below 0.2 K.

The observation of a low-temperature saturation of the dephasing time is not only limited to GaAs/AlGaAs heterojunctions and Si MOSFETs, but has also been reported for Si/SiGe quantum wires, and two-dimensional-electron-gas systems, and InGaAs/InAlAs wires and rings. Kurdak *et al* [272] used wet etching to fabricate quasi-ballistic wires and rings in InGaAs/InAlAs heterojunctions, and used the weak-localization magnetoresistance and Aharonov–Bohm oscillations to extract an estimate for the dephasing time. In both types of structure, evidence for saturation was found at temperatures below 0.35 K. van Veen *et al* [279] used reactive-ion etching to fabricate quasi-ballistic, Si/SiGe quantum wires and obtained values for the dephasing time from the weak-localization magnetoresistance. A weak temperature dependence of this parameter was found below a kelvin, suggestive of saturation. Interestingly, a saturated dephasing time has even been found in studies of the two-dimensional electron gas in Si/SiGe heterojunctions [280], and in GaAs/InGaAs/GaAs single quantum wells [281] and GaAs/AlGaAl quantum wells [282]. Many of the findings on the saturation of the dephasing time in semiconductor wires are summarized in table 4.

In contrast to the above, in the more recent investigations of Khavin *et al* [283], dephasing was studied in GaAs/AlGaAs quantum wires, in the region near the crossover from strong to weak localization. Estimates for the dephasing time were extracted from the one-dimensional weak-localization magnetoresistance, and the values of L_ϕ inferred in this manner were found to be in excellent agreement with the predictions of equation (45). While *no* evidence for saturation was found in the experiment, the lowest-temperature data reported in this study were obtained at 0.7 K, so the possibility of saturation having its onset at much lower temperatures cannot be discounted.

4.3. Dephasing in ballistic quantum dots

In comparison to the situation in metal and semiconductor quantum wires, the problem of dephasing in ballistic quantum dots has thus far attracted much less attention. Experimental investigations have focused exclusively on the coherent characteristics of GaAs/AlGaAs gated quantum dots, in which structure estimates for the dephasing time have been extracted by

Table 4. Transport parameters for different dephasing experiments on semiconductor quantum wires (1D) and dots (0D). The sheet carrier density (n_s) and mobility (μ) values shown here are typically those reported for the two-dimensional electron gas, prior to processing to form the microstructure. T_{on} is the temperature at which the saturation is observed to onset, while τ_ϕ^0 and L_ϕ^0 are the reported values of the saturated dephasing time, and length, respectively (in those experiments where no saturation was reported, the values for τ_ϕ and L_ϕ at 1 K are indicated).

Sample	n_s (10^{11} cm^{-2})	μ (10^3 cm^2 V^{-1}s^{-1})	T_{on} (K)	τ_ϕ^0 (ps)	L_ϕ^0 (μm)	Reference
1D GaAs/AlGaAs	5.2	170	2	30	—	[278]
1D GaAs/AlGaAs	1.4–5.4	53–490	> 1	260–52	4–6	[122]
2D GaAs/AlGaAs	1.6	27	None	30 @ 1 K	—	[71]
1D GaAs/AlGaAs	1.6	27	None	10 @ 1 K	—	[71]
1D GaAs/AlGaAs	35	34	0.4[a]	—	2	[150]
1D GaAs/AlGaAs	1.7–28	2–780	< 3	0.5–100	—	[229]
1D GaAs/AlGaAs	5.6	420	< 0.5	—	4	[272]
1D GaInAs/AlInAs	7–17	70–160	< 0.5	—	3–6	[272]
1D GaAs/AlGaAs	6.2	47	< 4	—	2	[121]
1D GaAs/AlGaAs	4	200	None	—	2 @ 1 K	[270]
1D Si/SiGe	8.8	86	0.5	—	< 2	[279]
0D GaAs/AlGaAs	4.4	400	0.15	200	—	[142]
0D GaAs/AlGaAs	3.5	1600	0.3	200	—	[136]

[a] In this case the authors clearly identified that the saturation resulted from the spin–orbit scattering time becoming the shortest timescale in the problem (i.e. $\tau_{so} < \tau_\phi$).

studying the characteristics of the fluctuations, and the zero-field peak, observed in their low-temperature magnetoresistance [135–137, 142, 144, 230, 284, 285]. The general behaviour revealed in these studies is fairly consistent, in spite of the different methods that are used to extract the dephasing time. At temperatures close to a kelvin, the dephasing time is found to exhibit a power-law scaling with temperature, which in most cases appears to be best described by $\tau_\phi \propto T^{-1}$ (figure 45). A power-law variation of this type has actually been obtained by Takane, who considered the dephasing of ballistic electrons due to Coulomb interactions in a *chaotic* quantum dot [286]:

$$\frac{1}{\tau_\phi} \sim \frac{\lambda_F}{W}\frac{k_B T}{\hbar}, \tag{50}$$

which expression is valid in the limit where the width of the leads (W) is much larger than the Fermi wavelength (λ_F). In most experiments, however, this condition is violated, since the leads are typically configured to support just a small number of propagating modes ($\lambda_F \approx W$). In another theoretical study, Sivan *et al* [287] have calculated the quasiparticle lifetime due to e–e scattering in a *disordered* quantum dot, and predict a temperature-dependent variation of the dephasing time that scales as $\tau_\phi \propto T^{-2}$. As indicated by the dotted line in figure 45, this dependence is much stronger than that typically found in most experiments.

Similar to the behaviour found in disordered quantum wires, a saturation of the dephasing time is observed in ballistic dots at very low temperatures (figure 45) [136, 142, 144, 230, 284]. Bird *et al* speculated that the saturation occurs once the thermal energy becomes comparable to the average level spacing in the dot, indicating a transition to zero-dimensional dephasing behaviour [142]. In a later experiment by Pivin *et al*, however, the saturation was studied in a self-aligned GaAs/AlGaAs quantum dot (figure 46, inset) and was found to persist to temperatures much higher than expected from the average level spacing [144]. These authors also found that the saturated value of the dephasing time *increased* as the coupling between the dot and the external reservoirs was reduced, and a similar effect has also been reported

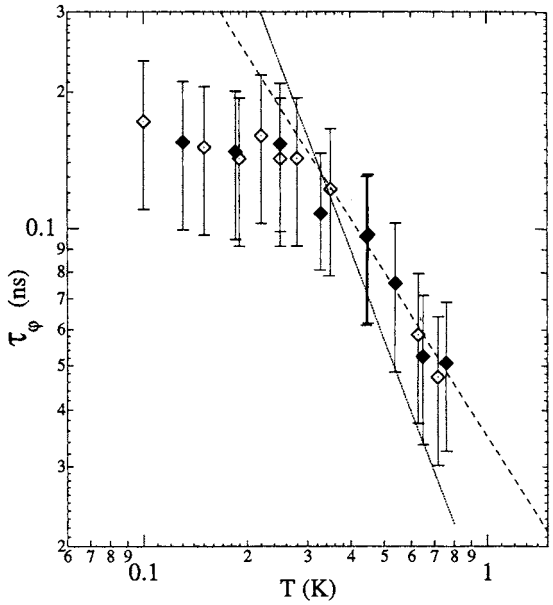

Figure 45. The variation of the phase-breaking time with temperature measured by Clarke *et al*. Solid and open symbols are the results for two different dots. The dotted line shows the T^{-2} variation predicted for isolated quantum dots, while the dashed line indicates a $T^{-1.2}$ dependence. The dots were realized by the split-gate technique and had a lithographic linear dimension of roughly 2 μm. This figure was reproduced with permission from [136]. Copyright 1995 by the American Physical Society.

in split-gate dots of similar size [285]. While Pivin *et al* suggested that the change in the dephasing time was associated with a change in electron number in the dot, the origin of this enhancement of the dephasing time remains unexplained.

A proposed mechanism for the low-temperature saturation of the dephasing time in studies of disordered quantum wires is the presence in experiment of extraneous RF radiation [41]. It has been argued that, even at levels insufficient to produce electron heating, this radiation may be sufficient to induce decoherence. In order to investigate whether such a mechanism may be responsible for the saturation of the dephasing time found in ballistic quantum dots, Huibers *et al* have studied the influence of *deliberate* microwave excitation on the value of the dephasing time [230]. The crucial point to note here is that, according to random-matrix theory, the variance of the conductance fluctuations is affected by both dephasing *and* thermal smearing, while the amplitude of the zero-field magnetoresistance peak depends only on the presence of dephasing [138, 139]. From comparing the temperature dependence of the conductance fluctuations, and the averaged amplitude of the zero-field peak, to the corresponding variations induced by the microwave irradiation, Huibers *et al* concluded that the effect of the microwave excitation was *identically equivalent* to an increase in the electron temperature. On this basis it was argued that the low-temperature saturation of the dephasing time *cannot* be due to unintentional sources of electromagnetic radiation. From studying metal (Au) wires exposed to an externally applied high-frequency noise, Webb *et al* [244] have similarly concluded that electron heating precedes dephasing by high-frequency noise.

In addition to studies of equilibrium dephasing, investigations of the mechanisms for decoherence have also been made in the non-equilibrium regime. In one report, Linke

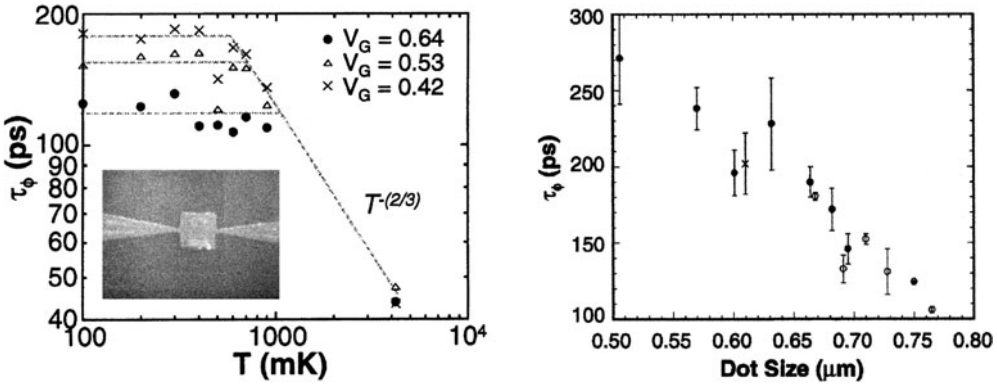

Figure 46. The left-hand panel shows the variation of the phase-breaking time with temperature measured in the gated dot shown in the inset. This dot was realized using the metallic gate as a self-aligning mask, which protected the underlying substrate during a subsequent chemical etch. The lithographic dimension of the central dot is approximately 0.8 μm, and by applying a *positive* voltage to the gate the conductance, and effective area, of the dot could be increased. The data in the main panel show that this increase is accompanied by a *reduction* in the saturated value of the dephasing time. The right-hand panel shows the variation of the saturated value of the dephasing time with dot size (different symbols denote the results of measurements performed under different illumination conditions). This figure was reproduced with permission from [144]. Copyright 1999 by the American Physical Society.

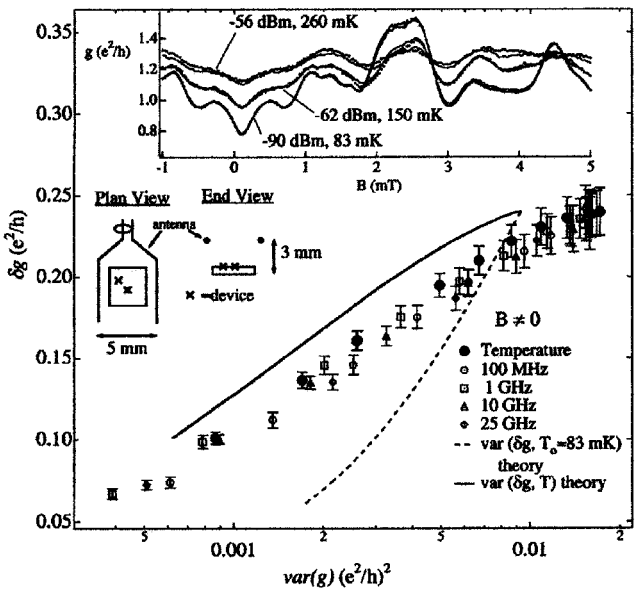

Figure 47. In this figure, the amplitude of the zero-field magnetoresistance peak is plotted versus the variance of the conductance fluctuations, for a split-gate quantum dot under conditions of different temperature or microwave excitation. This figure establishes that the effect of microwave irradiation is indistinguishable from an increase in the electron temperature in the dot. The inset further clarifies this point, showing magnetoresistance traces obtained under conditions of different temperature and microwave irradiation. This figure was reproduced with permission from [230]. Copyright 1999 by the American Physical Society.

et al [284] compared the influence of temperature and dc bias on the lineshape of the zero-field magnetoresistance peak, and found a bias-dependent variation of the dephasing time reminiscent of that observed in temperature-dependent studies. On the basis of this comparison it was suggested that the effect of a given bias voltage (V) could simply be understood to increase the effective electron temperature to a value eV/k_B. The resulting variation of the dephasing time was found to be saturated for small voltage biases, but to decay as $\tau_\phi \propto V^{-2}$ at higher values—reminiscent of the theoretical predictions of Sivan *et al* [287]. In contrast, Switkes *et al* [288] studied the influence of the measurement current on the electron temperature in a much larger dot, and found this temperature to be determined by an equilibrium condition where the energy supplied to the dot by hot electrons is balanced by loss to the reservoirs via the point contact leads. More recently, Prasad *et al* [145] have used electron heating studies to obtain the dephasing and energy relaxation times in arrays of coupled quantum dots. The temperature-dependent variation of the dephasing time in these structures was found to be very similar to that exhibited by single dots, while the energy relaxation time showed a very *different* functional dependence to the dephasing time. The value of $\tau_\mathcal{E}$ at low temperatures was typically several orders of magnitude longer than the dephasing time, while little evidence for saturation was found in its temperature dependence. These observations were taken to be consistent with the notion that energy relaxation in these structures arises by e–ph scattering.

4.4. Dephasing in other ballistic systems

In this section, we consider the results of studies of dephasing in a variety of different ballistic, and near-ballistic, systems. One of the few experimental investigations of dephasing in clean *two-dimensional* electron systems was undertaken by Yacoby *et al* [267, 289], who utilized a novel interferometer to study the dependence on DC bias of the phase-breaking length (figure 48). The device was realized in the high-mobility two-dimensional electron gas of a GaAs/AlGaAs heterojunction, and is illustrated in the inset to figure 48. By varying the voltage applied to either of the centre finger gates, the phase difference of electrons arriving at the voltage probe P from the emitter could be varied, giving rise to oscillations in the probe voltage V_p. These phase oscillations were found to be suppressed with increasing DC emitter bias, which effect was attributed to an associated reduction in electron coherence. This reduction was found to be consistent with theoretical predictions for the dephasing rate, due to large-energy-transfer, e–e, scattering in *clean* two-dimensional metals (equation (41)) [266, 290]. An important conclusion of this study is that, in contrast to the situation for dephasing due to e–e scattering in dirty metals at low temperatures, dephasing of electrons in high-mobility systems can occur via a *single* e–e scattering event. In such systems, this study shows that the phase-breaking length can actually be *shorter* than the mean free path ($L_\phi < l$), indicating that dephasing events involve a transfer of energy of order the quasiparticle energy Δ [267]. While this situation may, at first, seem counterintuitive, we point out that the mean free path is the distance over which *large-angle* backscattering occurs, and is therefore not necessarily equal to the mean distance travelled between any *pair* of scattering events. In high-mobility systems, large-angle backscattering events are rare, which is presumably the situation that allows the limit $L_\phi < l$ to be accessed.

An interesting example of a ballistic system is provided by the two-dimensional electron gas at high magnetic fields, where current flow occurs via one-dimensional edge states (for an extensive review see [70], for example). The edge states arise from the Fermi-level intersections of successive Landau levels, whose energies diverge rapidly as the sample walls are approached, and may be viewed as one-dimensional transport channels. One important length scale that arises in the discussion of edge-state transport is the inter-edge-state *equilibration length*, the

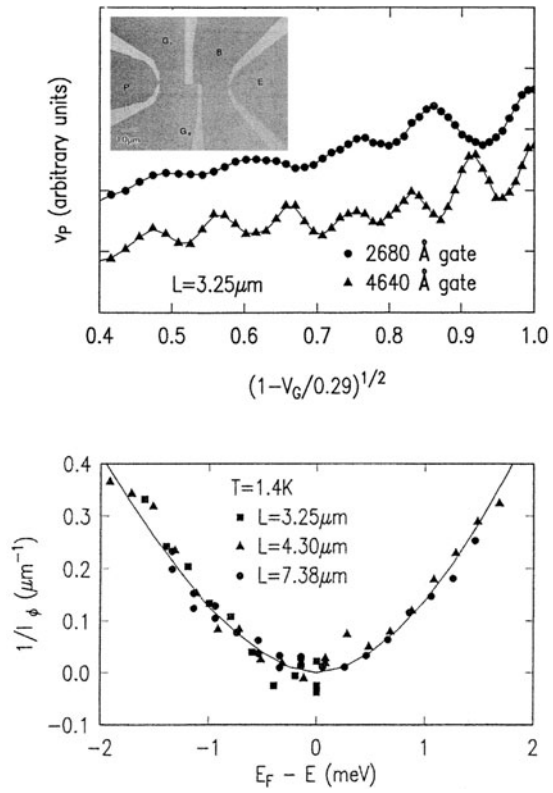

Figure 48. The inset to the upper panel shows a micrograph of the Young's-slit interferometer used to determine the dephasing time for ballistic two-dimensional electrons. Electrons are injected from the emitter (E) and their transmission is detected by measuring the voltage (V_p) of the probe P. The centre finger gates are used to modulate the interference of electron partial waves arriving at the voltage probe, giving rise to the oscillations shown in the main figure. The lower panel shows the variation of the phase-breaking length with the injection energy, for a number of different experiments. The solid curve is the prediction of theory for a clean two-dimensional electron gas. This figure was reproduced from [267]. Copyright 1991 by the American Physical Society.

distance over which two edge states, injected into a two-dimensional electron gas at different electrochemical potentials, come into equilibrium with each other. At high magnetic fields, where current is carried by just a few edge states, it is well known from experiment that this length scale may exceed several *hundred* microns [291–294]. As has been pointed out by Buttiker [295], however, this equilibration length is quite distinct from, and should not be confused with, the phase-breaking length of the edge channels. An attempt to measure this latter length scale directly in experiment has been performed by Machida *et al* [296], who investigated the behaviour in the quantum-Hall transitions at high magnetic fields. They derived an inelastic scattering *length* that shows no evidence for saturation down to the lowest experimental temperatures, but which increases strongly with magnetic field. The results of their analysis are shown in figure 49, from which it can be seen that the extrapolated value of the inelastic scattering length exceeds 1 mm at 10 mK. We also note that the variation of the inelastic scattering length implies a temperature-dependent timescale that varies as T^{-3}. Such a power-law variation is typical for e–ph scattering in three dimensions [7, 165], suggesting that the length scale Machida *et al* derive from their experiment is related to energy relaxation, rather than dephasing.

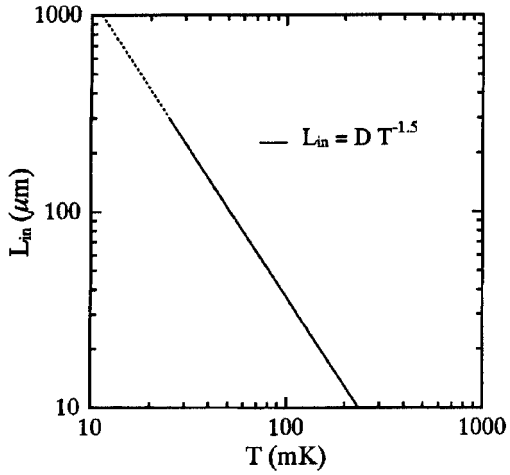

Figure 49. The temperature dependence of the edge-state inelastic scattering length obtained in the experiment of Machida *et al* [296]. This figure was reproduced with permission from [296]. Copyright 1996 by the American Physical Society.

Finally, studies of phase coherence have also been performed in near-ballistic Aharonov–Bohm rings, in which current is carried by only a small number of one-dimensional subbands [297, 298]. Liu *et al* studied the low-temperature magnetoresistance of shallow-etched GaAs/AlGaAs rings, and extracted estimates for the phase-breaking length from the decay in the harmonic content of their Aharonov–Bohm oscillations. The results of this analysis suggest that the phase-breaking length in these near-ballistic structures increases with magnetic field (figure 50), although it is unclear whether this behaviour is due to an increase in the dephasing time, or a change in the nature of electron motion at high magnetic fields [124, 125] (the same may also be said of the study of Machida *et al* discussed above). Hansen *et al* [298] also considered the decay in the harmonic content of the Aharonov–Bohm effect as a means to determine the temperature dependence of the dephasing time, which they found to decay according to $\tau_\phi \propto T^{-1}$—reminiscent of the behaviour found in open quantum dots [136, 137, 142]. In contrast to the behaviour exhibited by these latter structures, however, Hansen *et al* found *no* evidence for saturation, at temperatures down to 0.3 K.

5. Conclusions

The electron dephasing time $\tau_\phi(T, l)$ is a quantity of fundamental interest and importance in metal and semiconductor mesoscopic structures. Both theoretical and experimental investigations of τ_ϕ have advanced significantly over the last 20 years. These advances have largely been due to the observation, in mesoscopic metals and semiconductors, of a variety of quantum-interference phenomena. Among these phenomena, weak localization is probably the *most* powerful probe of the electron dephasing times in mesoscopic structures. The advances in our understanding of weak-localization effects have made feasible systematic and quantitative measurements of different electron scattering times, such as the e–ph scattering time τ_{ep}, the e–e scattering time τ_{ee}, the critical e–e scattering time τ_{EE}, the magnetic spin–spin scattering time τ_s, the spin–orbit scattering time τ_{so}, and the 'saturated' dephasing time τ_ϕ^0 ($=\tau_\phi(T \to 0)$). In the case of superconductors, the electron–superconducting-fluctuation

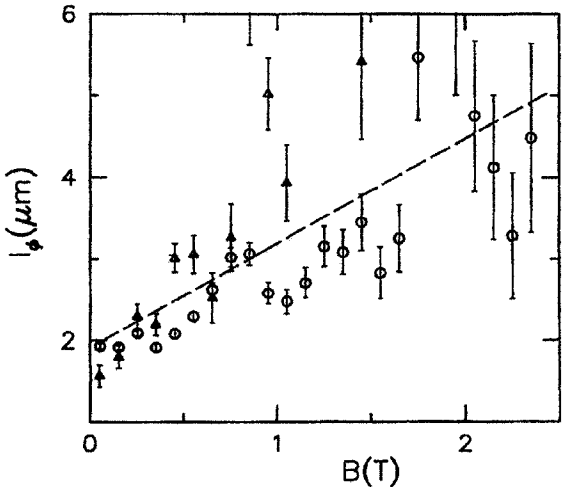

Figure 50. The inferred dependence of the phase-breaking length on the magnetic field, obtained in the experiment of Liu *et al* in their experimental studies of near-ballistic GaAs/AlGaAs rings. This figure was reproduced from [297]. Copyright 1994 by the American Physical Society.

scattering time τ_{e-sf} can also be deduced from weak-localization studies. Despite great efforts in theoretical calculations and experimental measurements of τ_ϕ, our current understanding of the microscopic mechanisms for different dephasing times (except the Nyquist e–e scattering time τ_{ee} in one and two dimensions) is still incomplete. Experimentally, carefully designed low-temperature magneto-transport measurements employing tailor-made structures, with sample specifics varying over a wide range of disorder and dimensionality, would be highly desirable to help with discerning the underlying physics of different electron dephasing times. Systematic information on the dependence of τ_ϕ on temperature T and electron elastic mean free path l will shed light on the underlying physics of the dephasing processes, helping with theoretical formulation of the problem. In addition to normal-metal and semiconductor structures, weak-localization study has also been applied to measure τ_ϕ in unconventional conductors, such as quasicrystals [51], high-temperature superconductors (in the normal state) [53], and carbon nanotubes [52].

In this review, we have surveyed the temperature and electron mean free path dependences of $1/\tau_{ep}$ in disordered metals (section 3). We have discussed why a quadratic temperature dependence of $1/\tau_{ep}$ in the dirty limit of $q_T l \ll 1$ is *often* (but not always) found in experiments [174], while the theoretically expected T^4 law is *rarely* seen in real materials [179] (where $q_T \approx k_B T/\hbar v_s$ is the wavelength of thermal phonons, and v_s is the sound velocity). Since a T^4 temperature dependence of $1/\tau_{ep}$ is quite firmly established theoretically, the consistent observations of a T^2 temperature dependence have recently led to a major revision of the standard Pippard–Rammer–Schmid theory of the e–ph interaction in the presence of strong impurity scattering [22, 33]. It is currently proposed that, in addition to the scattering of electrons by the 'vibrating' potential considered in the standard theory, there might also occur scattering of electrons by the 'static' potential [95, 96] due to heavy defects and/or tough boundaries. Under such circumstances, a T^2 temperature dependence of $1/\tau_{ep}$ due to *transverse* phonons can be expected. Depending on the degree of disorder (i.e. the value of $q_T l$), and also on the contribution of the scattering by the 'static' potential relative to the 'vibrating' potential, the temperature exponent p can take any value between 2 and 4. In realistic measurements, covering a not-too-wide range of temperature, a (single) effective

value of p can be assumed. As for the disorder dependence of τ_{ep}, experimental results do *not* support a universal dependence of $1/\tau_{ep}$ on the electron mean free path l, as is evident from table 2. (Compared with the information of τ_ϕ on T, experimental information of τ_ϕ on l has been extremely limited in the literature.) These results of different temperature and disorder dependences indicate that the nature of the e–ph interaction in disordered metals is fairly sensitive to the local material environment of a particular material system. In addition to the possible existence of 'static'-potential scattering, the phonon excitation spectrum might be subtly affected by the microscopic quality of the disorder. Besides, while the existing theories are formulated on the basis of a model with a spherical Fermi surface, the Fermi surfaces in real alloys are often more complicated. Therefore, it is probably not entirely surprising that (significant) discrepancies are often found between the theory and experiment.

While the theory predicts both the temperature and disorder dependences of $1/\tau_{ep}$ to be extremely sensitive to the value of $q_T l$ [22,48,96], the experimental situation is less clear. An inspection of the experimental results listed in tables 1 and 2 reveals *hardly* any systematic variation of the temperature exponent p with $q_T l$. This might imply that the quantity $q_T l$ alone is *not sufficient* to determine the complete temperature (and disorder) behaviour of $\tau_{ep}(T, l)$. As just mentioned, the non-monotonic variation of p with $q_T l$ found in different measurements might further be complicated by the possible coexistence of 'vibrating'-potential and 'static'-potential scattering in real systems.

For e–ph scattering in the clean limit of $q_T l \gg 1$, it is often taken for granted that the T^3 temperature dependence of $1/\tau_{ep}$ is well established theoretically [157] and experimentally [191]. However, in contrast to this long-standing belief, a close inspection of tables 1 and 2 indicates that e–ph scattering in the clean limit has *scarcely* been explored experimentally, since extremely few, if any, measurements have achieved a sufficiently large value of $q_T l$ ($\gg 1$). Instead, in most of the previous measurements where a $1/\tau_{ep} \propto T^3$ dependence was reported, the e–ph interaction was more probably falling in the intermediate-disorder regime ($q_T l \sim 1$), rather than in the clean limit. According to current theoretical understanding [95, 96], the frequently observed T^3 temperature dependence of $1/\tau_{ep}$ might correspond to a crossover from the clean-limit to the dirty-limit regime for *transverse* phonons. Thus, it would be of interest to carry out measurements on samples having a large value of $q_T l \gg 1$ to test the T^3 temperature dependence due to the longitudinal phonons.

Taking into account both the temperature and disorder dependences, an e–ph scattering rate $1/\tau_{ep} \propto T^4 l$ due to complete 'vibrating'-potential scattering (the Pippard ineffectiveness condition) [22, 33], and a scattering rate $1/\tau_{ep} \propto T^2 l^{-1}$ due to a partial contribution from 'static'-potential scattering (the 'breakdown' of the Pippard ineffectiveness condition) [95,96], have been theoretically predicted. These two different temperature and disorder variations have been observed experimentally in different material systems (see table 2). However, there are other systems, such as three-dimensional Au–Pd [94] and Ag–Pd [182] thick films, and $V_{100-x}Al_x$ alloys [183], and two-dimensional Sb [187] and Nb [186] thin films, in which an abnormal $1/\tau_{ep} \propto T^2 l$ dependence was observed. Such a combined $T^2 l$ temperature and disorder behaviour cannot be understood, even qualitatively, in terms of any current theories for the e–ph interaction. This observation therefore deserves serious theoretical attention.

In addition to the e–ph scattering time τ_{ep}, we have also discussed the role of critical e–e scattering in very low-diffusivity conductors. In three-dimensional conductors near the mobility edge, a dependence $1/\tau_{EE} \propto T$ is observed in experiments (figure 26). Moreover, it is found that $1/\tau_{EE}$ depends only very weakly, if at all, on the electron mean free path l (figure 25(b)) [219, 222]. This is due to the critical, as opposed to diffusive, current dynamics in the presence of very strong impurity scattering [34]. Thus, insofar as inelastic electron scattering in disordered conductors is concerned, the experimental picture suggests a crossover

from e–ph dephasing to critical e–e dephasing, as the level of disorder greatly increases and the system moves significantly toward the Anderson transition. The critical e–e scattering time has not attracted much theoretical and experimental attention in the literature.

In low-dimensional systems, such as semiconductor heterojunctions and quantum wires, we have seen that, in the range of temperature from approximately 1–30 K, the dominant source of dephasing can clearly be attributed to e–e scattering [71]. At the low-temperature end of this range, this scattering is predominantly quasielastic in nature, and phase randomization results from the cumulative effect of a large number of scattering events, each involving a small energy transfer. This so-called *Nyquist mechanism* is essentially equivalent to a process in which the phase of the electron is gradually randomized by fluctuations in the background electromagnetic field, generated by the thermal motion of the electron sea [35]. At higher temperatures, the dephasing behaviour exhibits a crossover to e–e scattering involving large energy transfer, and evidence for this process has been found to persist to temperatures as high as 30 K [229]. It is interesting that, even at such elevated temperatures, e–e scattering still dominates the dephasing, and no evidence is found for the role of e–ph scattering. This is, in fact, consistent with the results of other studies. In the recent report by Prasad *et al* [145], for example, estimates for the dephasing *and* the energy relaxation time were obtained in studies of quantum-dot arrays. While the upper limit of measurement was limited to about 10 K in this work, the authors were able to show that the dephasing time remained at least *two* orders of magnitude smaller than the energy relaxation time, over the entire temperature range studied.

While the experimental results for dephasing in heterojunctions and semiconductor wires can be well explained within the framework of accepted theories for e–e scattering (at least in the regime where τ_ϕ does not exhibit a saturation), our understanding of the sources of dephasing in semiconductor quantum dots is clearly less well established. A common feature of the few experimental studies performed thus far is a dephasing rate that varies close to linearly in T, at temperatures close to a kelvin [136,137,142]. It has previously been noted that such a variation is similar to that predicted for the Nyquist mechanism in two dimensions, and Huibers *et al* have argued that the observed temperature dependence of τ_ϕ can be well fitted with the predictions of this theory [137]. The success of this approach relies on the introduction of a fitting parameter, whose significance is not well understood at present, however. The suggestion of other experiments [143,144] is that the dephasing time in these structures may depend strongly on a number of additional factors, such as the strength of the coupling between the dot and its reservoirs, the number of electrons in the dot, and its specific potential landscape. While the number of theoretical studies of this problem continues to grow [286, 287, 299], further effort is required to clarify the origins of dephasing in these structures. At the same time, new experiments that are able to probe phase coherence *directly*, possibly in real time, are highly desired.

In addition to the inelastic electron scattering times at finite temperatures, the behaviour of the dephasing time near zero temperature, $\tau_\phi^0 = \tau_\phi(T \to 0)$, has recently attracted vigorous experimental and theoretical attention (figure 27). One of the central themes of this renewed interest is concerned with whether τ_ϕ^0 should reach a finite or an infinite value as $T \to 0$. While it is accepted that τ_ϕ^0 should diverge if there exists only inelastic e–e and e–ph scattering, several recent careful measurements, performed on different mesoscopic conductors, have found that τ_ϕ^0 depends only very weakly on temperature, if at all, when the temperature is sufficiently low. These measurements have demonstrated that hot-electron effects, external microwave noise, and very dilute magnetic impurities can *at most* play a *subdominant* role in the finite dephasing of τ_ϕ^0 as $T \to 0$. Therefore, the microscopic origin(s) for the widely observed 'saturation' behaviour of τ_ϕ^0 remain undetermined. In addition to the systematic studies on high-disorder

three-dimensional polycrystalline metals [13, 246], combined measurements of the electron energy exchange rate, dephasing rate, and Aharonov–Bohm oscillations will shed light on this issue [38, 39, 254].

In this review, we have surveyed available proposals for the observed saturation of τ_ϕ^0 and have also discussed recent systematic efforts aimed at testing these proposals. We have discussed several early measurements of τ_ϕ in different metals that deserve renewed investigation with a focus on the temperature, disorder, and sample-geometry behaviour of τ_ϕ^0. However, we have not attempted to discuss in detail any theoretical models of the saturation behaviour of τ_ϕ^0. Various theoretical proposals have appeared in the literature, including dynamical-defect-induced dephasing [14, 15], zero-temperature 'vacuum' fluctuations [235, 238], coupling to gravity [234], phonon emission [232], wavefunction collapse [236], and the role of sample-to-sample averaging [239], to list but a few (see, for example, [242] and [300] for a brief summary). Theoretically, we note that quantitative calculations of τ_ϕ^0 could be rather difficult, because there are many different processes that might cause dephasing at very low temperatures.

In addition to the case of disordered metals in the diffusive regime, a saturation of τ_ϕ^0 has also been observed in semiconductor, diffusive and quasi-ballistic, quantum wires, and ballistic dots. In many regards, the features of this saturation appear reminiscent of that found in dirty-metal wires. As we illustrate in table 4, the saturated value of the dephasing time is typically of similar orders in semiconductor wires and dots, and is also of comparable magnitude to that found in studies of dirty-metal wires and films (figure 27). The characteristic temperature for onset of the saturation also varies widely in these structures—again reminiscent of the behaviour found in dirty mesoscopic systems. There are some important differences between the saturation characteristics in semiconductors and metals, however. In contrast to the *inverse* scaling of τ_ϕ^0 with the diffusion constant, found in dirty systems by Lin and co-workers (figure 34), Noguchi *et al* have shown a more complicated behaviour in studies of semiconductor wires. In their lowest-mobility (<3000 cm^2 V^{-1} s^{-1}) samples, evidence for a decreasing τ_ϕ^0 with increasing mobility was indeed found. At higher ($>10\,000$ cm^2 V^{-1} s^{-1}) mobilities, however, τ_ϕ^0 was instead found to increase with increasing mobility [229]. Studies of ballistic quantum dots have suggested that τ_ϕ^0 also increases as the strength of the coupling between the dot and its reservoirs is decreased, and this effect has been discussed in terms of a suppression of the density of states for scattering [285], and a change in the number of electrons in the dot [144]. It is therefore not completely clear that the origins of the saturation are the same in these different systems (semiconductor wires and dots, metal wires and films).

Another important issue revealed in a number of studies is a sensitivity of the electron dephasing to the microscopic quality of disorder. Ovadyahu [43] has studied the energy relaxation time $\tau_\mathcal{E}$ and dephasing time τ_ϕ at low temperatures in diffusive In_2O_{3-x} and In_2O_{3-x}:Au thin films. He found that, although the Au doping is only $\lesssim 3\%$ in In_2O_{3-x}:Au thin films, the behaviour of $\tau_\mathcal{E}$ and τ_ϕ in these two materials could be *significantly different*. His observation suggests some very sensitive impurity-related, or defect-related, influence on the nature of the electron scattering processes. A similar conclusion has been reached by Fournier *et al* [53] from their study of underdoped $Pr_{2-x}Ce_xCuO_4$ thin films. Bird and co-workers [143] have studied semiconductor quantum dots and found that their dephasing time can show significant dot-to-dot variations, in samples realized in materials with similar mobilities. These measurements reflect a critical sensitivity of the dephasing processes to disorder. Using Ag–Pd thick films prepared by RF and DC sputtering deposition, Zhong *et al* [182] have found $1/\tau_{ep} = A_{ep}(l)T^2 \propto T^2 l$ in both types of film. However, they also observed that the variation of the strength of e–ph coupling A_{ep} with the electron mean free

path is a factor ∼2 higher in DC sputtered films than that in RF sputtered films. Indeed, as discussed above, the e–ph scattering time is very sensitive to the microscopic quality of disorder. These experiments clearly suggest that both τ_{ep} and τ_ϕ^0 are not only dependent on the *total* level of disorder, but are also very sensitive to the microscopic *quality* of the disorder. This can be particularly critical for mesoscopic devices, whose disorder profile is known to be highly sample specific. This is a key point that needs to be taken into consideration in future theories of electron dephasing times.

In our discussion of the e–ph scattering time τ_{ep} in section 3, we have pointed out that three-dimensional mesoscopic systems are more advantageous than lower-dimensional structures. It is worth noting that, apart from the e–ph scattering time, the saturation problem can also be better addressed in three-dimensional, rather than lower-dimensional, structures. While in the case of lower-dimensional structures surface effects due to interfaces, substrates, and paramagnetic oxidation are probably non-negligible, such effects are much less important in bulk structures. In addition, one of the advantages of bulk samples in this problem is the increased contrast between the 'saturation' and the strong dependence of $\tau_{\rm i}(T)$ in three dimensions. In three dimensions, e–ph scattering dominates the inelastic scattering, resulting in $1/\tau_{\rm i} \approx 1/\tau_{ep} \propto T^p$, with the temperature exponent $p \gtrsim 2$. Such a temperature variation is much stronger than the dominating $p = 2/3$ in one dimension and the $p = 1$ in two dimensions. For example, inspection of the solid lines, which are drawn proportional to T^{-2} in figures 29(*a*) and 35(*b*), reveals that the measured τ_ϕ^0 at 0.3 K is already approximately *two orders of magnitude* lower than that extrapolated from the measured τ_{ep} at a few kelvins. Such a huge discrepancy is well outside any experimental uncertainty.

It has been 20 years since the theoretical and experimental realization of the weak-localization effect, and related quantum-interference phenomena, in metal and semiconductor mesoscopic structures. The richness of these effects, and their wide appearance in different materials and dimensionalities, have also been well established. It is now also appreciated that these effects provide the most powerful probe of electron dephasing processes in mesoscopic and disordered systems. While several excellent reviews in this direction have appeared in the literature over the past two decades, there have been very few in-depth surveys of the *experimental* results and their physical implications for the various electron dephasing times. We hope that the present work will therefore help to provide up-to-date, quantitative, information on $\tau_\phi(T, l)$, as well as those issues of high current interest (such as 'the saturation problem' of τ_ϕ as $T \to 0$).

Acknowledgments

The authors are grateful to N O Birge, M Buttiker, C S Chu, D K Ferry, N Giordano, V Mitin, P Mohanty, G Schön, A Sergeev, G Y Wu, and A Zawadowski for helpful discussions, and for N O Birge and N Giordano for critically reading the manuscript. The motivation for this review was provided by a visit of JPB to the National Centre for Theoretical Sciences (Taiwan), and the authors would like to acknowledge the kind hospitality of the NCTS and support provided by them for this task. One of us (JJL) would also like to thank the organizers of the NATO Advanced Research Workshop on *Size Dependent Magnetic Scattering*, which took place from 29 May to 1 June 2000 in Pécs, Hungary. The ardent discussions among the participants at that Workshop greatly inspired him to respond to the need for an in-depth experimental survey on the electron dephasing in real metals and semiconductors. Part of this manuscript was written (by JJL) at the low-temperature laboratory of Professor C Uher at the University of Michigan–Ann Arbor, whose hospitality is gratefully acknowledged. This work was supported at NCTU by the Taiwan National Science Council, and at ASU by the Office of Naval Research and the Department of Energy.

References

[1] Bergmann G 1984 *Phys. Rep.* **107** 1
[2] Kobayashi S and Komiri F 1985 *Prog. Theor. Phys. Suppl.* **84** 224
[3] Altshuler B L and Aronov A G 1985 *Electron–Electron Interactions in Disordered Systems* ed A L Efros and M Pollak (Amsterdam: Elsevier)
[4] Fukuyama H 1985 *Electron–Electron Interactions in Disordered Systems* ed A L Efros and M Pollak (Amsterdam: Elsevier)
[5] Lee P A and Ramakrishnan T V 1985 *Rev. Mod. Phys.* **57** 287
[6] Chakravarty S and Schmid A 1986 *Phys. Rep.* **140** 194
[7] Altshuler B L, Aronov A G, Gershenson M E and Sharvin Yu V 1987 *Sov. Sci. Rev.* A **9** 223
[8] Giordano N 1991 *Mesoscopic Phenomena in Solids* ed B L Altshuler, P A Lee and R A Webb (Amsterdam: Elsevier)
[9] Washburn S and Webb R A 1986 *Adv. Phys.* **35** 375
[10] Imry Y 1997 *Introduction to Mesoscopic Physics* (Oxford: Oxford University Press)
[11] Natelson D, Willett R L, West K W and Pfeiffer L N 2001 *Phys. Rev. Lett.* **86** 1821
[12] Mohanty P, Jariwala E M Q and Webb R A 1997 *Phys. Rev. Lett.* **78** 3366
[13] Lin J J and Kao L Y 2001 *J. Phys.: Condens. Matter* **13** L119
[14] Zawadowski A, von Delft J and Ralph D C 1999 *Phys. Rev. Lett.* **83** 2632
Ujsaghy O, Zarand G and Zawadowski A 2001 *Solid State Commun.* **117** 167
[15] Imry Y, Fukuyama H and Schwab P 1999 *Europhys. Lett.* **47** 608
[16] Kaminski A and Glazman L I 2001 *Phys. Rev. Lett.* **86** 2400
[17] Polyanskaya T A and Shmartsev Yu V 1989 *Sov. Phys.–Semicond.* **23** 1
Ootuka Y and Kawabata A 1985 *Prog. Theor. Phys. Suppl.* **84** 249
[18] Van Haesendonck C, Vloeberghs H and Bruynseraede Y 1991 *Quantum Coherence in Mesoscopic Systems* ed B Kramer (New York: Plenum)
[19] Bouchiat H 1995 *Mesoscopic Quantum Physics* ed E Akkermans, G Montambaux, J-L Pichard and J Zinn-Justin (Amsterdam: Elsevier)
[20] Bird J P 1999 *J. Phys.: Condens. Matter* **11** R413
[21] Kobayashi S 1992 *Surf. Sci. Rep.* **16** 1
[22] Rammer J and Schmid A 1986 *Phys. Rev.* B **34** 1352
[23] Belitz D and Wybourne M N 1995 *Phys. Rev.* B **51** 689
[24] Gershenson M E 1999 *Ann. Phys., Berlin* **8** 559
[25] Mui K C, Lindenfeld P and McLean W L 1984 *Phys. Rev.* B **30** 2951
[26] Komori F, Okuma S and Kobayashi S 1987 *J. Phys. Soc. Japan* **56** 691
[27] Koike Y, Okamura M and Fukase T 1985 *J. Phys. Soc. Japan* **54** 3018
[28] Kuzmenko V M, Vladychkin A N, Melnikov V I and Sudovtsov A I 1984 *Sov. Phys.–JETP* **59** 102
[29] Howson M A and Gallagher B L 1988 *Phys. Rep.* **170** 265
[30] Dugdale J S 1995 *The Electrical Properties of Disordered Metals* (Cambridge: Cambridge University Press)
[31] Wu C Y and Lin J J 1994 *Phys. Rev.* B **50** 385
[32] Wu C Y, Jian W B and Lin J J 1998 *Phys. Rev.* B **57** 11 232
[33] Reizer M Yu and Sergeev A Y 1986 *Sov. Phys.–JETP* **63** 616
Sergeev A V and Reizer M Yu 1996 *Int. J. Mod. Phys.* B **10** 635
[34] Belitz D and Wysokinski K I 1987 *Phys. Rev.* B **36** 9333
[35] Altshuler B L, Aronov A G and Khmelnitzky D E 1982 *J. Phys. C: Solid State Phys.* **15** 7367
[36] Lin J J and Giordano N 1987 *Phys. Rev.* B **35** 1071
[37] Mohanty P and Webb R A 1997 *Phys. Rev.* B **55** R13 452
[38] Gougam A B, Pierre F, Pothier H, Esteve D and Birge N O 2000 *J. Low Temp. Phys.* **118** 447
[39] Pierre F, Pothier H, Esteve D, Devoret M H, Gougam A B and Birge N O 2001 *Kondo Effect and Dephasing in Low-Dimensional Metallic Systems* ed V Chandrasekhar, C Van Haesendonck and A Zawadowski (Dordrecht: Kluwer)
[40] Goppert G and Grabert H 2001 *Phys. Rev.* B **64** 033301
[41] Altshuler B L, Gershenson M E and Aleiner I L 1998 *Physica* E **3** 58
[42] Aleiner I L, Altshuler B L and Gershenson M E 1999 *Waves Random Media* **9** 201
Aleiner I L, Altshuler B L and Vavilov 2002 *J. Low Temp. Phys.* **126** 1377
[43] Ovadyahu Z 2001 *Phys. Rev.* B **63** 235403
[44] Golubev D S and Zaikin A D 1998 *Phys. Rev. Lett.* **81** 1074
Golubev D S and Zaikin A D 1999 *Phys. Rev. Lett.* **82** 3191
Golubev D S and Zaikin A D 1999 *Phys. Rev.* B **59** 9195

[45] Golubev D S, Zaikin A D and Schön G 2002 *J. Low Temp. Phys.* **126** 1355
[46] Hikami S, Larkin A I and Nagaoka Y 1980 *Prog. Theor. Phys.* **63** 707
[47] Geier S and Bergmann G 1992 *Phys. Rev. Lett.* **68** 2520
Papanikolaou N, Stefanou N, Dederichs P H, Geier S and Bergmann G 1992 *Phys. Rev. Lett.* **69** 2110
[48] Pippard A B 1955 *Phil. Mag.* **46** 1104
Holstein T 1959 *Phys. Rev.* **113** 479
[49] Altshuler B L, Aronov A G and Khmelnitsky D E 1981 *Solid State Commun.* **39** 619
[50] Belitz D and Das Sarma S 1987 *Phys. Rev.* B **36** 7701
[51] Rodmar M, Ahlgren M, Oberschmidt D, Gignoux C, Delahaye J, Berger C, Poon J S and Rapp O 2000 *Phys. Rev.* B **61** 3936
[52] Appenzeller J, Martel R, Avouris Ph, Stahl H, Hunger U Th and Lengeler B 2001 *Phys. Rev.* B **64** 121404
Liu K, Avouris Ph, Martel R and Hsu W K 2001 *Phys. Rev.* B **63** 161404
[53] Fournier P, Higgins J, Balci H, Maiser E, Lobb C J and Greene R L 2000 *Phys. Rev.* B **62** R11 993
[54] Altshuler B L and Aronov A G 1981 *JETP Lett.* **33** 499
[55] Echternach P M, Gershenson M E, Bozler H M, Bogdanov A L and Nilsson B 1993 *Phys. Rev.* B **48** 11 516
[56] Kawabata A 1980 *Solid State Commun.* **34** 431
[57] Fukuyama H and Hoshino K 1981 *J. Phys. Soc. Japan* **50** 2131
[58] Webb R A 1998 *Superlatt. Microstruct.* **23** 969
[59] Ando T and Fukuyama H (ed) 1988 *Anderson Localization* (Berlin: Springer)
[60] Kramer B, Bergmann G and Bruynseraede Y (ed) 1985 *Localization, Interaction, and Transport Phenomena* (Berlin: Springer)
[61] Kittel C 1996 *Introduction to Solid State Physics* 7th edn (New York: Wiley)
[62] Larkin A I 1980 *JETP Lett.* **31** 219
[63] Lopes dos Santos J M B and Abrahams E 1985 *Phys. Rev.* B **31** 172
[64] Aslamazov L G and Larkin A I 1968 *Phys. Lett.* A **26** 238
[65] Altshuler B L, Aronov A G, Larkin A I and Khmelnitskii D E 1981 *Sov. Phys.–JETP* **54** 411
[66] Baxter D V, Richter R, Trudeau M L, Cochrane R W and Strom-Olsen J O 1989 *J. Physique* **50** 1673
[67] Bruynseraede Y, Gijs M, Van Haesendonck C and Deutscher G 1983 *Phys. Rev. Lett.* **50** 277
[68] Giannouri M, Rocofyllou E, Papastaikoudis C and Schilling W 1997 *Phys. Rev.* B **56** 6148
Giannouri M, Papastaikoudis C and Rosenbaum R 1999 *Phys. Rev.* B **59** 4463
[69] Meiners-Hagen K and Gey W 2001 *Phys. Rev.* B **63** 052507
[70] Beenakker C W J and van Houten H 1991 *Solid State Physics* vol 44, ed H Ehrenreich and D Turnbull p 1
[71] Choi K K, Tsui D C and Alavi K 1987 *Phys. Rev.* B **36** 7751
[72] Beenakker C W J and van Houten H 1988 *Phys. Rev.* B **38** 3232
[73] Foxon C T and Harris J J 1986 *Philips J. Res.* **41** 313
[74] Beenakker C W J and van Houten H 1988 *Phys. Rev.* B **37** 6544
[75] van Houten H, Beenakker C W J, van Wees B J and Mooij J E 1988 *Surf. Sci.* **196** 144
[76] Chang A M, Timp G, Chang T Y, Cunningham J E, Mankiewich P, Behringer R E and Howard R E 1988 *Solid State Commun.* **67** 769
[77] Hiramoto T, Hirakawa K, Iye Y and Ikoma T 1989 *Appl. Phys. Lett.* **54** 2103
[78] Chandrasekhar V, Prober D E and Santhanam P 1988 *Phys. Rev. Lett.* **61** 2253
[79] Nguyen V L, Spivak B Z and Shklovskii B I 1985 *Sov. Phys.–JETP* **62** 1021
[80] Wu G Y 2001 *J. Phys.: Condens. Matter* **13** 9739
[81] Sheng P J and Lin J J 1999 unpublished
[82] Hsu S Y, Sheng P J and Lin J J 1999 *Phys. Rev.* B **60** 3940
[83] Abrikosov A A and Gorkov L P 1962 *Sov. Phys.–JETP* **15** 752
[84] Bergmann G 1982 *Phys. Rev. Lett.* **48** 1046
[85] Sahnoune A, Strom-Olsen J O and Fischer H E 1992 *Phys. Rev.* B **46** 10 035
[86] McGinnis W C and Chaikin P M 1985 *Phys. Rev.* B **32** 6319
[87] Lin J J and Giordano N 1986 *Phys. Rev.* B **33** 1519
[88] Lin J J and Giordano N 1987 *Phys. Rev.* B **35** 545
[89] Natelson D, Willett R L, West K W and Pfeiffer L N 2000 *Appl. Phys. Lett.* **77** 1991
Natelson D, Willett R L, West K W and Pfeiffer L N 2000 *Solid State Commun.* **115** 269
[90] Kanskar M and Wybourne M N 1994 *Phys. Rev. Lett.* **73** 2123
[91] Kanskar M and Wybourne M N 1994 *Phys. Rev.* B **50** 168
[92] Giordano N, Gilson W and Prober D E 1979 *Phys. Rev. Lett.* **43** 725
Giordano N 1980 *Phys. Rev.* B **22** 5635
[93] Dolan G J and Osheroff D D 1979 *Phys. Rev. Lett.* **43** 721

[94] Zhong Y L and Lin J J 1998 *Phys. Rev. Lett.* **80** 588
[95] Sergeev A and Mitin V 2000 *Phys. Rev.* B **61** 6041
[96] Sergeev A and Mitin V 2000 *Europhys. Lett.* **51** 641
[97] Mooij J E and Klapwijk T M 1985 *Localization, Interaction, and Transport Phenomena* ed B Kramer, G Bergmann and Y Bruynseraede (Berlin: Springer)
[98] Matthias B, Compton V B, Suhl H and Corenzwit E 1959 *Phys. Rev.* **115** 1597
Martin I and Phillips P 1997 *Phys. Rev.* B **56** 14 650
[99] Jian W B and Lin J J 1996 unpublished
[100] Gordon J M, Lobb C J and Tinkham M 1984 *Phys. Rev.* B **29** 5232
[101] Stolovits A, Sherman A, Ahn K and Kremer R K 2000 *Phys. Rev.* B **62** 10 565
[102] Ebisawa H, Maekawa S and Fukuyama H 1983 *Solid State Commun.* **45** 75
Brenig W, Chang M, Abrahams E and Wolfe P 1985 *Phys. Rev.* B **31** 7001
Reizer M Yu 1992 *Phys. Rev.* B **45** 12 949
Devereaux T P and Belitz D 1996 *Phys. Rev.* B **53** 359
[103] Rosenbaum R, Hsu S Y, Chen J Y, Lin Y H and Lin J J 2001 *J. Phys.: Condens. Matter* **13** 10 041
[104] Bergmann G 1986 *Phys. Rev. Lett.* **57** 1460
Bergmann G 1987 *Phys. Rev. Lett.* **58** 1236
Beckmann H, Ye F and Bergmann G 1994 *Phys. Rev. Lett.* **73** 1715
[105] Peters R P, Bergmann G and Mueller R M 1987 *Phys. Rev. Lett.* **58** 1964
Peters R P, Bergmann G and Mueller R M 1988 *Phys. Rev. Lett.* **60** 1093
[106] Van Haesendonck C, Vranken J and Bruynseraede Y 1987 *Phys. Rev. Lett.* **58** 1968
[107] Vranken J, Van Haesendonck C and Bruynseraede Y 1988 *Phys. Rev.* B **37** 8502
[108] Bergmann G and Hossain M 2001 *Phys. Rev. Lett.* **86** 2138
[109] Johnson M 1995 *Mater. Sci. Eng.* B **31** 199
[110] Bergmann G 1982 *Z. Phys.* B **48** 5
[111] Petta J R and Ralph D 2001 *Phys. Rev. Lett.* **87** 266801
[112] Mueller R M, Stasch R and Bergmann G 1994 *Solid State Commun.* **91** 255
[113] Weissmann M B 1993 *Rev. Mod. Phys.* **65** 829
[114] Umbach C P, Washburn S, Laibowitz R B and Webb R A 1984 *Phys. Rev.* B **30** 4048
[115] Lee P A, Stone A D and Fukuyama H 1987 *Phys. Rev.* B **35** 1039
[116] Licini J C, Bishop D J, Kastner M A and Melngailis 1985 *Phys. Rev. Lett.* **55** 2987
[117] Ralls K S, Skocpol W J, Jackel L D, Howard R E, Fetter L A, Epworth R W and Tennant D M 1984 *Phys. Rev. Lett.* **52** 228
[118] Lee P A and Stone A D 1985 *Phys. Rev. Lett.* **55** 1622
[119] Altshuler B L and Khmelnitskii D E 1986 *JETP Lett.* **42** 359
[120] Timp G, Chang A M, Mankiewich P, Behringer R, Cunningham J E, Chang T Y and Howard R E 1987 *Phys. Rev. Lett.* **59** 732
[121] Taylor R P, Main P C, Eaves L, Beaumont S P, McIntyre I, Thoms S and Wilkinson C D W 1989 *J. Phys.: Condens. Matter* **1** 10 413
[122] Bird J P, Grassie A D C, Lakrimi M, Hutchings K M, Harris J J and Foxon C T 1990 *J. Phys.: Condens. Matter* **2** 7847
[123] Bykov A A, Gusev G M, Kvon Z D, Katkov A V and Plyuchin V B 1991 *Superlatt. Microstruct.* **10** 287
[124] Geim A K, Main P C, Beton P H, Eaves L, Beaumont S P and Wilkinson C D W 1992 *Phys. Rev. Lett.* **69** 1248
[125] Brown C V, Geim A K, Foster T J, Langerak C J G M and Main P C 1993 *Phys. Rev.* B **47** 10 935
[126] Morgan A, Cobden D H, Pepper M, Jin G, Tang Y S and Wilkinson C D W 1994 *Phys. Rev.* B **50** 12 187
[127] Bird J P, Ishibashi K, Ochiai Y, Lakrimi M, Grassie A D C, Hutchings K M, Aoyagi Y and Sugano T 1995 *Phys. Rev.* B **52** 1793
[128] Thornton T J, Pepper M, Ahmed H, Andrews D and Davies G J 1986 *Phys. Rev. Lett.* **56** 1198
[129] Bird J P, Akis R, Ferry D K, Vasileska D, Cooper J, Aoyagi Y and Sugano T 1999 *Phys. Rev. Lett.* **82** 4691
[130] Marcus C M, Rimberg A J, Westervelt R M, Hopkins P F and Gossard A C 1992 *Phys. Rev. Lett.* **69** 506
[131] Jalabert R A, Baranger H U and Stone A D 1990 *Phys. Rev. Lett.* **65** 2442
[132] Baranger H U, Jalabert R A and Stone A D 1993 *Phys. Rev. Lett.* **70** 3876
[133] Nakamura K 1997 *Chaos, Solitons and Fractals* vol 8, ed K Nakamura, number 7/8 (Exeter: Pergamon)
[134] Baranger H U and Westervelt R M 1999 *Nanotechnology* ed G Timp (Berlin: Springer) p 537
[135] Marcus C M, Westervelt R M, Hopkins P F and Gossard A C 1993 *Phys. Rev.* B **48** 2460
[136] Clarke R M, Chan I H, Marcus C M, Duruoz C I, Harris J S Jr, Campman K and Gossard A C 1995 *Phys. Rev.* B **52** 2656
[137] Huibers A G, Switkes M, Marcus C M, Campman K and Gossard A C 1998 *Phys. Rev. Lett.* **81** 200

[138] Baranger H U and Mello P A 1994 *Phys. Rev. Lett.* **73** 142
[139] Baranger H U and Mello P A 1995 *Phys. Rev.* B **51** 4703
[140] Buttiker M 1988 *IBM J. Res. Dev.* **32** 63
[141] Efetov K B 1995 *Phys. Rev. Lett.* **74** 2299
[142] Bird J P, Ishibashi K, Ferry D K, Ochiai Y, Aoyagi Y and Sugano T 1995 *Phys. Rev.* B **51** R18 037
[143] Micolich A P, Taylor R P, Newbury R, Bird J P, Wirtz R, Dettmann C P, Aoyagi Y and Sugano T 1998 *J. Phys.: Condens. Matter* **10** 1339
[144] Pivin D P Jr, Anderson A, Bird J P and Ferry D K 1999 *Phys. Rev. Lett.* **82** 4687
[145] Prasad C, Ferry D K, Shailos A, Elhassan M, Bird J P, Lin L-H, Aoki N, Ochiai Y, Ishibashi K and Aoyagi Y 2000 *Phys. Rev.* B **62** 15 356
[146] Ferry D K, Edwards G, Ochiai Y, Yamamoto K, Bird J P, Ishibashi K, Aoyagi Y and Sugano T 1995 *Japan. J. Appl. Phys.* **34** 4338
[147] Bending S, von Klitzing K and Ploog K 1990 *Phys. Rev. Lett.* **65** 1060
[148] Sheng P 1995 *Introduction to Wave Scattering, Localization and Mesoscopic Phenomena* (Boston, MA: Academic)
[149] Labeyrie G, de Tomasi F, Bernard J C, Muller C A, Miniatura C and Kaiser R 1999 *Phys. Rev. Lett.* **83** 5266
[150] Fukai Y K, Yamada S and Nakano H 1990 *Appl. Phys. Lett.* **56** 2123
[151] Ketzmerick R 1996 *Phys. Rev.* B **54** 10 841
[152] Sachrajda A S, Ketzmerick R, Gould C, Feng Y, Kelly P J, Delage A and Wasilewski Z 1998 *Phys. Rev. Lett.* **80** 1948
[153] Huckstein B, Ketzmerick R and Lewenkopf C 2000 *Phys. Rev. Lett.* **84** 5504
[154] Takagaki Y, Elhassan M, Shailos A, Prasad C, Bird J P, Ferry D K, Ploog K H, Lin L-H, Aoki N and Ochiai Y 2000 *Phys. Rev.* B **62** 10 255
[155] Micolich A P *et al* 2001 *Phys. Rev. Lett.* **87** 036802
[156] de Moura A P S, Lai Y-C, Akis R, Bird J P and Ferry D K 2002 at press
[157] Reizer M Yu 1989 *Phys. Rev.* B **40** 5411
[158] Bergmann G 1969 *Phys. Lett.* A **29** 492
Bergmann G 1969 *Z. Phys.* **228** 25
Bergmann G 1971 *Phys. Rev.* B **3** 3797
[159] Takayama H 1973 *Z. Phys.* **263** 329
[160] Schmid A 1973 *Z. Phys.* **259** 421
[161] Belitz D 1987 *Phys. Rev.* B **36** 2513
[162] Ziman J M 1960 *Electrons and Phonons* (Oxford: Clarendon)
[163] Tsuneto T 1961 *Phys. Rev.* **121** 402
[164] Eisenriegler E 1973 *Z. Phys.* **258** 185
Grunewald G and Scharnberg 1974 *Z. Phys.* **268** 197
Grunewald G and Scharnberg 1975 *Z. Phys.* B **20** 61
[165] Chow E, Wei H P, Girvin S M and Shayegan M 1996 *Phys. Rev. Lett.* **77** 1143
[166] Aronov A G, Gershenson M E and Zhuravlev Yu E 1984 *Sov. Phys.–JETP* **60** 554
[167] Dynes R C, Geballe T H, Hull G W Jr and Garno J P 1983 *Phys. Rev.* B **27** 5188
[168] Newson D J, Pepper M, Hall H Y and Marsh J H 1985 *J. Phys. C: Solid State Phys.* **18** L1041
[169] Richter R, Baxter D V and Strom-Olsen J O 1988 *Phys. Rev.* B **38** 10 421
[170] Bergmann G, Wei W, Zou Y and Mueller R M 1990 *Phys. Rev.* B **41** 7386
[171] Komnik Yu F, Kashirin V Yu, Belevtsev B I and Beliaev E Yu 1994 *Phys. Rev.* B **50** 15 298
[172] Liu J and Giordano N 1991 *Phys. Rev.* B **43** 3928
[173] Lin J J and Wu C Y 1995 *Europhys. Lett.* **29** 141
[174] Lin J J 2000 *Physica* B **279** 191
[175] Lin J J and Wu C Y 1993 *Phys. Rev.* B **48** 5021
[176] Liu S, Zhang D L, Jing X, Lu L, Li S, Kang N, Wu X and Lin J J 2000 *Phys. Rev.* B **62** 8695
[177] Wiesmann H, Gurvitch M, Ghosh A K, Lutz H, Kammerer O F and Strongin M 1978 *Phys. Rev.* B **17** 122
Leitner A, Olaya D, Rogers C T and Price J C 2000 *Phys. Rev.* B **62** 1408
[178] Lin J J and Wu C Y 1996 *Physica* B **219–20** 68
[179] Gershenson M E, Gong D, Sato T, Karasik B S and Sergeev A V 2001 *Appl. Phys. Lett.* **79** 2049
[180] Ptitsina N G, Chulkova G M, Il'in K S, Sergeev A V, Pochinkov F S, Gershenzon E M and Gershenson M E 1997 *Phys. Rev.* B **56** 10 089
[181] Wu C Y 1996 *PhD Thesis* National Taiwan University
[182] Zhong Y L, Kao L Y and Lin J J 2002 at press
[183] Meikap A K and Lin J J 2002 at press

[184] Peters R P and Bergmann G 1985 *J. Phys. Soc. Japan* **54** 3478
[185] Schmid A 1985 *Localization, Interaction, and Transport Phenomena* ed B Kramer, G Bergmann and Y Bruynseraede (Berlin: Springer)
[186] Gershenzon E M, Gershenzon M E, Gol'tsman G N, Lyul'kin A M, Semenov A D and Sergeev A V 1990 *Sov. Phys.–JETP* **70** 505
[187] Butenko A V and Bukhshtab E I 1985 *Sov. Phys.–JETP* **61** 618
[188] Jan W, Wu G Y and Wei H S 2001 *Phys. Rev.* B **64** 165101
Jan W and Wu G Y 2001 *J. Phys.: Condens. Matter* **13** 10 925
[189] Sergeev A, Karasik B S, Gershenson M and Mitin V 2002 *Physica* B at press
[190] Friedrichowski S and Dumpich G 1998 *Phys. Rev.* B **58** 9689
[191] Roukes M L, Freeman M R, Germain R S, Richardson R C and Ketchen M B 1985 *Phys. Rev. Lett.* **55** 422
[192] Dalrymple B J, Wolf S A, Ehrlich A C and Gillespie D J 1986 *Phys. Rev.* B **33** 7514
[193] Kwong Y K, Lin K, Isaacson M S and Parpia J M 1992 *J. Low Temp. Phys.* **88** 261
[194] Echternach P M, Thoman M R, Gould C M and Bozler H M 1992 *Phys. Rev.* B **46** 10 339
[195] DiTusa J F, Lin K, Park M, Isaacson M S and Parpia J M 1992 *Phys. Rev. Lett.* **68** 1156
[196] Dumpich G and Carl A 1991 *Phys. Rev.* B **43** 12 074
[197] Stolovits A, Sherman A, Avarmaa T, Meier O and Sisti M 1998 *Phys. Rev.* B **58** 11 111
[198] Dorozhkin S I and Schoepe W 1986 *Solid State Commun.* **60** 245
[199] Moon J S, Birge N O and Golding B 1996 *Phys. Rev.* B **53** R4193
[200] Licini J C, Dolan G J and Bishop D J 1985 *Phys. Rev. Lett.* **54** 1585
[201] Lin J J, Li T J and Wu T M 2000 *Phys. Rev.* B **61** 3170
[202] Chun K and Birge N O 1994 *Phys. Rev.* B **49** 2959
[203] Abraham D and Rosenbaum R 1984 *J. Phys. C: Solid State Phys.* **17** 2627
[204] Poon S J, Wong K M and Drehman A J 1985 *Phys. Rev.* B **31** 1668
[205] Trudeau M L and Cochrane R W 1988 *Phys. Rev.* B **38** 5353
[206] Trudeau M L and Cochrane R W 1990 *Phys. Rev.* B **41** 10 535
[207] Chen J T, Chen T T, Leslie J D and Smith H J T 1967 *Phys. Lett.* A **25** 679
Bergmann G 1976 *Phys. Rep.* **27** 161
Watson P W III and Naugle D G 1995 *Phys. Rev.* B **51** 685
[208] Keck B and Schmid A 1975 *Solid State Commun.* **17** 799
Keck B and Schmid A 1976 *J. Low Temp. Phys.* **24** 611
[209] Mittal A, Wheeler R G, Keller M W, Prober D E and Sacks R N 1996 *Surf. Sci.* **361–2** 537
[210] Chow E, Wei H P, Girvin S M, Jan W and Cunningham J E 1997 *Phys. Rev.* B **56** R1676
[211] Eschner W, Gey W and Warnecke P 1984 *Proc. 17th Int. Conf. on Low Temperature Physics* ed U Eckern, A Schmid, W Weber and H Wuhl (Amsterdam: Elsevier) p 497
[212] Il'in K S, Ptitsina N G, Sergeev A V, Goltsmann G N, Gershenzon E M, Karasik B S, Pechen E V and Krasnosvobodtsev S I 1998 *Phys. Rev.* B **57** 15 623
[213] Seyler J and Wybourne M N 1992 *Phys. Rev. Lett.* **69** 1427
[214] Wind S, Rooks M J, Chandrasekhar V and Prober D E 1986 *Phys. Rev. Lett.* **57** 633
[215] Schmid A 1974 *Z. Phys.* **271** 251
[216] Altshuler B L and Aronov A G 1979 *JETP Lett.* **30** 482
[217] Ovadyahu Z 1984 *Phys. Rev. Lett.* **52** 569
[218] Beutler D E and Giordano N 1988 *Phys. Rev.* B **38** 8
[219] Li T J and Lin J J 1997 *Phys. Rev.* B **56** 8032
[220] Aleiner I L, Altshuler B L and Gershenson M E 1999 *Phys. Rev. Lett.* **82** 3190
[221] Gershenson M E, Khavin Yu B, Mikhalchuk A G, Bolzer H M and Bogdanov A L 1997 *Phys. Rev. Lett.* **79** 725
[222] Lin J J, Xu W, Zhong Y L, Huang J H and Huang Y S 1999 *Phys. Rev.* B **59** 344
[223] Dai P, Zhang Y and Sarachik M P 1992 *Phys. Rev.* B **46** 6724
[224] Ghosh A and Raychaudhuri A K 2000 *Phys. Rev. Lett.* **84** 4681
[225] Aleshin A N, Mironkov N B and Suvorov A V 1996 *Phys. Solid State* **38** 72
Menon R, Yoon C O, Moses D, Heeger A J and Cao Y 1993 *Phys. Rev.* B **48** 17 685
Ghosh M, Barman A, Das A, Meikap A K, De S K and Chatterjee S 1998 *J. Appl. Phys.* **83** 4230
[226] Black J L, Gyorffy B L and Jackle J 1979 *Phil. Mag.* B **40** 331
[227] Cukier R I, Morillo M, Chun K and Birge N O 1995 *Phys. Rev.* B **51** 13 767
Chun K and Birge N O 1993 *Phys. Rev.* B **48** 11500
Golding B, Zimmerman N M and Coppersmith S N 1992 *Phys. Rev. Lett.* **68** 998
[228] Lin J J, Sheng P J and Hsu S Y 2000 *Physica* B **280** 460
[229] Noguchi M, Ikoma T, Odagiri T, Sakakibara H and Wang S N 1996 *J. Appl. Phys.* **80** 5138

[230] Huibers A G, Folk J A, Patel S R, Marcus C M, Duruoz C I and Harris J S Jr 1999 *Phys. Rev. Lett.* **83** 5090
[231] Aleshin A N, Kozub V I, Suh D S and Park Y W 2001 *Phys. Rev.* B **64** 224208
[232] Houshangpour K and Maschke K 1999 *Phys. Rev.* B **59** 4615
[233] Raimondi R, Schwab P and Castellani C 1999 *Phys. Rev.* B **60** 5818
[234] Ben-Jacob E, Hermon Z and Shnirman A 1999 *Phys. Lett.* A **256** 369
[235] Wang X R, Xiong G and Wang S D 2000 *Phys. Rev.* B **61** R5090
[236] Flores J C 2000 *Phys. Rev.* B **62** R16291
[237] Volker A and Kopietz P 2000 *Phys. Rev.* B **61** 13 508
Volker A and Kopietz P 2002 *Phys. Rev.* B **65** 045112
[238] Seelig G and Buttiker M 2001 *Phys. Rev.* B **64** 245313
Cedraschi P and Buttiker M 2001 *Ann. Phys., NY* **289** 1
Buttiker M 2001 *Preprint* cond-mat/0106149
Nagaev K E and Buttiker M 2001 *Preprint* cond-mat/0108243
[239] Mourokh L G, Smirnov A Yu, Puller V I and Horing N J M 2001 *Phys. Lett.* A **288** 49
[240] Kirkpatrick T R and Belitz D 2001 *Preprint* cond-mat/0111398
Golubev D S, Zaikin A D and Schön 2001 *Preprint* cond-mat/0111527
Kirkpatrick T R and Belitz D 2001 *Preprint* cond-mat/0112063
[241] Mohanty P 2000 *Physica* B **280** 446
Mohanty P 2001 *Complexity from Microscopic to Macroscopic Scales: Coherence and Large Deviations (NATO ASI Series)* ed A T Skjeltorp and T Vicsek (Dordrecht: Kluwer)
[242] Mohanty P 1999 *Ann. Phys., Berlin* **8** 549
[243] Kravtsov V E and Altshuler B L 2000 *Phys. Rev. Lett.* **84** 3394
Schwab P 2000 *J. Eur. Phys.* B **18** 189
Cedraschi P, Ponomarenko V V and Buttiker M 2000 *Phys. Rev. Lett.* **84** 346
Cedraschi P and Buttiker M 2001 *Phys. Rev.* B **63** 165312
Eckern U and Schwab P 2002 *J. Low Temp. Phys.* **126** 1291
[244] Webb R A, Mohanty P, Jariwala E M Q, Stevenson T R and Zhaiikov A G 1998 *Quantum Coherence and Decoherence* ed K Fujikawa and Y A Ono (Amsterdam: North-Holland)
[245] Webb R A, Mohanty P and Jariwala E M Q 1998 *Fortschr. Phys.* **46** 779
[246] Lin J J, Zhong Y L and Li T J 2002 *Europhys. Lett.* **57** 872
[247] Pouydebasque A, Pogosov A G, Budantsev M V, Maude D K, Plotnikov A E, Toropov A I and Portal J C 2001 *Physica* B **298** 287
[248] Burke P J, Pfeiffer L N and West K W 2001 *Preprint* cond-mat/0107454
[249] Liu J and Giordano N 1991 *Phys. Rev.* B **43** 1385
[250] Komori F, Kobayashi S and Sasaki W 1983 *J. Phys. Soc. Japan* **52** 4306
[251] Kumar N, Baxter D V, Richter R and Strom-Olsen J O 1987 *Phys. Rev. Lett.* **59** 1853
Rammer J, Shelankov A L and Schmid A 1988 *Phys. Rev. Lett.* **60** 1985
Bergmann G 1988 *Phys. Rev. Lett.* **60** 1986
[252] Anthore A, Pierre F, Pothier H, Esteve D and Devoret M H 2001 *Preprint* cond-mat/0109297
Goppert G, Galperin Y M, Altshuler B L and Grabert H 2002 *Preprint* cond-mat/0202353
[253] Kroha J 2001 *Preprint* cond-mat/0102185
[254] Pierre F and Birge N O 2002 unpublished
[255] Pierre F 2001 *Ann. Phys., Paris* **26** 4
[256] Dikin D A, Black M J and Chandrasekhar V 2001 *Phys. Rev. Lett.* **87** 187003
[257] Aleiner I L, Altshuler B L and Galperin Y M 2001 *Phys. Rev.* B **63** 201401
Ahn K H and Mohanty P 2001 *Phys. Rev.* B **63** 195301
[258] Aleiner I L, Altshuler B L, Galperin Y M and Shutenko T A 2001 *Phys. Rev. Lett.* **86** 2629
[259] Blachly M A and Giordano N 1995 *Phys. Rev.* B **51** 12537
Blachly M A and Giordano N 1994 *Europhys. Lett.* **27** 687
[260] Dolan G J, Licini J C and Bishop D J 1986 *Phys. Rev. Lett.* **56** 1493
[261] Umbach C P, Haesendonck C V, Laibowitz R B, Washburn S and Webb R A 1986 *Phys. Rev. Lett.* **56** 386
[262] Milliken F P, Washburn S, Umbach C P, Laibowitz R B and Webb R A 1987 *Phys. Rev.* B **36** 4465
[263] White E A, Dynes R C and Garno J P 1984 **29** 3694
[264] Komori F, Kobayashi S and Sasaki W 1983 *J. Phys. Soc. Japan* **52** 368
[265] Ashcroft N W and Mermin N D 1976 *Solid State Physics* (Philadelphia, PA: Saunders)
[266] Giuliani G F and Quinn J J 1982 *Phys. Rev.* B **26** 4421
[267] Yacoby A, Sivan U, Umbach C P and Hong J M 1991 *Phys. Rev. Lett.* **66** 1938
[268] Abrahams E, Anderson P W, Lee P A and Ramakrishnan T V 1981 *Phys. Rev.* B **24** 6783

[269] Fukuyama H and Abrahams E 1983 *Phys. Rev.* B **27** 5976
[270] Thornton T J, Pepper M, Ahmed H, Davies G J and Andrews D 1987 *Phys. Rev.* B **36** 4514
[271] Pooke D M, Paquin N, Pepper M and Gundlach A 1989 *J. Phys.: Condens. Matter* **1** 3289
[272] Kurdak C, Chang A M, Chin A and Chang T Y 1992 *Phys. Rev.* B **46** 6846
[273] Linke H, Omling P, Xu H and Lindelof P E 1997 *Phys. Rev.* B **55** 4061
[274] de Graaf C, Caro J and Radelaar S 1992 *Phys. Rev.* B **46** 12 814
[275] Wheeler R G, Choi K K, Goel A, Wisnieff R and Prober D E 1982 *Phys. Rev. Lett.* **49** 1674
[276] Altshuler B L, Aronov A G and Zyuzin A 1984 *JETP* **59** 415
[277] Bergmann G 1983 *Phys. Rev.* B **28** 2914
[278] Aihara K, Yamamoto M, Iwadate K and Mizutani T 1991 *Japan J. Appl. Phys.* **9B** L1627
[279] van Veen R G, Verbruggen A H, van der Drift E, Schaffler F and Radelaar S 1999 *Semicond. Sci. Technol.* **14** 508
[280] Stoger G, Brunthaler G, Bauer G, Ismail K, Meyerson B S, Lutz J and Kuchar F 1994 *Semicond. Sci. Technol.* **9** 765
[281] Minkov G M, Germanenko A V, Rut O E, Sherstobitov A A, Zvonkov B N, Uskova E A and Birukov A A 2001 *Phys. Rev.* B **64** 193309
[282] Prasad R S, Thornton T J, Matsumura A, Fernandez J M and Williams D 1995 *Semicond. Sci. Technol.* **10** 1084
[283] Khavin Yu B, Gershenson M E and Bogdanov A L 1998 *Phys. Rev. Lett.* **81** 1066
[284] Linke H, Bird J P, Cooper J, Omling P, Aoyagi Y and Sugano T 1997 *Phys. Rev.* B **56** 14 937
[285] Bird J P, Micolich A P, Linke H, Ferry D K, Akis R, Ochiai Y, Aoyagi Y and Sugano T 1998 *J. Phys.: Condens. Matter* **10** L55
[286] Takane Y 1998 *J. Phys. Soc. Japan* **67** 3003
[287] Sivan U, Imry Y and Aronov A G 1994 *Europhys. Lett.* **28** 115
[288] Switkes M, Huibers A G, Marcus C M, Campman K and Gossard A C 1998 *Appl. Phys. Lett.* **72** 471
[289] Yacoby A, Heiblum M, Shtrikman H, Umansky V and Mahalu D 1994c *Semicond. Sci. Technol.* **9** 907
[290] Chaplik A V 1971 *Sov. Phys.–JETP* **33** 997
[291] Komiyama S, Hirai H, Sasa S and Hiyamizu S 1989 *Phys. Rev.* B **40** 12 566
[292] Alphenaar B W, McEuen P L, Wheeler R G and Sacks R N 1990 *Phys. Rev. Lett.* **64** 677
[293] van Wees B J, Kouwenhoven L P, Willems E M M, Harmans C J P M, Mooij J E, van Houten H, Beenakker C W J, Williamson J G and Foxon C T 1989 *Phys. Rev.* B **43** 12 431
[294] Muller G, Weiss D, Khaetskii A V, von Klitzing K, Koch S, Nickel H, Schlapp W and Losch R 1992 *Phys. Rev.* B **45** 3932
[295] Buttiker M 1992 *Semiconductors and Semimetals* vol 35, ed M Reed (San Diego, CA: Academic) p 253
[296] Machida T, Hirai H, Komiyama S and Shiraki Y 1996 *Phys. Rev.* B **54** 16 860
[297] Liu J, Gao W X, Ismail K, Lee K Y, Hong J M and Washburn S 1994 *Phys. Rev.* B **50** 17 383
[298] Hansen A E, Kristensen A, Pedersen S, Sorensen C B and Lindelof P E 2001 *Phys. Rev.* B **64** 045327
[299] Altshuler B L, Gefen Y, Kamenev A and Levitov L S 1997 *Phys. Rev. Lett.* **78** 2803
Clerk A A, Waintal X and Brouwer P W 2001 *Phys. Rev. Lett.* **86** 4636
Clerk A A, Brouwer P W and Ambegaokar V 2001 *Phys. Rev. Lett.* **87** 186801
Leyronas X, Tworzydlo J and Beenakker C W J 1999 *Phys. Rev. Lett.* **82** 4894
Mirlin A D and Fyodorov Y V 1997 *Phys. Rev.* B **56** 13 393
Silvestrov P G 1997 *Phys. Rev. Lett.* **79** 3994
[300] Imry Y 2002 *Preprint* cond-mat/0202044